POTENTIAL OF RADIO FREQUENCY HEATING OF FRESH FRUITS AS AN ALTERNATIVE QUARANTINE METHOD

By

SOHAN L. BIRLA

A dissertation submitted in partial fulfillment of
the requirements for the degree of

DOCTOR OF PHILOSOPHY

in

ENGINEERING SCIENCE

WASHINGTON STATE UNIVERSITY

College of Engineering and Architecture

Department of Biological Systems Engineering

December 2006

To the Faculty of Washington State University:

The members of the Committee appointed to examine the dissertation of SOHAN LAL BIRLA find it satisfactory and recommend that it be accepted.

_____
Chair

_____

_____

_____

A C K N O W L E D G M E N T

I express my greatest gratitude to Dr. Juming Tang for his advice, guidance and encouragement throughout my studies and research at Washington State University. I am at a loss of words to express fully the importance and value of his helpful insights, understanding, and moral support that enabled me to stay focused on my PhD research. I also express hearty thanks to my doctoral committee members: Drs. John Fellman, Joan Wu, and Prashanta Dutta for their suggestions and valuable comments whenever I approached them with problems. Dr. Fellman was instrumental in grooming me as a postharvest engineer.

I thank Dr. Shaojin Wang, Research Assistant Professor, for his support and perceptivity during technical brain-storming sessions. I learned a tremendous amount from him, especially experimental design and scientific writing. I acknowledge the contribution of Dr. Susan Lurie, Israel in designing experiments for quality assessment of fresh fruits. I am indebted to Mr. Scott Mattinson, Research Associate in the Department of Horticulture and Landscape Architecture, for teaching me flavor analysis.

I thank Frank Younce, Wayne Dewitt, and Vince Himsl for providing all needed technical support and fabrication of requisite instrumentation. I acknowledge the assistance provided by Gopal Tewari in conducting the last part of my experimentations. And my colleagues Ram, Ali, Jian, and Hao were highly supportive and stood by me through the thick and thin of my doctoral study.

Last but not least, I want to express my heartfelt thanks to my wife Veena, who bore all the pain of forced separation and single-handedly fulfilled our common responsibilities in raising our kids Sovin and Reva. Without her vital moral support I could never have accomplished this research.

I acknowledge the funding of BARD (US-3276-01), USDA-IFAFS (00-52103-9656), and the WSU IMPACT Center for supporting my doctoral research.

POTENTIAL OF RADIO FREQUENCY HEATING OF FRESH FRUITS AS AN ALTERNATIVE QUARANTINE METHOD

ABSTRACT

By Sohan L. Birla, Ph.D.
Washington State University
December 2006

Chair: Juming Tang

Methyl bromide fumigation, the most widely used contemporary quarantine method for fresh fruits, has raised public concerns because of its high ozone-depletion potential. To respond to the urgency of finding alternative methods, many researchers have explored radio frequency (RF) energy to disinfest fresh fruits. Although damage to fruit has been a major stumbling block for commercial applications, there is renewed interest in RF energy stems after successful demonstration of its ability to control fruit flies in dry nuts. The research upon which this dissertation was based has the broad objective of developing RF energy-based treatment protocols for apples and citrus fruits.

A computer model that solves electro-magnetic field and Navier-Stokes equations using FEMLAB software was developed to predict transient temperature profiles in fruits. Simulation results suggested that the problem of non-uniformity can be resolved by continuously moving and rotating fruits in an RF field, so a fruit mover was designed and developed to impart 3-D movement and rotation of fruits in a saline water solution. This resulted in a significant improvement in heating uniformity of fruits. Dielectric properties of constituent parts of fruits, namely oranges, grapefruits, apples, avocados, and peaches, were measured to understand the RF heating charteristics of the fresh fruits using the developed model. The simulation and

experimental results corroborated that the physical and dielectric properties of peel and pulp, geometric shape of fruits, and the medium around the fruits all play crucial roles in their heating patterns. The model also helped to determine the effects of parameters on heating patterns and design of practical RF treatments.

RF treatments were designed based on literature about the thermal death kinetics of fruit flies. Evaluation of quality parameters such as weight loss, peel and pulp color, and change in volatile flavor profiles after simulated storage for 30 days revealed that an RF treatment including a 48°C temperature exposure for 15 min can be an effective. RF-assisted hot water heating (preheating fruits in hot water at non-damaging temperatures for specific times and then exposing to RF heating) was efficacious against codling moth in apples. However, the margin for maintaining the quality of treated apples was small. Because of significant changes in volatile flavor profiles in the fruits subjected to RF-based high-temperature-short-time treatment hence low temperature RF treatment should be explored.

Lastly, issues of energy and induction in current packing house operations were addressed. By demonstrating the feasibility of designing a continuous RF heat treatment for packing houses, this research opened up a new vista for exploring RF energy-based treatment for disinfecting fresh fruits. Due to specific heating patterns in RF fields, each fruit category needs a special approach to ascertain the benefits associated with RF heating.

TABLE OF CONTENTS

LIST OF TABLES

Chapter 6

Chapter 7

Chapter 8

LIST OF FIGURES

Chapter 2

Chapter 3

Chapter 4

Chapter 5

Chapter 6

Chapter 7

Chapter 8

Dedication

This dissertation is dedicated to my late mother

who taught me that

"The important thing about a problem is not its solution, but the strength we gain in finding the solution"

.....Anonymous

OUTLINE OF DISSERTATION

This dissertation has been organized into eight self-contained chapters. The first chapter is a general introduction to quarantine methods and the motivation for exploring the use of RF energy in quarantine treatments of fresh fruits. The following chapters are stand-alone articles, and hence, some repetition was unavoidable.

Chapter 2 develops a fundamental understanding of RF heating fruits in parallel plate systems and pinpoints the problem of non-uniform heating. Chapter 3 suggests ways and means to overcome the problem of non-uniform RF heating of fresh fruits.

Chapter 4 describes the measurement and effects of dielectric properties of component parts of fruits on RF heating patterns. Chapter 5 identifies potential RF treatments for oranges based on post-treatment quality analysis. Chapter 6 evaluates the efficacy of RF-assisted hot water treatments against codling moth in red delicious apples, in addition to a quality evaluation of RF-treated apples.

Chapter 7 describes the development of a simulation model and its uses for studying the effects of various parameters on an RF heating pattern. The last chapter explores prospects for designing continuous RF treatments of fresh fruits.

Since the dissertation is composed of individually published and prepared manuscripts, the chapter formats vary according to the submitted journals. A list of articles published/manuscripts prepared from this research is shown below:

1. Birla S.L., Wang S., Tang J., and Hallman G. 2004. Improving heating uniformity of fresh fruits in radio frequency treatments for pest control. Postharvest Biology and Technology, 33(2), 205–217 (Chapter 3).

2. Birla S.L., Wang S., and Tang J. 2006. RF heating pattern as influenced by dielectric properties of fresh fruits. Transactions of the ASABE (Internal review, Chapter 4).
3. Birla S.L., Wang S., Tang J., Fellman J., Mattinson D., and Lurie S. 2005. Identification of a potential quarantine radio frequency heat treatment for oranges. Postharvest Biology and Technology, 38(3), 66–79 (Chapter 5).
4. Wang S., Birla S.L., Tang J., and Hansen, J. 2006. Postharvest treatment to control codling moth in fresh apples using water assisted radio frequency heating. Postharvest Biology and Technology, 40(1), 89–96 (Chapter 6).
5. Birla S.L., Wang S., and Tang J. 2006. Characterization of heating of spherical fruit in parallel plate radio frequency system. Journal of Food Engineering (Internal review, Chapter 7).

C H A P T E R 1

RADIO FREQUENCY HEATING AS A QUARANTINE METHOD: A REVIEW

Abstract:

Alternative quarantine methods for fresh fruits are evaluated in response to the ban on methyl bromide fumigation. The literature review focuses on radio frequency (RF) heating so that various issues pertinent to development of RF energy-based quarantine treatment protocols can be identified and resolved. Damage to fruit quality due to uneven RF heating was identified as the major bottleneck in the development of RF energy-based thermal treatment. Therefore, research was planned with a broad objective to resolve these issues and develop practical RF energy-based quarantine treatments for fresh fruits.

Keywords: Quarantine, disinfestation, fruit flies, radio frequency, heat treatment

1. Introduction

The United States is second only to Brazil in the production of oranges (*Citrus sinensis L. Osbeck*), which was 22.9% of world production and 11.7 million tons from the 2004-2005 season (USDA-NASS, 2004). About 67% of citrus fruits produced in the world are marketed as fresh, with major citrus-producing countries also acting as major fresh fruit exporters. Washington state contributed 58% of 4.7 million tons of the apples produced in the United States, valued at more than $1.6 billion in 2004. Of this production, 522,692 metric tons of fresh apples were exported, mainly destined for Japan and South Korea (USDA-NASS, 2004).

The major citrus fruit-producing regions in the Unites States such as Hawaii, California, and Florida have climates favorable for an epidemic of Mexican (*Anastrepha ludens* Loew), Mediterranean (*Ceratitis capitata* Wiedemann), and Caribbean fruit flies (*Anastrepha suspensa* Loew), whereas the climate in Washington state provides a conducive environment for the growth of codling moth (*Cydia pomonella*) in apples (Calkins, 1993). The export and import of fresh produce is one of the easiest ways to introduce invasive exotic insects into new geographic regions. However, strict quarantine systems and regulations can prevent the introduction of infested fruit. Endemic populations of fruit flies are not found in countries like Japan, Korea, the Republic of China, Australia, New Zealand, or the mainland United States even though these countries have climates conducive for the establishment of the flies. Generally a postharvest quarantine treatment is required to guarantee that no life stages of the insect/pest are present in imported fruits. Accepted quarantine treatments include fly-free production zones, fumigation with methyl bromide (MeBr), cold storage, and high-temperature forced-air (Mangan et al., 1998). Effective quarantine treatments must be efficacious, non-damaging to fruit, environmentally sound, safe, and cost-effective (Wang and Tang, 2001).

2. Drawbacks of Current Quarantine Methods

Importing countries establish the requirements for quarantine treatments. For example, citrus shipments destined from states such as California, Arizona, and Florida to Japan and other Pacific Rim countries require MeBr fumigation to meet import quarantine security requirements. On average, 80 to 95% of the used MeBr that enters the atmosphere has a 0.6 ozone depletion potential (USEPA, 1998). According to the Montreal Protocol, MeBr uses have been restricted or eliminated in developed countries for most applications since 2005 (USEPA, 1998). Moreover, MeBr fumigation often damages the commodity. Many chemicals have been proposed, but none

for use on fresh fruit because of unacceptable phototoxic damage that reduces quality, shelf life, and marketability (Armstrong, 1992).

Some of the alternative methods investigated include ionizing radiation (Burditt, 1982), cold storage (Schiffman-Nadel et al., 1972; 1975), controlled atmosphere (Neven, 2005), conventional hot air and water heating (Sharp and McGuire, 1996; Sharp, 1991; Shellie and Mangan, 2002; Shellie et al., 1993), and radio frequency (RF) treatments (Ikediala et al., 1999; Ikediala et al., 2002; Tang et al., 2000) for various fruits and other agricultural commodities.

Use of irradiation has raised public concern over safety of the technology (Hatton et al., 1984). It also requires significant capital investments for special treatment facilities because precise control and verification of doses are necessary. Moreover, excessive irradiation doses bring undesirable quality changes in fruits. Common symptoms of radiation injury are browning or discoloring of either the surface or flesh, cavitation, flesh softening, and abnormal ripening (Morris and Jessup, 1994).

Cold storage treatment as a quarantine method has been explored to control exotic fruit flies and other insects in some fruit (Gould, 1994). Cold treatment usually takes several weeks to achieve this purpose, so integrating it with existing storage or shipping facilities would be the best approach. Import of grapefruit, oranges, and tangerines from countries having Mediterranean fruit fly problems to the USA requires cold treatment at 0, 0.6, 1.1, 1.7, or 2.2°C for 10, 11, 12, 14, or 16 days, respectively (USDA-APHIS-PPQ, 2002). One of the major drawbacks of cold storage is that its long treatment time (~16 days at 0 to 2°C) to be effective against fruit flies may induce chilling injury and lead to enhanced decay susceptibility, interruption of ripening, and damage to peel, pulp, and texture (Couey, 1982).

Controlled atmosphere (CA) has been used for many years to extend commodity shelf life. Many researchers have demonstrated its efficacy in controlling fruit flies, but low commodity tolerance to treatment is a limiting factor (Mitcham et al., 1997). In general, O_2 concentrations must be below 1% and CO_2 concentrations above 20% for insect control (Zhou et al., 2000). For most applications, however, CA treatments require long exposures that sometimes lead to quality damage.

Conventional heating methods have been explored for different fruit types and insect species using different thermal treatments alone or in combination with cold or controlled storage conditions (Neven, 2005; Neven et al., 1996; Neven et al., 2000; Sharp, 1990 & 1992, 1993; Sharp and Gould, 1994; Sharp and McGuire, 1996; Sharp et al., 1989; Shellie and Mangan, 2002a, 2002b). The fruit core must reach certain temperatures so that the treatment is effective even in the most insulated areas such as inside seed kernels. A common difficulty with hot air or water heating methods is the slow rate of heat transfer in fruit from outside to inside, resulting in hours of treatment time, especially for large fruits (Wang et al., 2001a). The temperature requirements of quarantine treatments (43–49°C) border between that which will not affect fruit quality but not kill all insects in the amount of time used for treatments (< 43°C) and those that will kill pests but might harm fresh commodities (> 49°C) (Mangan and Hallman, 1998). External and internal damage caused by long exposure times to heat include peel browning, pitting, poor color development, and abnormal softening (Lurie, 1998). The desire to eliminate these problems and achieve fast and effective thermal processing has resulted in increased interest in using electromagnetic (EM) energy to control insect pests in agricultural commodities.

3. RF Heating

EM energy at RF or microwave (MW) frequency can be used to rapidly raise fruit temperature volumetrically. The Federal Communications Commission (FCC) in the USA reserves three RFs (13.56, 27.12 and 40.68 MHz) and two MW frequencies (915 and 2,450 MHz) for industrial, scientific, and medical applications. Headlee and Burdette (1929) first explored the use of RF energy as a rapid disinfestation treatment. In subsequent years, Frings (1952) studied the factors affecting insect/pests mortality during RF heating. He concluded that RF energy-based disinfestation would damage fruit quality. Hayes et al. (1984) explored the use of 2,450 MHz MW energy to disinfest papaya, but uneven heating (> 20°C variation) deterred further trial on other fruits. To overcome the problem of uneven heating of mango fruit, Seo et al. (1970) tried intermittent MW heating, but was unsuccessful. Most recently, (Fang et al., 2001) explored RF heating to eliminate decay fungi in roundwood sections of fencing poles during processing.

Hallman and Sharp (1994) summarized the research on potential uses of RF/MW heating in fresh fruit disinfestation. They concluded that damage to the fruit was the major concern in commercial application of this technology. RF treatment may hold potential for grains, pulses, nuts, dried fruits, cured tobacco, and other similar commodities because of their relatively higher thermal tolerance than that of fresh fruits. (Hallman and Sharp, 1994) suggested a need for research that deals with non-uniform heating of fresh fruit, including a combination of RF heating with other quarantine methods to overcome problems associated with individual methods. The bottom line is that RF heat treatment can be effectively applied if the problem of uneven heating is resolved.

4. Current Research Directions

Wang et al. (2002) developed RF treatment protocols for in-shell walnuts, but when fresh fruits are RF-heated in air, they suffer thermal damage (burn) at the points of contact with the container or other fruits. This is the result of overheating caused by a concentration of electric fields around the contact areas, which have the least resistance to RF energy. To avoid fruit-to-fruit contact during RF heating and make the load more homogeneous to RF fields, Ikediala et al. (2002) suggested immersion of fruits in water. Water immersion indeed improved RF heating uniformity in cherries; however, for large fruits such as oranges and apples, the immersion technique did not work. Since mode stirrers and turntables in home MW ovens successfully deal with spatial non-uniformities, a similar approach is proposed to improve the heating uniformity in RF systems.

To better understand the causes of non-uniform heating of fruit and improve their heating uniformity, it is desirable to develop a computer simulation model. A model also helps in the design of commercial-scale quarantine treatments (Mangan and Hallman, 1998). Similar to the development of any new technology or process, one has to address many issues prior to its successful commercial adoption. Following are the general objectives of this research geared toward developing RF energy-based treatment protocols for fresh fruit:

1 Develop a system to rotate and move fruit to facilitate uniform RF heating.

2 Identify potential RF heat treatments based on postharvest quality analysis.

3 Verify the efficacy of the potential treatments on artificially-infested fruit.

4 Measure the dielectric properties of fresh fruit peel and pulp.

5 Model and simulate the complete RF heating process.

6 Explore the design feasibility of a continuous RF treatment.

Each sub-objective leading to development of a treatment protocol for fresh fruits is elaborated in Chapters 2 through 8.

5. Conclusions

Literature review suggested that uneven RF heating of fresh fruit is the major challenge in the development of RF quarantine treatments. If the problem of non-uniformity is resolved, RF energy-based treatment protocol can be developed.

References

Armstrong, J.W., 1992. Fruit-fly disinfestation strategies beyond Methyl-Bromide. New Zealland J. Crop Hort .20, 181–193.

Bailey, S.W., Banks, H.J., 1980. A review of recent studies on the effects of controlled atomspheres on stored product pests. In: Shejbal, J. (Ed.), Controlled atmosphere of grains. Elsevier, Amsterdam, pp. 101–118.

Burditt, A.K.J., 1982. Food irradiation as a quarantine treatment of fruits. Food Technol. 51–54–58–60, 62.

Calkins, C.O., 1993. Future directions in control of the Caribbean fruit fly. Flo. Entomol. 76, 263–270.

Couey, H.M., 1982. Chilling injury of crops of tropical and subtropical origin. HortSci. 17, 162–165.

Fang, F., Ruddick, J.N.R., Avramidis, S., 2001. Application of radio-frequency heating to utility poles. Part 3. The use of RF heating to eradicate decay fungi in pole material. Forest Prod. J. 51, 51–55.

Frings, H., 1952. Factors determining the effects of radio-frequency electromagnetic fields and materials they infest. J. Econ. Entomol. 45, 396–408.

Gould, W.P., 1994. Cold storage. In: Sharp, J.L., Hallman, G.J. (Eds.), Quarantine treatments for pests of food plants. Westview Press, Boulder, pp. 119–132.

Hallman, G.J., Sharp, J.L., 1994. Radio frequency heat treatments. In: Sharp, J.L., Hallman, G.J. (Eds.), Quarantine treatments for pests of food plants. Westview Press, San Francisco, CA, pp. 165–170.

Hatton, T.T., Cubbredge, R.H., Risse, L.A., Spalding, D.H., Windeguth, D.L., Chew, V., 1984. Phytotoxic responses of Florida grapefruit to low-dose irradiation. J. Ame. Soc. Hortic. Sci. 109, 607–610.

Hayes, C.F., Chingon, T.G., Nitta, F.A., Wang, W.J., 1984. Temperature control as an alternative to ethylene dibromide fumigation for the control of fruit flies (Diptera: Tephritidae) in papaya [Dacus dorsalis]. J. Econ. Entomol. 77, 683–686.

Headlee, T.J., Burdette, R. C., 1929. Some facts relative to the effect of high frequency radio waves on insect activity. J. New York Entomol. Soc. 37, 59–64.

Ikediala, J.N., 2000. Quarantine treatment for fruits using radio frequency and microwave energy. PhD Thesis, Biological Systems Engineering, Washington State University, 183.

Ikediala, J.N., Tang, J., Neven, L.G., Drake, S.R., 1999. Quarantine treatment of cherries using 915 MHz microwaves: temperature mapping, codling moth mortality and fruit quality. Postharvest Biol. Technol. 16, 127–137.

Ikediala, J.N., Hansen, J.D., Tang, J., Drake, S.R., Wang, S., 2002. Development of a saline water immersion technique with RF energy as a postharvest treatment against coding moth in cherries. Postharvest Biol. Technol. 24, 25–37.

Lurie, S., 1998. Postharvest heat treatments. Postharvest Biol. Technol. 14, 257–269.

Mangan, R.L., Hallman, G.J., 1998. Temperature Treatments for Quarantine Security: New Approaches for Fresh Commodities. In: Hallman, G.J., Denlinger, D.L. (Eds.), Temperature sensitivity in insects and application in integrated pest management. Westview Press, Boulder, pp. vi, 311.

Mangan, R.L., Shellie, K.C., Ingle, S.J., Firko, M.J., 1998. High temperature forced-air treatments with fixed time and temperature for 'Dancy' tangerines, 'Valencia' oranges, and 'Rio Star' grapefruit. J. Econ. Entomol. 91, 933–939.

Mitcham, E.J., Zhou, S.J., Bikoba, V., 1997. Controlled atmospheres for quarantine control of three pests of table grape. J. Econ. Entomol. 90, 1360–1370.

Morris, S.C., Jessup, A.J., 1994. Irradiation. In: Paull, R.E., Armstrong, J.W. (Eds.), Insect Pests and fresh horticultural products: Treatments and responses. CAB International, Wallington, UK, pp. 163–190.

Neven, L.G., 2005. Combined heat and controlled atmosphere quarantine treatments for control of codling moth in sweet cherries. J. Econ. Entomol. 98, 709–715.

Neven, L.G., Rehfield, L.M., Shellie, K.C., 1996. Moist and vapor forced air treatments of apples and pears: Effects on the mortality of fifth instar codling moth (Lepidoptera: Tortricidae). J. Econ. Entomol. 89, 700–704.

Neven, L.G., Drake, S.R., Ferguson, H.J., 2000. Effects of the rate of heating on apple and pear fruit quality. J. Food Quality 23, 317–325.

Schiffman-Nadel, M., Chalutz, E., Wax, J. Dagan, M., 1975. Reduction of chilling injury in grapefruit by thiabendazole and benomyl during long term storage. J. Ame. Soc. Hortic. Sci. 100, 276–276.

Schiffman-Nadel, M., Chalutz, E., Wax, J., Lattar, F.S., 1972. Reduction of pitting of grapefruit by thiabendazole during long term cold storage. HortSci. 7, 394–394.

Seo, S.T., Chambers, D.L., Komura, M., Lee, C.Y.L., 1970. Mortality of mango weevils in mangoes treated by dielectric heating. J. Econ. Entomol 63, 1977–1978.

Sharp, J.L., 1990. Immersion in heated water as a quarantine treatment for California Stone fruits infested with the Caribbean fruit-fly (Diptera, Tephritidae). J. Econ. Entomol. 83, 1468–1470.

Sharp, J.L., 1992. Hot-air quarantine treatment for mango infested with Caribbean fruit-fly (Diptera, Tephritidae). J. Econ. Entomol. 85, 2302–2304.

Sharp, J.L., 1993. Hot-air quarantine treatment for Marsh White grapefruit infested with Caribbean fruit-fly (Diptera, Tephritidae). J. Econ. Entomol. 86, 462–464.

Sharp, J.L., Gould, W.P., 1994. Control of Caribbean fruit-fy (Diptera, Tephritidae) in grapefruit by forced hot air and hydrocooling. J. Econ. Entomol. 87, 131–133.

Sharp, J.L., McGuire, R.G., 1996. Control of Caribbean fruit fly (Diptera: Tephritidae) in navel orange by forced hot air. J. Econ. Entomol. 89, 1181–1185.

Sharp, J.L., Ouye, M.T., Ingle, S.J., Hart, W.G., 1989. Hot-water quarantine treatment for mangoes from Mexico infested with mexican fruit-fly and West-Indian fruit-fly (Diptera, Tephritidae). J. Econ. Entomol. 82, 1657–1662.

Sharp, J.L., Gaffney, J.J., Moss, J.I., Gould, W.P., 1991. Hot-air treatment device for quarantine research. J. Econ. Entomol. 84, 520–527.

Shellie, K.C., Mangan, R.L., 2002a. Cooling method and fruit weight: Efficacy of hot water quarantine treatment for control of Mexican fruit fly in mango. HortSci. 37, 910–913.

Shellie, K.C., Mangan, R.L., 2002b. Hot water immersion as a quarantine treatment for large mangoes: Artificial versus cage infestation. J. Ame. Soc. Hortic. Sci. 127, 430–434.

Shellie, K.C., Firko, M.J., Mangan, R.L., 1993. Phytotoxic response of dancy tangerine to high-temperature, moist, forced-air treatment for fruit-fly disinfestation. J. Ame. Soc. Hortic. Sci. 118, 481–485.

Tang, J., Ikediala, J.N., Wang, S., Hansen, J.D., Cavalieri, R.P., 2000. High-temperature-short-time thermal quarantine methods. Postharvest Biol. Technol. 21, 129–145.

USDA-APHIS-PPQ, 2002. Treatment manual: interim edition. In: Agric., U.S.D. (Ed.). Animal Plant Health Inspection Service, Plant protection Quarantine, Riverdale, MD.

USDA-NASS, 2004. Agricultural statistics 2004. Chapter V: Statistics of fruits, tree nuts and horticultural specialties U. S. Dep. Agric., Nat. Agric. Stat. Serv. Washington, D.C. U. S. Dep. Agric., Nat. Agric. Stat. Serv. Washington, D.C.

USEPA, 1998. United States Environmental Protection Agency. Reregistration Eligibility Decision. Aluminum and Magnesium Phosphide. Cases 0025 & 0645. USEPA, Office of Pesticide Programs, Special Review and Reregistration Division.

Wang, S., Tang, J., 2001a. Radio frequency and microwave alternative treatments for insect control in nuts: Review. Agric. Eng. J. 10, 105–120.

Wang, S., Tang, J., Cavalieri, R.P., 2001b. Modeling fruit internal heating rates for hot air and hot water treatments. Postharvest Biol. Technol. 22, 257–270.

Wang, S., Tang, J., Johnson, J.A., Mitcham, E., Hansen, J.D., Cavalieri, R.P., Bower, J., Biasi, B., 2002. Process protocols based on radio frequency energy to control field and storage pests in in-shell walnuts. Postharvest Biol. Technol. 26, 265–273.

Zhou, H.W., Lurie, S., Lers, A., Khatchitski, A., Songeo, L., Ben Arie, R., 2000. Delayed storage and controlled atmosphere storage of nectarines: two strategies to prevent woolliness. Postharvest Biol. Technol. 18, 133–141.

C H A P T E R 2

FUNDAMENTAL OF RF HEATING OF OBJECTS IN PARALLEL PLATES SYSTEM

S. L Birla, S Wang, and J. Tang

Manuscript prepared for Journal of Microwave Power and Electromagnetic Energy

Abstract:

Historically, radio frequency (RF) heating has been explored for rapid and volumetric heating of various materials. However, a problem of uneven heating of materials has deterred the possible use of RF energy for heat-sensitive materials such as fruits. A systematic understanding of RF heating as influenced by the geometrical shape of objects is needed to overcome uneven heating problems. In the present study, a simulation model was developed using commercial finite element method-based FEMLAB software. The model provided insight into the influence of various geometries on heating uniformity in a parallel plate RF system. The analytical and numerical solutions of Laplace equation for electric field in sphere, slab and cylindrical objects were compared. It was established in this study that heating potential did not increase linearly with increasing loss factor of the objects but reached a broad maximum depending on the geometric shape of the objects, surrounding medium and air gap above the object. Beyond that point, further increase in loss factor diminished the heating potential. A condition was also derived for uniform heating of the medium and objects. It is highly recommended that computer simulation should be adopted for developing further understanding of the RF heating mechanism in arbitrary-shaped objects and temperature dependent dielectric material.

Keywords: radio frequency, parallel plate electrodes, dielectric heating, fringe field

1. Introduction

RF heating systems usually consist of a high voltage AC signal generator attached with applicators enclosed in a metallic enclosure. Heat is generated in the object by ionic conductance, dipole movement and flow of displacement current. Absorbed RF power per unit volume (P, W m^{-3}) in any lossy media (composed of linear homogenous isotropic material of known properties) is proportional to the square of the electric field strength ($\boldsymbol{E}$, V m^{-1}), the dielectric loss factor (ε''), and frequency (f, Hz) (Choi and Konrad, 1991):

$$P = 2\,\pi\, f\, \varepsilon_{o}\, \varepsilon''\, \boldsymbol{E}_{rms}^{2} = \pi\, f\, \varepsilon_{o}\, \varepsilon''\, |\boldsymbol{E}|^{2} \tag{1}$$

where ε_0 is permittivity in free space (8.854×10^{-12} F m^{-1}) and $\boldsymbol{E}_{rms}$ is the root mean square value of electric field equal to $\sqrt{2}$ times of the E-field amplitude.

Evaluation of the absorbed RF power density at any point inside the material requires the value of electric field strength which is impractical to measure. This is further complicated by the fact that the '$\boldsymbol{E}$' at any point within the material depends on the geometry of the object and electrode configuration (Marshall and Metaxas, 1998). Electromagnetic (EM) field pattern in the heated material within a RF enclosure is governed by Maxwell equations. Analytical solutions of Maxwell equations are available in literature for regular geometrical shapes sandwiched between parallel plate electrodes (Roussy and Pearce, 1995). Evan (2000) mentioned that at a given frequency, information on loss factor and dielectric constant are sufficient in principle to calculate the heat dissipation at any point, but it is not straightforward in predicting the heating profile over the cross section of objects because it is influenced by shape and size of the object. Therefore, a numerical simulation is desirable to gain a better understanding of RF heating processes and design of thermal processes. For arbitrary-shaped geometries and heterogeneous

materials, numerical methods, such as Finite Difference Method (FDM) and Finite Element Method (FEM), are usually used for EM-field solutions.

Use of RF heating has been explored in disinfestation of fresh fruits (Tang et al., 2000). Several potential problems associated with the RF heating of fruits need to be resolved prior to commercial application. For example, fresh fruits, which are mostly spherical in shape, are heated excessively at points of contacts with containers or between fruits. Ikediala et al. (2002) suggested saline water immersion of fresh fruits to eliminate contact heating. While this approach alleviate the uneven heating problem to some extend, but for large size fruits such as apple, citrus, mango, etc., the problems of core heating, uneven heating persisted. Birla et al. (2004) showed that uneven RF heating of the large fresh fruits can be overcome by movement and rotation of spherical objects in saline water. Recently we have observed that even rotating and movement of fruits did not provide uniform heating all over the entire fruit cross section. Uneven heating may be either due to size and nature of materials or electrode configurations. There was a need to develop a computer model to investigate the causes of uneven heating and suggest means to resolve this problem. A computer simulation of RF heating of various load geometries under the parallel plates heating system would reduce the trial and error processes used in current of RF heating system design practices. A clear and systematic understanding of RF heating may help in improving the design of RF heating systems and processes (Burfoot et al., 1996; Fleischman, 1999).

Neophytou and Metaxas (1996) and Marshall and Metaxas (1998; 1999; 1997) conducted pioneering work on modeling of RF heating systems, and published a series of papers on the RF modeling. They suggested that for small size RF applicator, electrostatic conditions can be used with adequate accuracy, whereas for large size electrodes, wave equations should be solved.

They also hinted that for frequencies above 27.12 MHz the electrostatic assumptions would lead to large inaccuracies. Chan et al. (2004) modeled a complete industrial RF heating system by solving electromagnetic wave equations using FEM. The predicted field patterns agreed with experimental results. But only slab shaped foods were considered in that study. Veen et al. (2004) developed an analytical model for dielectric heating potential in spherical objects immersed in an infinitely large surrounding medium, in which Maxwell equations for plane wave were solved by adopting the Mie theory for the electric field. They assumed that the electromagnetic field in a small sphere was uniform over the cross section. In the case of large objects, such as oranges and apples, this assumption is not valid because of the relative large size of objects with respect to that of the electrodes and the gap between them.

Evan (2000) showed that heating potential inside a sphere surrounded by air in a uniform electric field would reach maximum when the loss factor was in the range of dielectric constant. We extended his work and systematically derived a condition for maximum heating potential of various object shapes surrounded by the lossy material. In this chapter we also compared characteristic heating pattern in various geometrical shapes in actual conditions using FEMLAB software.

2. Materials and Methods

2.1. RF heating system

A RF heating system consists of two parts -generator and applicator. The applicator is a metal structure which directs the RF field to the product or load to be heated. The applicator functions as a capacitor and its electric characteristics depend on its geometry and the material to be heated. The most common type of RF applicator is a pair of parallel plates in which the lossy

material is sandwiched to form a parallel plate capacitor (Fig. 1). The top electrode plate with adjustable height is inductively coupled to the tank oscillator circuit via feed strips. When the size of the applicators is comparable or larger than the wavelength, the plate voltage does not remain constant from the feed points (Metaxas, 1996).It causes uneven distribution of surface charges, in addition to fringe effects at the edges of the electrodes and loads. A RF applicator is usually housed in a metallic enclosure and inductively connected with a tank circuit as shown in Fig. 1. The power supplied to the sandwiched object is typically controlled by varying the electrode gap in most industrial systems (Wang et al.).

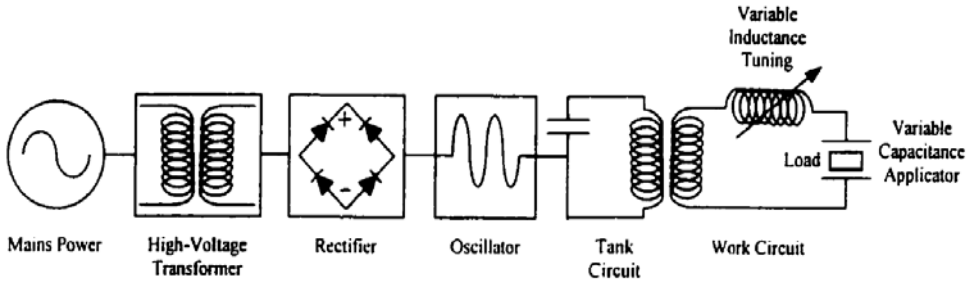

Fig. 1. Schematic diagram of RF generator and applicator (Courtesy:Wig, 2000)

2.2. Design consideration for RF system

The RF system design is dictated by requirements for energy efficiency, heating uniformity, and control. Moreover, electrical and physio-chemical properties of a lossy object play a critical role in the design and operation of RF processes. Heating uniformity is important due to the fact that the correct temperature over the whole mass may be critical to the effectiveness and efficiency of the process.

The RF heating process suffers from two distinct forms of non-uniformity. The first is the fundamental "standing wave" effect. This is a repeated pattern of field intensity variation within a RF applicator, which for the most part, follows a half-sine pattern (Brown et al., 1947). In a distance of one quarter of the operating wavelength the field intensity can change from a

maximum to zero, or in a one-tenth of a wavelength the intensity can change by 60%. Uniformity considerations can also play a role in the choice of frequency. The lower the frequency, the larger is the uniform volume. The second type of non-uniformity is the limited penetration depth problem. The RF fields attenuate within the bulk of conductive materials or materials with high dielectric losses. Both types of non-uniformities described above are frequency dependent and become less severe as frequency is lowered (Cable, 1954).

Table 1. FCC allocated frequency bands designated for ISM applications (FCC, 1988)

Frequency Range	Center Frequency (MHz)	Frequency Tolerance +/– %	Free Space Wavelength (m)
Radio frequency	13.56	0.052	22.1
	27.12	0.6	11.1
	40.68	0.005	7.4
Microwave (MW)	915	1.4%	0.328
	2450	2.0%	0.122

Other than frequency, object shape and size, and distribution of particles in the matrix also contribute to the non-uniformity. Particle size is an important parameter in dielectric heating. Stack of grains or fruits sandwiched between RF electrodes makes a heterogeneous matrix of air-fruit mass. The electrical circuit between the electrodes consists of a network of small resistances and capacitances, the values of each component being governed by the physical characteristics of the particles or air spaces between them. This affects the voltage gradients built up across the bulk of the material and can result in unusual temperature distribution. Jelinek et al. (1949) observed that in bulk, peas, lima beans, and corn tended to burn at points of contact as a result of the high current concentrations at these points. If the

material such as fresh fruit is susceptible to damage from localized heating, the investigation of such effects is essential in the primary stages of development of the RF energy based processes.

2.3. Governing equations

Because the wavelength in the RF range is often much larger than the maximum size of the object to be heated, quasi-static approximation can be applied for the solution of Maxwell's electromagnetic field equations. Maxwell equations for electromagnetic fields are written as (Roussy and Pearce, 1995):

$$\nabla \times \boldsymbol{H} = \sigma \boldsymbol{E} + \frac{\partial \boldsymbol{D}}{\partial t} \tag{2}$$

where, $\boldsymbol{H}$ is magnetic field intensity (A m^{-1}); $\boldsymbol{D}$ is electric flux density ($\boldsymbol{D}$= ε $\boldsymbol{E}$), ε is the absolute permittivity of the material.

Time harmonic electric field intensity ($\boldsymbol{E}$, V m^{-1}) at angular frequency (ω= 2 π f, rad/s) and period variation (t, s) may be expressed as:

$$\boldsymbol{E} = \boldsymbol{E}_0 e^{j\omega t} \tag{3}$$

In RF systems, the time variations are of co-sinusoidal form and are referred to time-harmonic condition. Under time-harmonic condition, the Maxwell's equation can be modified to (Roussy and Pearce, 1995):

$$\nabla \times \boldsymbol{H} = \sigma \boldsymbol{E} + \frac{\partial(\varepsilon \boldsymbol{E})}{\partial t} = (\sigma + j\varepsilon_o \varepsilon \omega)\boldsymbol{E} = \boldsymbol{J} \tag{4}$$

The right hand term is the current density ($\boldsymbol{J}$, A m^{-2}) due to combined loss of all possible mechanisms in the medium such as ionic conduction, dielectric relaxation, Maxwell-Wagner losses, etc. When a material has a complex permittivity under the influence of a time harmonic EM field then:

$$\boldsymbol{J} = \sigma \boldsymbol{E} + \mathrm{j}\omega\varepsilon_o(\varepsilon' - \mathrm{j}\varepsilon'')\boldsymbol{E} \quad (5)$$

where ε' is dielectric constant.

Scalar voltage potential (V) is related to electric field by $\boldsymbol{E} = -\nabla V$, and current density $\nabla \boldsymbol{J}=0$, hence, Maxwell's equations for quasi-static electric field become Laplace equation (Metaxas, 1996):

$$-\nabla \cdot ((\sigma + j\ \varepsilon_o \omega \varepsilon')\nabla V) = 0 \quad (6)$$

where electrical conductivity (σ, S m^{-1}) is related to loss factor (ε'') in RF range as $\sigma = \varepsilon_o \omega \varepsilon''$.

Analytical solution of Laplace Equation (6) is well documented in the literature (Roussy and Pearce, 1995). The solution requires to specify boundary conditions of either fixed potential or to specify flux or flux density at interfaces.

2.4. Maximum heating potential

For comparison of heating ability of different geometry, we defined a term 'heating potential'(P, W m^{-3}) which is a direct function of power density of any solid geometry in the event of slow thermal diffusion rate. We assumed that the rate of heat generation in the solid object is much faster than the thermal diffusion. In the following sections we analytically derived expressions for maximum heating potential in slabs, spheres and cylinders using the classical analytical solutions of the Laplace equation (Roussy and Pearce, 1995).

2.4.1. Slab

The actual field distribution in a RF applicator can be very complex, particularly if the fringing field effect is included in the analytical solution (Metaxas, 1996). But to simplify the analysis, we assume a uniform electric field between two parallel plate electrodes with no fringing field at the edges (Fig. 2). The electric field strength ($\boldsymbol{E}_s$,) in a lossy dielectric slab

having complex permittivity ($\varepsilon_s^* = \varepsilon_s^{'} - \mathrm{j}\varepsilon_s^{''}$) and thickness '*d*' sandwiched between two parallel plate RF electrodes is expressed as (Roussy and Pearce, 1995):

$$\boldsymbol{E}_s = -\frac{\varepsilon_m^*}{a\,\varepsilon_s^* + d\,\varepsilon_m^*} V_o\,\hat{\mathbf{k}}_z \tag{7}$$

where '*a*' is the gap above the slab occupied by dielectric medium ($\varepsilon_m^* = \varepsilon_m^{'} - \mathrm{j}\varepsilon_m^{''}$), V_o is applied electric potential (V) between two plate electrodes, unit vector $\boldsymbol{k_z}$ converts scalar potential into to vector field .

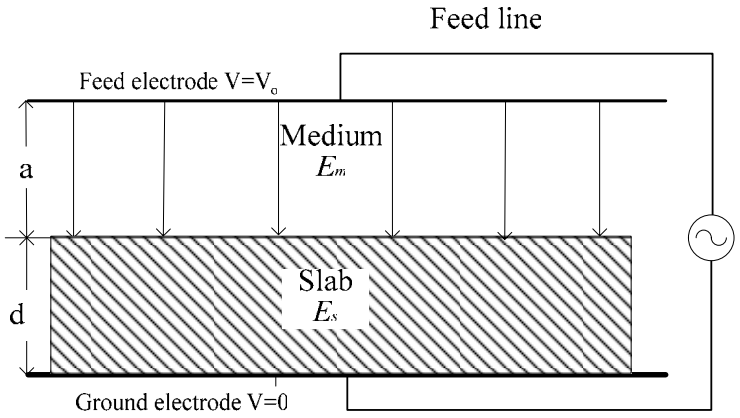

Fig. 2. Plan slab in between RF electrode

Power dissipation (P) according to Eq. (1) in the slab can be expressed as:

$$\mathrm{P} = \frac{\pi f\ \varepsilon_o\ \varepsilon_s^{''}\ V_o^2}{\left| a\,\dfrac{(\varepsilon_s^{'} - \mathrm{j}\varepsilon_s^{''})}{(\varepsilon_m^{'} - \mathrm{j}\varepsilon_m^{''})} + d \right|^2} \tag{8}$$

$$\mathrm{P} = \frac{\pi f\,\varepsilon_o\ V_o^2\,\varepsilon_s^{''}}{\left(a\,\dfrac{\varepsilon_s^{'}\,\varepsilon_m^{'} + \varepsilon_s^{''}\varepsilon_m^{''}}{\varepsilon_m^{'\,2} + \varepsilon_m^{''\,2}} + d \right)^2 + \left(a\,\dfrac{\varepsilon_s^{'}\,\varepsilon_m^{''} - \varepsilon_s^{''}\varepsilon_m^{'}}{\varepsilon_m^{'\,2} + \varepsilon_m^{''\,2}} \right)^2} \tag{9}$$

Differentiating Eq. (9) with respect to loss factor of the slab and equating with zero gives a condition for maximum heating potential as shown below:

$$\frac{dP}{d\varepsilon_s^{"}} = \pi f \varepsilon_o V_o^2 \frac{\varepsilon_m^{'2} + \varepsilon_m^{"2}\left(d^2\varepsilon_m^{'2} + d^2\varepsilon_m^{"2} + 2ad\varepsilon_m^{'}\varepsilon_s^{'} + a^2\varepsilon_s^{'2} - a^2\varepsilon_s^{"2}\right)}{\left(d^2\varepsilon_m^{'2} + d^2\varepsilon_m^{"2} + 2ad\,\varepsilon_m^{'}\varepsilon_s^{'} + 2ad\varepsilon_m^{"}\varepsilon_s^{"} + a^2\varepsilon_s^{'2} + a^2\varepsilon_s^{"2}\right)^2} = 0 \qquad (10)$$

$$d^2\varepsilon_m^{'2} + d^2\varepsilon_m^{"2} + 2ad\varepsilon_m^{'}\varepsilon_s^{'} + a^2\varepsilon_s^{'2} - a^2\varepsilon_s^{"2} = 0 \qquad (11)$$

$$\left(\frac{d}{a}\right)^2(\varepsilon_m^{'2} + \varepsilon_m^{"2}) + 2\frac{d}{a}\varepsilon_m^{'}\varepsilon_s^{'} + \varepsilon_s^{'2} - \varepsilon_s^{"2} = 0 \qquad (12)$$

$$\varepsilon_s^{"} = \sqrt{\frac{d^2}{a^2}(\varepsilon_m^{'2} + \varepsilon_m^{"2}) + 2\frac{d}{a}\varepsilon_m^{'}\varepsilon_s^{'} + \varepsilon_s^{'2}} \qquad (13)$$

If the medium is air ($\varepsilon_m^{'} = 1, \varepsilon_m^{"} = 0$), the maximum heating will occur when:

$$\varepsilon_s^{"} = \varepsilon_s^{'} + \frac{d}{a} \qquad (14)$$

2.4.2. Sphere

Fig. 3 shows a small homogenous lossy sphere immersed in a medium in which E- field is uniform ($\boldsymbol{E_m}$) in absence of the sphere. The uniform electric field strength ($\boldsymbol{E_s}$) inside the sphere was given by (Stratton, 1941):

$$\boldsymbol{E_s} = \frac{3\varepsilon_m^*}{\varepsilon_s^* + 2\varepsilon_m^*}\boldsymbol{E_m} \qquad (15)$$

Power density in sphere:

$$P = \frac{\pi f \varepsilon_o \varepsilon_s^{"} 9\left|\boldsymbol{E_m}\right|^2}{\left|\frac{(\varepsilon_s^{'} - j\varepsilon_s^{"})}{(\varepsilon_m^{'} - j\varepsilon_m^{"})} + 2\right|^2} \qquad (16)$$

Comparing Eq. (16) with Eq. (9) we discern that when $a = 1$, $d = 2$ are put in the Eq. (9) then we get Eq. (16). Therefore the condition for maximum potential in the sphere can be similarly derived by differentiating Eq. 16 with respect to loss factor.

$$\varepsilon_s^{"} = \sqrt{4(\varepsilon_m^{'2} + \varepsilon_m^{"2} + \varepsilon_m^{'}\varepsilon_s^{'}) + \varepsilon_s^{'2}} \tag{17}$$

If the surrounding medium is air ($\varepsilon_m^{'} = 1, \varepsilon_m^{"} = 0$), the condition becomes:

$$\varepsilon_s^{"} = \varepsilon_s^{'} + 2 \tag{18}$$

If power density in sphere (Eq.15) is plot with respect to increasing loss factor of sphere then a peak should occur as per Eq. 18(Evan 2000).

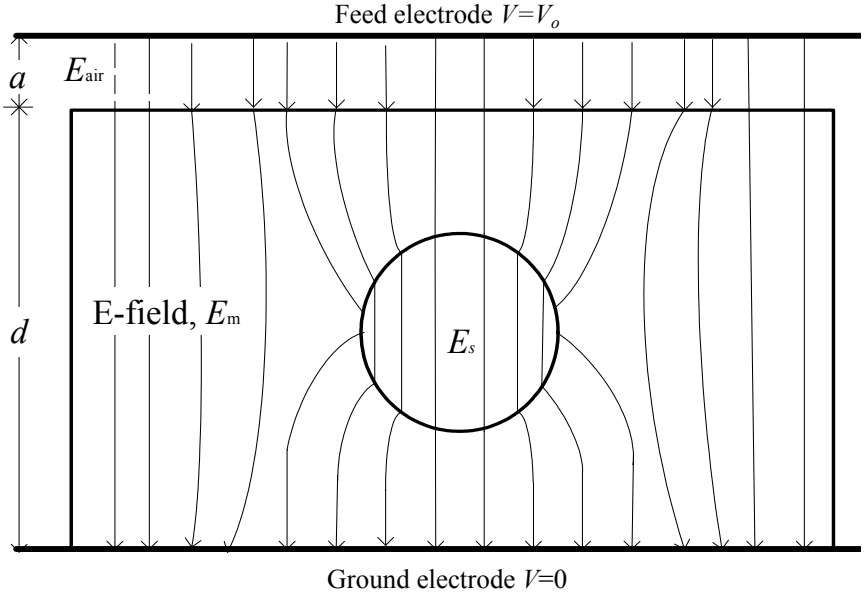

Fig. 3. E-field pattern in between RF electrodes and spherical object

2.4.3. Cylinder

Electric field in a transversely placed cylinder in the parallel plate RF system is given as (Roussy and Pearce, 1995):

$$\boldsymbol{E}_s = \frac{2\,\varepsilon_m^*}{\varepsilon_s^* + \varepsilon_m^*}\,\boldsymbol{E}_m \tag{19}$$

$$P = \frac{\pi f\, \varepsilon_o\, \varepsilon_s'' 4\left|\boldsymbol{E}_m\right|^2}{\left|\frac{(\varepsilon_s' - j\varepsilon_s'')}{(\varepsilon_m' - j\varepsilon_m'')} + 2\right|^2} \tag{20}$$

Similar to the slab and the sphere, a condition for maximum heating potential in the cylinder can be obtained by differentiating Eq. (20) with respect to the loss factor of the cylinder.

$$\varepsilon_s'' = \sqrt{\varepsilon_m''^{\,2} + (\varepsilon_m' + \varepsilon_s')^2} \tag{21}$$

2.5. Condition for matching heating potentials of water and fruit

Earlier we have emphasized on the importance of uniform heating of food materials. Therefore, it is imperative to find a means to overcome this problem. Ikediala et al.(2002) suggested immersion of fruits in a medium whose dielectric properties are properly matched with that of the fruit to overcome the uneven heating of fresh fruits in RF system. Hence it is important to find out appropriate combination of the dielectric properties of medium for a particular object. A condition for equal heating potentials of the medium and the object can be obtained by equating the power densities of the medium and the object. For simplification, it is assumed that heat capacity of both the medium and the object is same.

From Eqs. (15 & 19) a general equation for electric field can be written as:

$$\boldsymbol{E}_s = \frac{C\,\varepsilon_m^*}{\varepsilon_s^* + B\,\varepsilon_m^*}\,\boldsymbol{E}_m \tag{22}$$

where coefficient 'C' is 3 for sphere, 2 for cylinder, and '*B*' is 2 for sphere, 1 for cylinder.

Power densities in the object and surrounded medium are expressed as:

$$P_s = \frac{\pi f \varepsilon_o \varepsilon_s^{''} C^2 \left|\boldsymbol{E}_m\right|}{\left|\frac{(\varepsilon_s^{'} - j\varepsilon_s^{''})}{(\varepsilon_m^{'} - j\varepsilon_m^{''})} + B\right|^2} = P_m = \pi f \varepsilon_o \varepsilon_m^{''} \left|\boldsymbol{E}_m\right| \tag{23}$$

$$C^2 \frac{\varepsilon_s^{''}}{\varepsilon_m^{''}} = \left(\frac{\varepsilon_s^{'}\varepsilon_m^{'} + \varepsilon_s^{''}\varepsilon_m^{''}}{\varepsilon_m^{'2} + \varepsilon_m^{''2}} + B\right)^2 + \left(\frac{\varepsilon_s^{'}\varepsilon_m^{''} - \varepsilon_s^{''}\varepsilon_m^{'}}{\varepsilon_m^{'2} + \varepsilon_m^{''2}}\right)^2 \tag{24}$$

$$\frac{\varepsilon_s^{''}}{\varepsilon_m^{''}} C^2 \left(\varepsilon_m^{'2} + \varepsilon_m^{''2}\right)^2 = \left(\varepsilon_s^{'}\varepsilon_m^{'} + \varepsilon_s^{''}\varepsilon_m^{''} + B(\varepsilon_m^{'2} + \varepsilon_m^{''2})\right)^2 + \left(\varepsilon_s^{'}\varepsilon_m^{''} - \varepsilon_s^{''}\varepsilon_m^{'}\right)^2 \tag{25}$$

Eq. (25) was solved for various loss factor of medium ($\varepsilon_m^{''}$) using MATLAB 7.0 (Mathworks Inc., Nattick, MA) 'solve' function. This equation is of 5th order and out of five roots, four roots are imaginary and only one root is real. The real root gives the relationship between dielectric properties of the systems for uniform heating.

2.6. Computer simulation

Analytical solutions of Laplace equation are only available for regular shaped homogenous objects. When objects and electrodes are of finite length and width, the assumption of uniform field between the RF electrodes may no longer remain valid. To take these effects into account and solving for arbitrary object geometry, numerical solution techniques are sought. Many researchers have used finite element elements method based software to solve Laplace equation. We used commercial software FEMLAB 3.2 (Comsol, Multi-Physics, Los Angeles, CA) to model a one quarter of RF system as shown in Fig. 4 because the object and RF plates are symmetric. The upper electrode was drawn as an embedded part in the 3-D geometry to avoid large numbers of mesh elements for the upper electrode.

Since the main purpose here is to develop a theoretical understanding of the distribution of power dissipation in the objects as affected by size, shape, surrounding medium hence heat

transfer was not incorporated into the simulation model. In Chapter 7, we have included the heat transfer module in the simulation to predicate transient temperature profile.

2.7. Boundary conditions

In this study we simulated heating potential inside the objects for two scenarios. In the first scenario, we assumed no fringing field at the edges. The calculation domain was restricted to the medium as shown in Fig. 4A so that simulation conditions were consistent with assumptions made in the analytical solutions. This facilitated the simulation of an infinite large length and width of electrodes assuming a constant voltage distribution over the entire electrodes. Electric insulation boundary condition was applied on the sides and symmetric faces of the domain. In the second scenario, the calculation domain was extended to the shielding walls of the RF system (Fig. 4B). The metallic enclosure confines the electromagnetic field inside the RF machine. An electrically shielding boundary condition was applied to the metallic enclosure walls such that $\mathbf{n}\cdot(\sigma\nabla V) = 0$; where $\mathbf{n}$ is the unit vector normal to the surface, σ is the electrical conductivity, and V is the electric potential at the insulating surface. In both cases, source generated 27.12 MHz electric power was fed to the upper electrode (1050 mm × 805 mm) at an electric potential of $V = 9500$ V. The bottom of the enclosure served as an electrical ground return ($V = 0$). FEM Mesh consisted of Lagrange tetrahedral quadratic elements. Accuracy of the numerical solution depends on mesh size; therefore simulations were solved recursively for decreasing mesh element size to ascertain that solutions are converging with mesh refinement. In one-quarter of geometry, 32650 mesh elements were found to be optimum considering the accuracy and simulation time. All computer simulations were performed on a Dell 670 with 2 each Dual-Core, 2.80GHz XEON processors Running Windows XP 64 bit operating system.

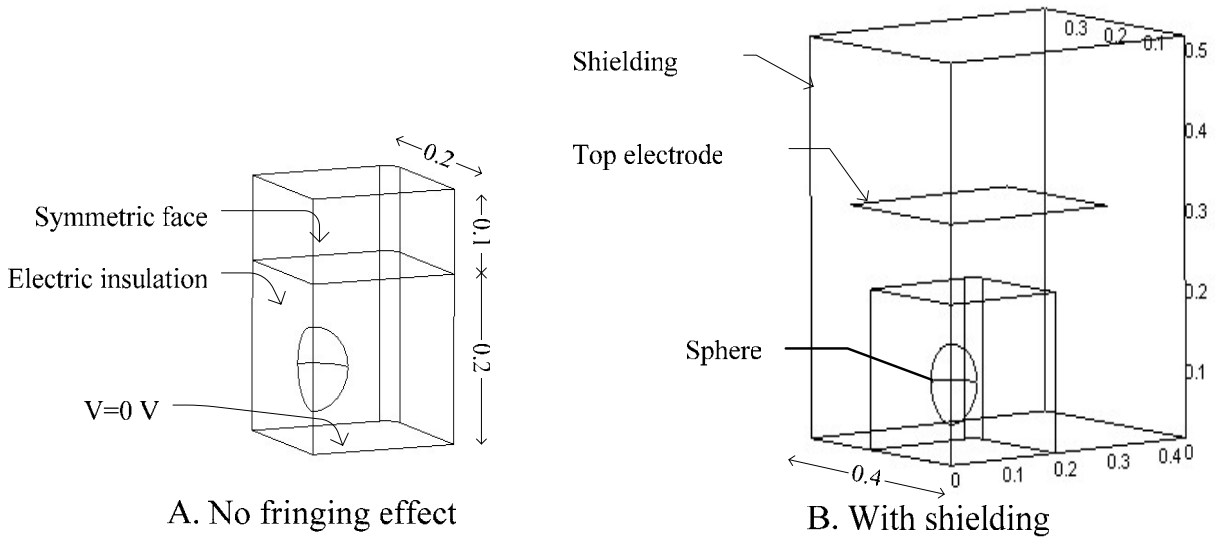

Fig. 4. Schematic diagram of 1/4th geometry of RF heating system showing boundary conditions (Dimensions are in meter).

3. Results and Discussions

Dielectrics properties of solid object (ε_s^* = 84 – j 220) representing the typical fresh fruits (Wang et al., 2003) were selected to study the effect of geometry on heating potential distribution over the cross section of the object. Ikediala et al. (2002) suggested that fruits immersion in saline water helps in improvement in heating uniformity of the fruits. Therefore water (ε_m^* =78 – j 20, at 20°C) was selected as a medium for immersion of fruits. Simulated and analytical solution of the heating potential in the slab, sphere and cylinder are discussed in the following sections.

3.1. Maximum heating potential

It is obvious from Eq. (9) that power density inside a lossy slab is a function of dielectric properties of both medium (air) and slab as well as relative thickness of the slab and air layer between electrodes. First we compared the analytical and the simulated heating potentials of 200

mm thick water slab sandwiched in 300 mm air gap between RF electrodes (Fig. 5). Assuming infinite length and width of slab and electrodes, the simulated power density of the slab matched well with the analytical solutions at the centre of the slab. However, if the finite length of electrode and slab and presence of the shielding walls are considered in the simulation, power density at geometry center of the slab was 27 % more than that of analytically calculated values. Moreover, the simulated power densities at edges were many fold of that center of the slab. It implies that the fringing field was prominent for the finite length and width of the slab and increases the power dissipation at the edges and corners (Roussy and Pearce, 1995).

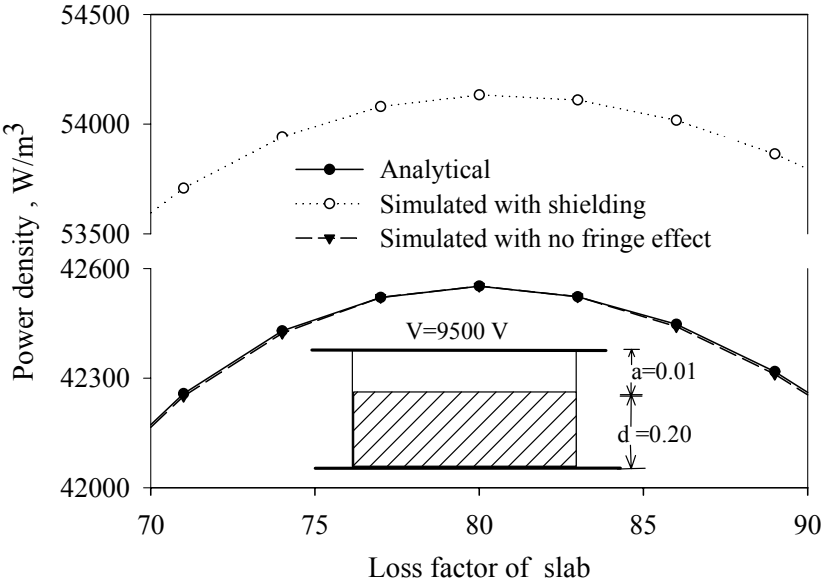

Fig. 5. Analytical and simulated power density at centre of 0.2 m thick water slab ($\varepsilon_s^{'}$ =78) sandwiched between two electrodes spaced at 0.3 m apart

Fig. 5 also shows that purposeful increase in the loss factor of the slab would not increase the power density infinitely, rather it reached a broad maximum when the loss factor of the slab was 80, which was equal to sum of dielectric constant of the slab (78) and ratio of slab thickness to air gap (2) according to Eq. (10).

Analytical solution of sphere power density (Eq. 12) suggests that it is independent of the size of the spherical object but computer simulation shows the contrary (Fig. 6). The simulated power density profile over the cross section of 0.02 and 0.04 m dia. sphere was uniform. But on a cross section of the 0.08 m sphere power density became non-uniform. It is implicit that the increasing size brought the sphere to the proximity of the electrode and left a smaller space for setting of uniform electric field in the medium. In practical applications such as RF heating of fresh spherical large fruit (apples and oranges), uniform heating may not be achieved even if the fruit are hypothetically hanging in the air between two electrodes. It is evident that analytical solutions are valid for very small sized spheres or when the air gap is many times larger than the sphere size. For a large size sphere in a fixed electrode gap, numerical methods should be employed for heating potential calculations.

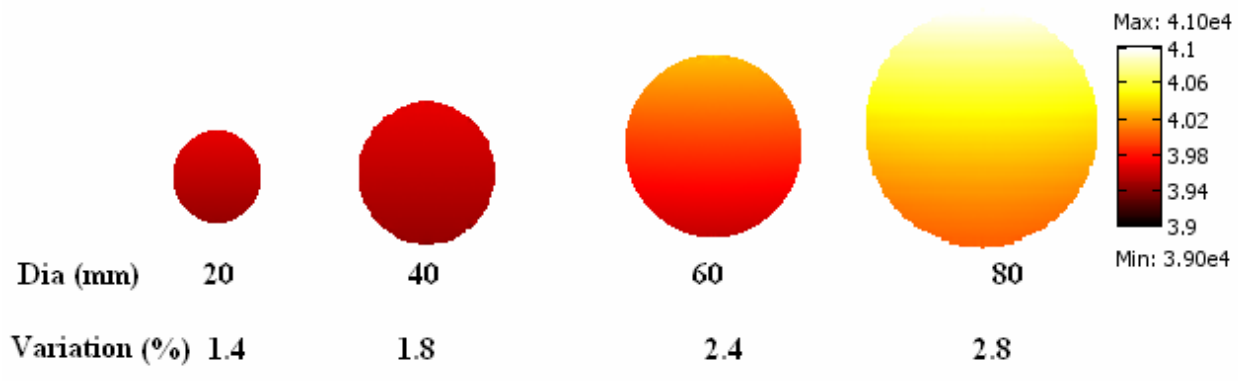

Fig. 6. Simulated effect of sphere size on distribution of power density (W m^{-3}) over the cross section. The sphere (84 – j 86) kept in middle of 0.3 m air gap between RF electrodes.

As per Eq. (17) maximum power density in sphere ($\varepsilon_s^{'}$ = 84) surrounded by air should occur when the loss factor of the sphere is 86, whereas in the case of surrounding medium water (ε_m^* =78 – j 20) heating should peak at 243 (Figures 7 and 8). A similar trend was observed for the 0.02 m dia sphere in computer simulation. However agreed well with the analytical solutions

with deviations of 0.1 – 0.14 % from the analytical solutions. Interestingly, the effect of shielding is not noticeable (Fig. 7).

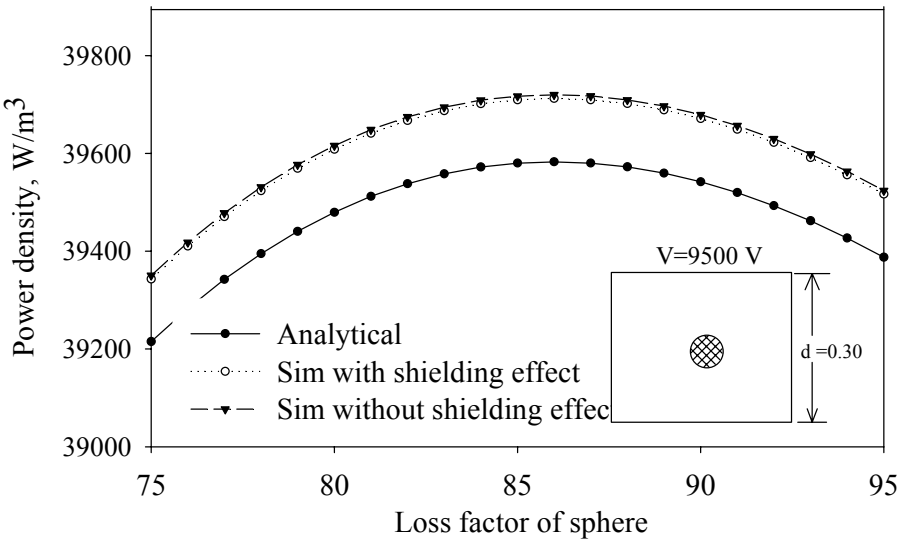

Fig. 7. Analytical and simulated power density at the centre of 0.02 m dia. sphere ($\varepsilon_s^{'}$ = 84) placed in middle of RF parallel plates separated by 0.3 m air gap.

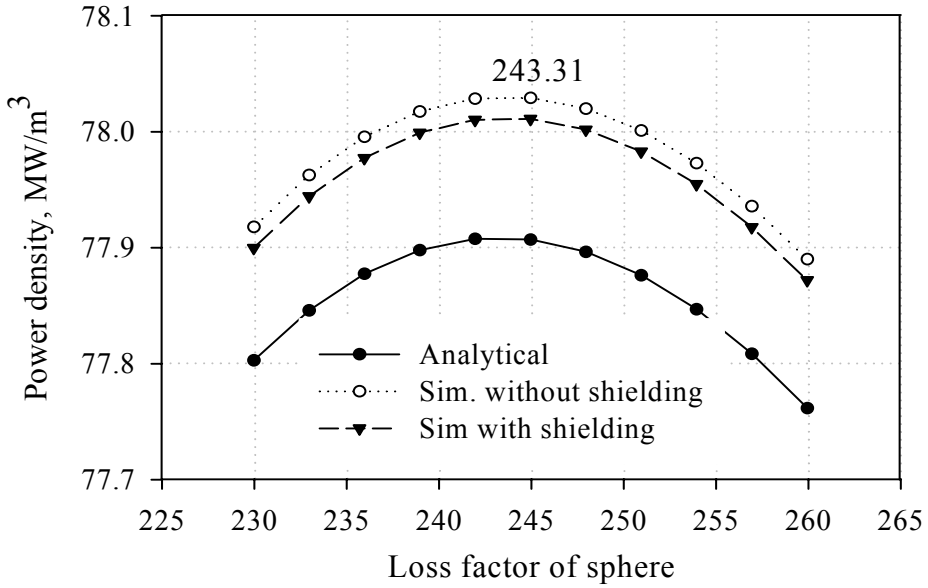

Fig. 8. Analytical and simulated power density in sphere ($\varepsilon_s^{'}$ = 84) immersed in water

Hypothetically, if the space between electrodes is filled with water, then simulation and analytical solutions were agreed well (Fig 8). However, in the case of the sphere immersed in water and air gap between water and upper electrodes as shown in Fig (9), an air gap above the water slab established fringing fields at the edges of the water slab and resulted in very high power density (>73 %) in sphere in comparison with analytical solutions (Fig. 9). Non-uniform and high power density in the sphere is also attributed to the fact that the sphere is close to ground electrode. However, in the case of the sphere immersed in water, an air gap above the water slab established fringing fields at the edges of the water slab and resulted in very high power density in sphere in comparison with analytical solutions (Fig. 9).

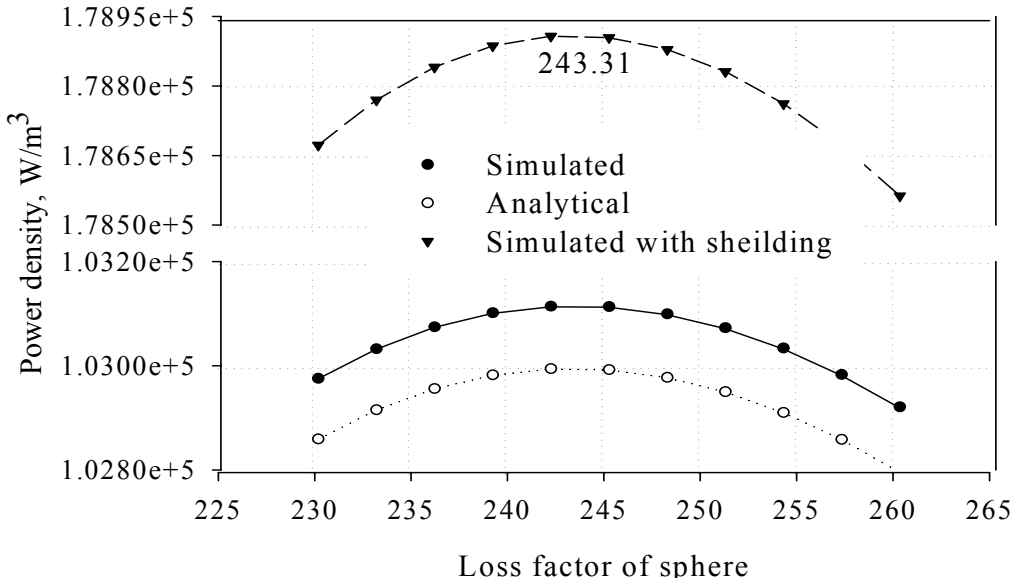

Fig. 9. Analytical and simulated power density at the centre of 0.02 m dia. sphere ($\varepsilon_s^{'}$ = 84) immersed in water (ε_m^* =78 – j 20) and placed between RF electrodes separated by 0.3 m gap.

3.2. Heating pattern in various geometrical objects

So far we discussed power dissipation in very small size spheres either immersed in water or air away from the electrodes. In practice, an object is often placed on a lower electrode, while

the upper electrode is adjusted vertically to tune maximum power in the load. Fig. 10 shows the simulated heating potential in a sphere, cylinder, and cube of the same size (80 mm) placed on the lower electrode with the upper electrode was 300 mm above the lower electrode. Under similar conditions, the maximum heating pontifical occurred at the top corners and edges of the cube, top edges of the cylinder but at the bottom of the sphere. Interestingly, minimum heating potential spot was always top central portion of all the object shapes. The problem of uneven heating can be further aggravated by the dielectric properties' dependency on temperature which may result in thermal runaway heating. Therefore, it is very important to devise means to eliminate these hot spots in the object. In the quest to deal with non-uniform RF heating of spherical objects, Ikediala et al. (2002) suggested a saline water immersion of the object in lossy medium, whose dielectric properties matched with that of the object. Saline immersion techniques worked for small fruit such as cherries but for large fruits it failed to provide uniform heating. The failure was attributed to the fact that the bottom of large fruits tended to come close to the ground electrode. Birla et al. (2004) suggested that moving and rotation of spherical objects in the immersed state eliminated the effect of proximity. However, matching the medium dielectric properties with that of the object is essential to minimize differential heating between the object and the medium.

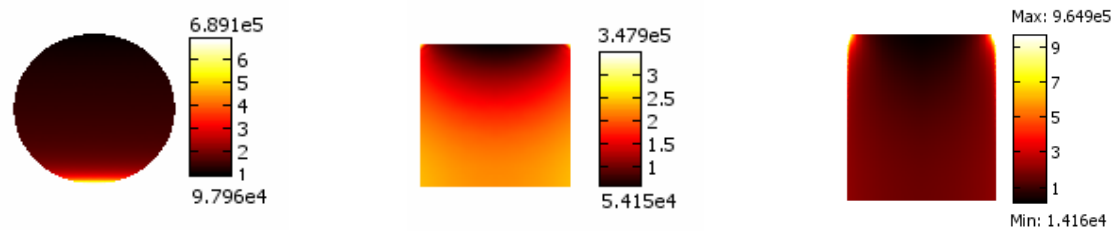

Sphere(Φ 80 mm) Cylinder (Φ 80 mm×80mm) Cube (80 mm×80mm ×80mm)

Fig. 10. Simulated power density (W m^{-3}) distribution in sphere, cylinder and cube made of material (84–j86) placed in 300 mm RF electrodes

3.3. Condition for matching heating potentials of medium and object

Power density in a sphere was simulated for various values of water loss factor. Increasing the water loss factor reduced the power density in the sphere steadily, and at a particular point the power densities in sphere and the medium became equal (Fig. 11). The condition was obtained graphically by locating this point on power density curves of the medium and sphere as shown in Fig. 11. The graphical solutions that use simulation results without shielding agreed with the analytical solution for the condition. For example, a 0.02 m dia. sphere (76 – j 120) immersed in water would heat evenly when the loss factor of the water is 121.6 and similarly for the sphere having dielectric properties 84 – j 220, the loss factor of water should be 216.8 (Fig. 11). Moreover, if fringing effect is taken into account, the estimated water loss factor is much lower (~150) than that of the analytically calculated (ε'' = 216.8) for uniform heating of sphere (84 – j 220) as depicted in Fig.12. Hence it is highly desirable to simulate heating pattern using temperature dependent dielectric and thermal properties of the objects and medium to precisely determine the combination of dielectric properties.

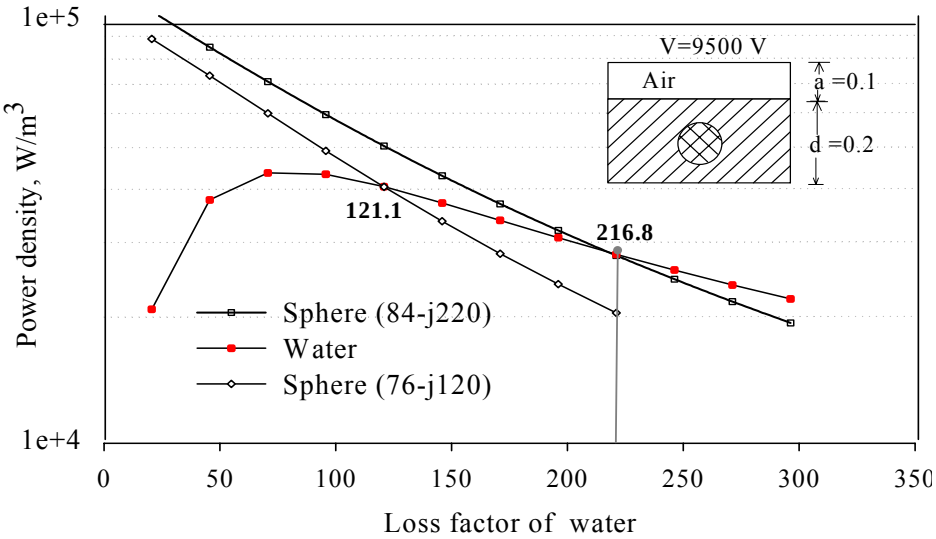

Fig. 11. Simulated effect of loss factor of water on heating potential of sphere (Φ 0.02 m)

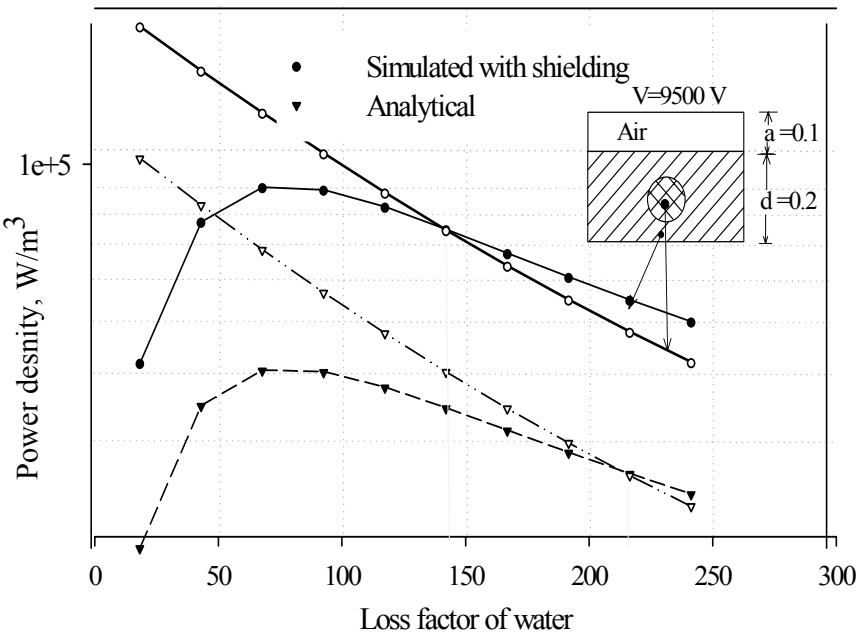

Fig. 12. Analytical and simulated heating potential in 20 mm dia. sphere (ε*=84 – j 220) and water

4. Conclusions

In this study we have developed an understanding of heating behavior of several geometrical objects, especially spheres in parallel plates RF system. The simulated heating potential was in close agreement with the analytical solutions when simulation was performed without fringing fields. It has been corroborated that the deliberate increase in loss factor of an object does not increase proportionally heating potential; rather it reaches a broad maximum when the loss factor is close to the value of the dielectric constant. Further increasing loss factor decreases the heating potential. The analytical solutions are valid for homogenous material RF heated in a relatively large electrodes gap in which the effect of the fringing effect is negligible. To simulate the actual heating pattern in arbitrarily-shaped objects, it is highly recommended that numerical methods should be used to account for temperature dependency of the dielectric properties.

References

Birla, S.L., Wang, S., Tang, J., Hallman, G., 2004. Improving heating uniformity of fresh fruit in radio frequency treatments for pest control. Postharvest Biol. Technol. 33, 205–217.

Brown, G.H., Hoyler, C.N., Bierwirth, R.A., 1947. Theory and application of radio-frequency heating. Van Nostrand Co. Inc., New York.

Burfoot, D., Railton, C.J., Foster, A.M., Reavell, S.R., 1996. Modeling the pasteurization of prepared meals with microwaves at 896 MHz. J. Food Eng. 30, 117–133.

Cable, J.W., 1954. Induction and dielectric heating. Reinhold, New York.

Chan, T.V.C.T., Tang, J., Younce, F., 2004. 3-Dienstional numerical modeling of an industrial Radio frequency heating systems using Finite elements. J. Microwave Power EE. 39, 87–105.

Choi, C.T.M., Konrad, A., 1991. Finite-Element Modeling of the RF Heating Process. IEEE Trans. Magn. 27, 4227–4230.

Evans, S., 2000. Electromagnetic rewarming: The effect of CPA concentration and radio source frequency on uniformity and efficiency of heating. Cryobiology 40, 126–138.

FCC, 1988. Federal Communication Commission, www.fcc.gov.

Fleischman, G.J., 1999. Predicting temperature range in food slabs undergoing short-term/high-power microwave heating. J. Food Eng. 40, 81–88.

Ikediala, J.N., Hansen, J.D., Tang, J., Drake, S.R., Wang, S., 2002. Development of a saline water immersion technique with RF energy as a postharvest treatment against coding moth in cherries. Postharvest Biol. Technol. 24, 25–37.

Jelinek, R.V., Linford, H.B., McMohan, E.K., Schutz, P.W., 1949. Dielectric heating of granular materials. Ind. Eng. Chem. 41, 852–856.

Marshall, M.G., Metaxas, A.C., 1998. Modeling of the radio frequency electric field strength developed during the RF assisted heat pump drying of particulates. J. Microwave Power EE. 33, 167–177.

Marshall, M.G., Metaxas, A.C., 1999. Radio frequency assisted heat pump drying of crushed brick. Appl. Therm. Eng. 19, 375–388.

Metaxas, A.C., 1996. Foundations of electoheat – A unified approach. John Wiley & Sons, New York.

Nelson, S.O., 1996. Review and assessment of radio-frequency and microwave energy for stored-grain insect control. Trans. ASAE 39, 1475–1484.

Neophytou, R.I., Metaxas, A.C., 1996. Computer simulation of a radio frequency industrial system. J. Microwave Power EE. 31, 251–259.

Neophytou, R.I., Metaxas, A.C., 1997. Characterisation of radio frequency heating systems in industry using a network analyser. IEE Proceedings-Science Measurement and Technology 144, 215–222.

Roussy, G., Pearce, J.A., 1995. Foundations and industrial applications of microwave and radio frequency fields: physical and chemical processes. John Wiley & Sons, New York, 475 pp.

Stratton, J.A., 1941. Electromagnetic Theory. McGraw-Hill, New York.

Tang, J., Ikediala, J.N., Wang, S., Hansen, J.D., Cavalieri, R.P., 2000. High-temperature-short-time thermal quarantine methods. Postharvest Biol. Technol. 21, 129–145.

Veen, M.E.v.d., Goot, A.J.v.d., Vriezinga, C.A., Meester, J.W.G.d., Boom, R.M., 2004. On the potential of uneven heating in heterogeneous food media with dielectric heating. J. Food Eng. 63, 403–412.

Wang, S., Ikediala, J.N., Tang, J., Hansen, J.D., Mitcham, E., Mao, R., Swanson, B., 2001. Radio frequency treatments to control codling moth in in-shell walnuts. Postharvest Biol. Technol. 22, 29–38.

Wang, S., Tang, J., Cavalieri, R.P., Davis, D.C., 2003. Differential heating of insects in dried nuts and fruits associated with radio frequency and microwave treatments. Trans. ASAE 46, 1175–1182.

Wig, T., 2000. Sterilization and Pasteurization of foods using radio frequency heating. PhD Thesis, Biological Systems Engineering, Washington State University.

C H A P T E R 3

IMPROVING HEATING UNIFORMITY OF FRESH FRUIT IN RADIO FREQUENCY TREATMENTS

S.L. Birla[1], S. Wang[1], J. Tang[1], G. Hallman[2]
[1]Washington State University,
[2] USADA-ARS Crop quality and Research Laboratory, TX 78596, USA
Published in Postharvest Biology and Technology, 33(2), 205–217, 2004

Abstract

Non-uniform heating of fresh fruit caused by variations in radio frequency (RF) fields is a major obstacle in developing postharvest insect control treatments based on RF energy. A fruit mover was developed to evaluate possibilities to improve RF heating uniformity of large fruit, such as oranges and apples, in a 12 kW batch type RF system. This fruit mover provided a means to rotate and move fruit in water when subjected to RF heating. Parameters for moving and rotating of fruit in the mover were selected based on consideration of vortex formation, foaming, damage to the fruit, and volume occupied by the fruit in water. RF heating uniformity of oranges and apples in the mover was assessed using an infra-red imaging technique and direct temperature measurement with fiber-optic sensors and thermocouples. The results showed that, with rotation and movement of fruit, temperature uniformity in oranges and apples was significantly improved with less than 2.8°C and 3.1°C standard deviations, respectively, after an average temperature rise of about 30°C in 7.8 min. The fruit mover can be used to develop a treatment protocol for disinfesting fresh fruit and to simulate industrial scale and continuous treatment systems.

Keywords: Apple; Fruit mover; Orange; Radio frequency; Temperature uniformity

1. Introduction

About 67% of citrus produced in the world is marketed as fresh, with major citrus-producing countries also acting as major fresh fruit exporters (USDA, 2001). The United States accounts for 53% world production of grapefruits (*Citrus paradise Macfad*.) and oranges (*Citrus sinensis L. Osbeck*). The Mexican (*Anastrepha ludens* Loew) and Carribbean fruit flies (*Anastrepha suspensa* Loew) are quarantine pests of citrus fruit as they threaten the entire fresh produce industry because of their broad host ranges (Calkins, 1993). In the U.S.A. citrus shipments destined for states such as California, Arizona, and Florida, as well as for export markets including Japan and other Pacific Rim countries, require methyl bromide fumigation to meet import quarantine security requirements. However, methyl bromide fumigation often damages the citrus. It is also an ozone depleting chemical and will be restricted or eliminated for most applications by the year 2005 (USEPA, 1998) according to the Montreal Protocol (UNEP, 1992). Thus, development of alternative physical treatments for disinfestation of fresh fruits is urgently needed.

Several alternative methods have been investigated, including ionizing radiation (Burditt, 1982), cold storage (Schiffman-Nadel et al., 1972; 1975), conventional hot air and water heating (Sharp et al., 1991; Shellie et al., 1992; Shellie and Mangan, 1993; 1995; 1998), and radio frequency (RF) treatments (Hallman and Sharp, 1994; Tang et al., 2000; Ikediala et al., 2002; Wang et al., 2001a; 2002) for different fruits and agricultural commodities. Use of irradiation has raised public concern over safety of the technology and over the effect on fruit (Hatton et al., 1984). It also requires significant capital investments for special treatment facilities. Cold storage requires lengthy treatment times (~16 Days at 0 to 2°C) for disinfestation, causes chilling injury due to the narrow safety margin for fruit quality. Heat treatments can be an effective control

against quarantined pests of certain commodities (Hansen, 1992). A common difficulty with hot air or water heating methods is the slow rate of heat transfer resulting in hours of treatment time, especially for large fruits (Wang et al., 2001b). For example, Soderstrom et al. (1996) showed that exposure to 39°C in air would take about 730 h to obtain Probit 9 quarantine security (99.996832% mortality). Prolonged heating may be detrimental to the quality of treated products, causing peel browning, pitting, poor color development and abnormal softening (Lurie, 1998), and may not be practical for industrial applications. New treatments are needed to replace ones that have been lost, are threatened, or have problems. The desire to eliminate these problems and achieve fast and effective thermal processing has resulted in the increased interest in using RF energy to control insect pests in commodities.

Radio frequency (RF) heating has been studied as a rapid disinfestation treatment (Headlee and Burdette, 1929; Frings, 1952; Nelson and Payne, 1982), with one of the chief problems being lack of uniform heating (Tang et al., 2000). Recently, treatment protocols have been developed using RF treatments that can effectively control codling moth (Wang et al., 2001a) and navel orangeworm (Wang et al., 2002) in in-shell walnuts without causing quality losses. These studies focus on dry nuts that have higher heat tolerance than fresh fruit. Fresh fruit suffers thermal damage (burn) at the points of contact with the container or with other fruits when heated with RF energy in air. This is the result of over-heating caused by a concentration of electric fields around the contact areas because the contact surfaces have the least resistance to RF energy. To avoid fruit-to-fruit contact during RF heating and to make the load more homogeneous to RF fields, a medium that has similar dielectric properties to fruit (Wang et al., 2003) can be selected to fill the void space between the fruit. Dielectric properties influence reflection of electromagnetic waves at interfaces and the attenuation of the wave energy within

materials. That in turn determines the amount of energy absorbed and converted into heat. Ikediala et al. (2002) used water as a medium to improve RF heating uniformity in cherries without their movement in the RF field. For larger fruit, such as citrus and apples, heating uniformity is impaired by variations of RF field along the length and width of the exposed area of the container as well as along the height of the water column in the container. Large temperature variations among and within fresh fruit can both reduce the effectiveness of a treatment and cause severe thermal damage to the fruit. Immersing fruit in a medium can solve the problem of contact surface overheating, but will not overcome non-uniform heating caused by varying RF fields in the large fruit and the medium. It is hypothesised that constant movement of fruit in a RF field will improve the heating uniformity of large fruit. Three-dimensional rotation and movement of fruit in a dielectrically matched medium may provide an opportunity for different parts of a fruit to absorb equal amounts of energy in an uneven RF field. The objectives of this study were (1) to develop a laboratory scale fruit mover for assessing the improvement in RF heating uniformity due to movement and spinning of fruit, and (2) to compare the RF heating uniformity of oranges with conventional heating methods such as hot air and hot water.

2. Materials and Methods

2.1 Design considerations for a fruit mover for RF heating

Non-uniform heating of fruit may be caused by non-uniform RF fields and non-uniform load between the two electrodes in a RF system. Moving and rotating fruit and filling the void space with a medium that has similar dielectric properties (Ikediala et al., 2002; Wang et al., 2003) to that of fruit may improve heating uniformity. Fresh fruit in general float in water, which

makes it easy to move and rotate it. Since dielectric properties of fresh fruit are much higher, i.e. heat at faster rate in RF field, than those of tap water, fruit should be immersed in a water solution with properly adjusted ionic conductivity to match that of the fruit to avoid surface burning and core overheating (Ikediala et al., 2002). Fruit should rotate on its axes to reduce the effect of non-uniform RF field throughout the container. In a fruit mover, fruit should not be in constant contact with other fruit or with the walls of container because contact spots concentrate RF energy causing overheating. A fruit mover was designed for RF heating of fresh fruit in a 12 kW batch type RF heating system (Strayfield Fastran with E-200, Strayfield International Limited, Wokingham, UK).

An appropriate container size was determined based on a desired heating rate when the container was filled with tap water. Assuming negligible energy loss to the surroundings, the rise in the water temperature in the fruit mover as a result of RF heating can be expressed as:

$$\rho V C_p \frac{\Delta T}{\Delta t} = \mathrm{P}\,\eta \tag{1}$$

where η is the power conversion efficiency (%) which was about 60% based on our preliminary tests, C_p is the specific heat of water at room temperature (4186 J.kg^{-1}.°C^{-1}), ρ is the density of water (1000 kg.m^{-3}), V is the volume of the fruit mover (m^3), P is displayed power absorbed by water in the RF machine (W), and ΔT is the water temperature rise (°C) in Δt duration (s). For a 12 kW RF system the maximum coupled power would be 7.2 kW. Based on Eq. (1) and assuming an 8°C/min heating rate, the net volume for water in the fruit mover should be:

$$V_{max} = 7.2/(1000\times4.186\times8/60) = 0.0129\ \mathrm{m}^3 \tag{2}$$

2.2. Description of the fruit mover

The fruit mover consisted of a container (425 × 425 × 127 mm^3), water jets, a spool, and a transparent top plate (Fig. 1). The container walls and the bottom were made of 10 mm thick polypropylene. Twelve Teflon water spray nozzles (spiral full cone angle 60°, 9 l/min discharge, 12.5 mm diameter) were mounted on the periphery of the container to rotate fruit on their axes and in a circular path. The nozzles were set at fixed angle of 35° from the wall of the container. To avoid inter-locking of fruit at the corners of the container, a polypropylene square skirt with filleted corners was placed in the container. The free-rotating polypropylene spool (75 mm in diameter and 60 mm in height) was placed in the center of the container to keep the fruit away from the center and to facilitate the rotation of the fruit in a specific fixed path along the periphery of the container. A centrifugal pump (1 hp, single phase, TEEL Model # 2PC27, Dayton Electrical Mfg. Co., Niles, IL) circulated water at 40–55 *l*/min through a suction pipe connected to one wall of the container and water nozzles. The suction pipe was placed under a perforated (8 mm diameter holes at spacing of 50 mm × 50 mm) polypropylene plate 20 mm above the bottom to maintain uniform suction pressure, and the water nozzles were mounted 2.5 cm below the water surface. An 8 mm thick transparent acrylic sheet was placed on the top of the water to keep the fruit immersed. A pair of baffles (half-circle rods) was glued to the bottom surface of the acrylic top plate to ensure that every fruit spun on its axes after completing about half of the circular motion in the container. To monitor the water temperature during RF heating, a thermocouple (Type-T, 0.8 mm diameter and 0.8 s response time, Omega Engineering Ltd, CT) was inserted in the water circulation line. Water flow rate was monitored and controlled with a digital flow meter (Flow Transmitter 3-8503, Signet-Scientific, El Monte, CA)(Fig. 2).

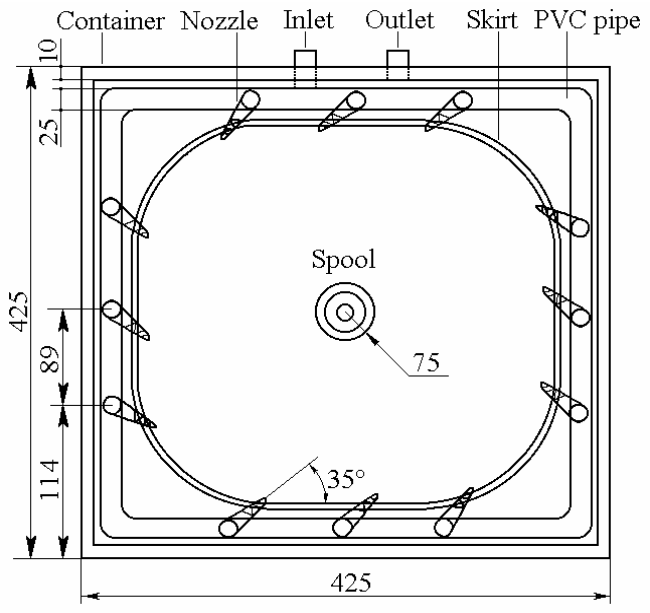

Fig. 1. Schematic diagram of top view of the fruit mover (all dimensions are in mm)

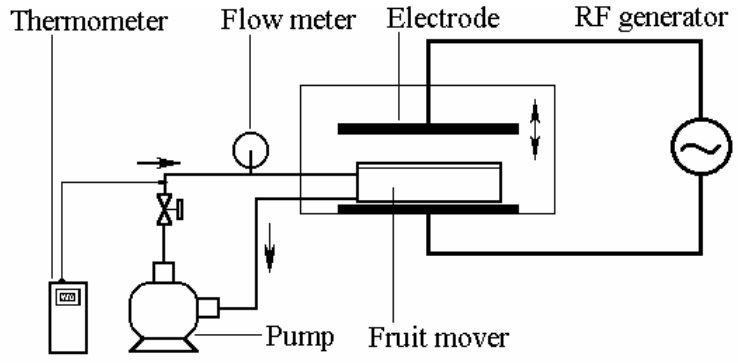

Fig. 2. Schematic diagram of the experimental set-up of RF heating system

2.3. Experimental procedures

2.3.1. Determination of operating parameters for fruit mover

The tap water without fruit in the fruit mover was heated first in the RF system to determine the temperature variation. Water temperatures at five locations (four in the corners and one in the center) 1 cm above the perforated plate and 1 cm below water surface were measured by thermocouples immediately after RF heating. A comparison of temperature uniformity in the

fruit mover was made with and without water circulation. The experiments were repeated three times.

'Naval' oranges (weight 255±20g, density 957 kg m^{-3}) and 'Fuji' apples (weight 245±15g, density 915 kg m^{-3}) were purchased from a local market and stored at 4°C. fruit was taken out of cold storage and allowed to equilibrate at room temperature (20°C) for 12 hrs. Fruit was randomly selected and each assigned an identification number. Experiments were carried out to determine the correct water circulation rates and fruit batch sizes. Factors important to the selection of correct batch size and water circulation rate were maximum peripheral velocity, axial rotational speed without formation of vortex, and bruising of fruit. The peripheral velocity is defined as linear velocity of the center of fruit moving along the periphery of the container. The axial rotational speed is the number of rotations a fruit made about its own axis per minute while moving along the container periphery. Too fast movement in the container might cause bruising whereas too slow movement might be inadequate for uniform heating. Experiments were carried out at water circulation rates of 45, 50, and 55 l/min, and each batch contained 7, 8, and 9 fruits.

2.3.2. Evaluation of RF heating uniformity

A pilot-scale RF system was used to heat oranges and apples in the fruit mover. Eight oranges or seven apples were placed in the fruit mover and tap water was poured in the container to completely submerge the fruit and the top plate. Based on our preliminary studies, differential heating of apples and water was observed when apples were heated in tap water. Tap water with 0.02 % table salt was appropriate to match the dielectric properties of the water with that of the apple (Wang et al., 2003). The transparent top plate was fixed at 2 cm below the top edge of the container. The water circulation rate was maintained at 50 and 55 l/min for orange and apple,

respectively. The gap between the two electrodes (that determined the RF power output) was set to achieve a heating rate of about 5°C/min. RF heating was stopped when the water temperature reached 50°C. Temperature in each individual fruit was immediately measured by the thermocouple at six different locations as shown in Fig. 3.

In order to assess improvement in temperature uniformity due to movement and rotation of fruit, oranges and apples were also heated without water circulation (zero water circulation rate) in the RF system as a reference. All experiments were repeated three times. Statistical analysis of data was conducted using PROC GLM procedure of SAS software (SAS Institute, 1989, Cary, NC). The significant difference ($P \leq 0.05$) was separated by the mean values using least significant difference (LSD) and multi pairwise comparisons (Tukey method).

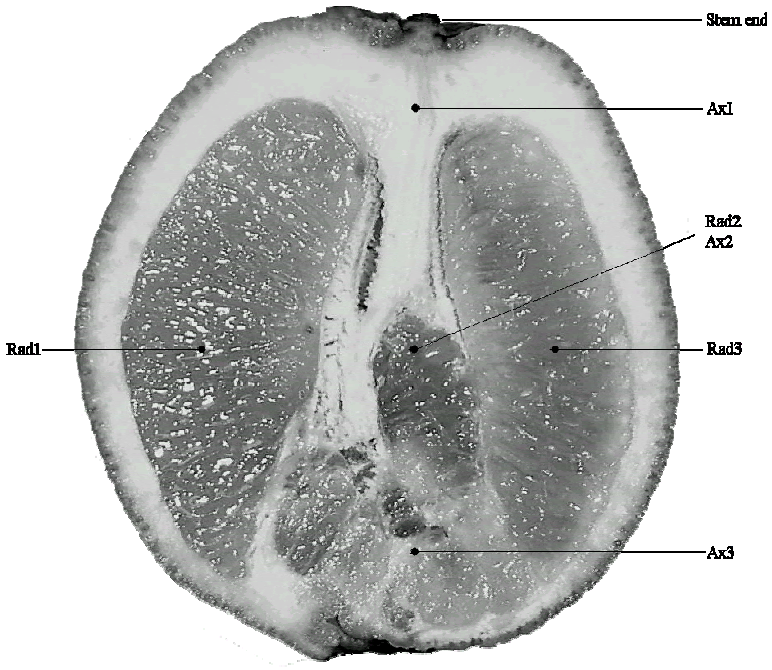

Fig. 3. Temperature measurement locations in an orange

2.3.3. Comparison of RF heating of oranges with hot air/ water heating

RF heating of 9 cm diameter navel oranges (250±10 g weight) was compared with forced hot air and hot water heating of same size of oranges. In RF heating, seven navel oranges (at 19°C) were placed in the fruit mover filled with 20°C tap water. During RF heating, water circulation was reduced until movement of fruit stopped. This was done because the measurement of core temperature was impossible during RF heating of moving or rotating fruit. The core temperature of the orange was measured by a FISO fiber-optic sensor (UMI, FISO Technologies Inc., Saint-Foy, Quebec, Canada) inserted into an orange through a pinhole. RF heating was done for 5 and 10 min. The forced air heating of oranges was conducted in a tray drier (UOP8, Armfield Limited, UK) in which air was moved by a fan through a square duct (28 cm × 28 cm) that housed a group of electric heating coils. Air speed and temperature were maintained at 1 m s^{-1} and 53°C, respectively. The oranges were placed in the middle section of an air heating duct.The hot water heating of oranges was carried out in a water bath (model ZD, Grant, Cambridge, UK) in which water was circulated at 1 m s^{-1} and temperature maintained at 53°C. The core and subsurface (20 mm blow surface) temperatures of one orange were measured by two type-T thermocouples.

Data were recorded every 5 s by a data logger (DL2e, Delta-T Devices Ltd., Cambridge, UK). The temperature distribution inside fruit at different stages of heating was mapped with an infrared imaging camera (ThermaCAM^{TM} Researcher 2001, accuracy ±2°C, 5 picture recordings per seconds, FLIR Systems, Portland, OR). In the hot air and hot water heating trials, fruit samples were taken out after 10, 20, 30, and 40 min from a batch of oranges for temperature distribution mapping. The heated orange was immediately cut into halves and a thermal image

was recorded for one of the cut surface. The temperature distribution in RF heated oranges was mapped for 5 and 10 min heating.

3. Results and Analyses

3.1. Operating parameters for Fruit mover

Table 1 shows the effect of batch size and water circulation rate on rotational characteristics of the fruit. Increasing flow rates increased the axial rotational speed and the linear velocity. However, it was observed that increasing the water circulation rate also increased the tendency of formation of vortex and foaming. Increasing batch size of fruit reduced both the axial and the peripheral motion of the fruit and increased the tendency of inter-locking of fruit and eventual cessation of fruit movement.

Table 1. Effect of water circulation rate and batch size on the linear velocity, and axial and peripheral rotation speed of oranges and apples.

Fruit	Water circulation rate, l/min	Fruit rotation and linear velocity (in parenthesis) at batch size of					
		7		8		9	
		Peripheral rpm(ms^{-1})	Axial rpm	Peripheral rpm(ms^{-1})	Axial rpm	Peripheral rpm(ms^{-1})	Axial rpm
Orange	45	20(0.28)	26	16(0.23)	26	13(0.19)	18
	50	23(0.32)	32	21(0.30)	30	17(0.24)	24
	55	26(0.37)$^{\#}$	35	24(0.34)$^{\#}$	34	20(0.29)	26
Apple	45	12(0.12)	13	0*	0	0	0
	50	14(0.20)	19	10(0.14)	16	0	0
	55	17(0.24)	22	13(0.19)	17	10(0.14)	13

* *Zero indicates the cessation of rotation and* $^{\#}$ *indicates overflow and vortex forming*

It was observed that slow rotation increased the chance for the fruit to be in contact with the container walls and top plate for extended times that might cause hot spots on contact surfaces during RF heating. On the other hand, we observed that reduced batch size caused non-uniformly distributed load (varying fruit-to-fruit distance) inside the RF field, and this in turn increased the variability in heating rates of individual fruits. Eight naval oranges per batch (fruit volume was 12.5 % of total volume of fruit and water) in the container met both requirements of uniformly distributed RF load and three dimensional rotation of the fruit in the RF field (Table 1). High water circulation rate imparted kinetic energy to fruit and caused frequent fruit to fruit collision and striking of fruit to the periphery of the container, which might cause bruising of fruit. Optimum flow rate was 50 l/min for eight oranges (the water jet velocity was 9 m s^{-1} at the end of nozzle tip) without overflowing of water from the container edges. At this flow rate the linear velocity of fruit centre was 0.30 m s^{-1} in the mover. It was observed that axial rotation was higher than the peripheral rotation of oranges in the mover (Table 1). This is desirable in view of RF heating of a large spherical shaped commodity because every part of a large fruit needs to be exposed to RF field for uniform heating. The axial rotation decreased with increasing batch size because of less free space available for movement of fruit in the container.

Table 1 shows that apples moved and spun at a slower speed compared with oranges for the same batch size and water circulation rate. With nine apples in the container, interlocking was frequently observed even at high water circulation rates. Interlocking and cessation of axial rotation of fruit were observed with eight apples at the water circulation rate of 45 l/min. The rotational ability of fruit was hampered by non-spherical shape and low density of 'Fuji' apples even at higher circulation rates. Therefore, seven apples per batch (fruit volume was 11 % of total volume of fruit and water) was found to be appropriate to obtain desired rotational

characteristics. A water flow rate at 55 l/min (peripheral velocity of fruit was 0.24 m s^{-1}, and water jet velocity was 10 m s^{-1} at end of the nozzle tip) was found to be a suitable flow rate that avoided bruising and vortex forming and provided desired rotational characteristics. Without water circulation, the mean water temperature at the 10 locations was 45.7°C with a 9.5°C standard deviation. The temperatures at all the measured points at the top layer (1 cm below water surface) were significantly higher ($p<0.05$) than those at the bottom layer (1 cm above the perforated plate). The maximum differences among five locations were 3.4 and 2.7°C for top and bottom layers, respectively. With water circulation, the temperature uniformity was significantly improved as the mean water temperature at the 10 locations in the container was 49.7°C with only 0.4°C standard deviation, and there was no significant difference ($p>0.05$) found in temperatures between top and bottom layers.

3.2. Heating uniformity of naval oranges

Fig. 4 shows temperature variations in RF heating of eight oranges without (A) and with (B) water circulation. The average heating rate for oranges was approximately 5°C/min at the coupled RF power of 7.0 kW. Without water circulation, the mean temperature of an individual orange after RF heating varied from 48.7 to 60.2°C with the standard deviation in each fruit varying from 2.5 to 4.9°C (Fig. 4A). The mean temperature of eight fruit was 53.6°C with an overall 4.8°C standard deviation. The mean temperatures were significantly different ($p<0.05$) among different oranges. With water circulation, the mean temperature at different locations in an individual orange after RF heating varied from 49.2 to 52.8°C with the standard deviation varying from 0.3 to 2.8°C (Fig. 4B).

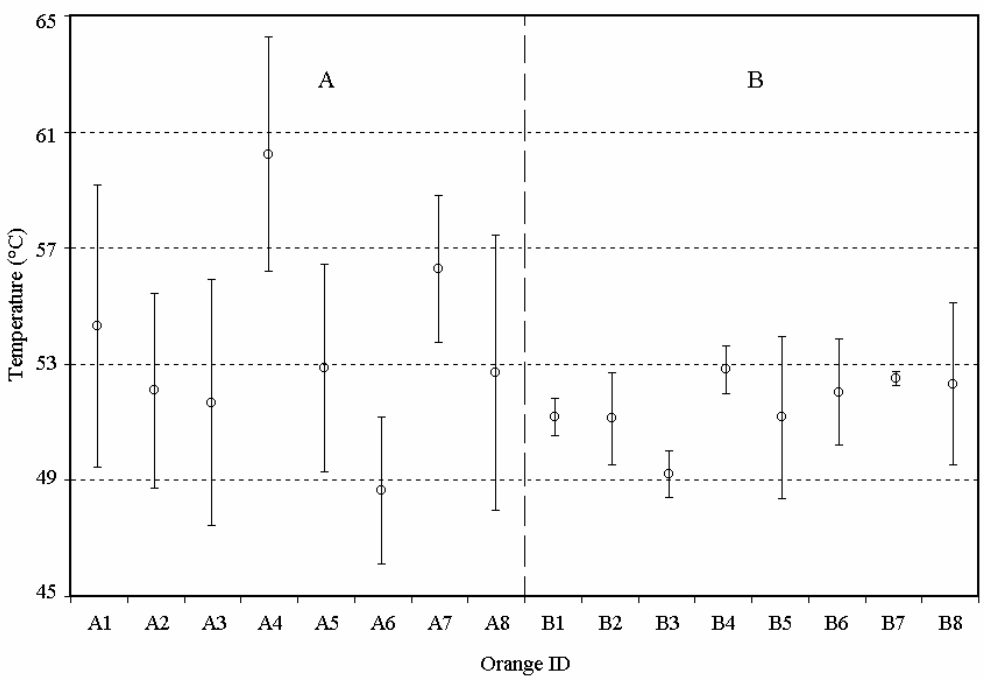

Fig. 4. Temperature variations (mean and standard deviation values over six locations) in eight oranges heated by RF for 5.5 min without (A) and with (B) water circulation from 20°C initial temperature of fruit

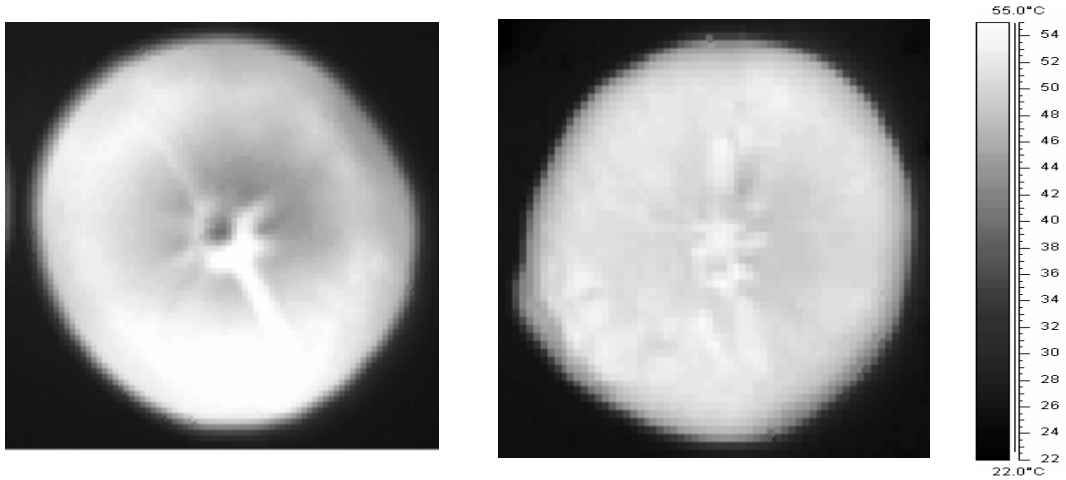

A). Without rotation B). With rotation

Fig. 5. Temperature distributions in oranges when subjected to RF heating for 5.5 min with and without rotation of oranges in the container (20^{o}C initial temperature)

The mean temperature among eight oranges was 51.6 °C with 2°C standard deviation and there was no significant difference in temperature ($p>0.05$) among oranges and within an orange. Therefore, with the proper movement and rotation, the variations of temperature among oranges and within individual fruits were significantly reduced. As shown in Fig. 4 with and without rotation of oranges during RF heating, the temperature variation was more prominent among oranges than within an orange. This variation might have been the result of natural variations in oranges such as different physical/chemical properties and internal structures. We have observed consistent hot spots on the naval end (Ax3 in Fig. 3) of an orange probably because of dense material at this end. The mean temperature of oranges was slightly higher than the temperature of water in the container probably because the dielectric loss factor of tap water was lower than that of oranges.

Fig. 5 shows temperature distribution in an orange as measured by an infra-red thermal imaging camera immediately after the oranges were subjected RF heating for 5.5 min. Without rotation, certain areas of the fruit were overheated (Fig 5A). Overheating was observed at the points where fruit surface was in contact with the top plate, which was placed above the fruit to keep them immersed in water. The non-uniform heating was eliminated by movement and rotation of oranges in RF field (Fig. 5B).

3.3. Heating uniformity of Fuji apples

Without water circulation, the mean temperature of individual apples varied from 54.4 to 70.0°C with the standard deviation varying from 1.0 to 9.6°C (Fig. 6A). The mean overall temperature of apples in a sample was 60.4°C with 4.3°C standard deviation and the mean temperatures of individual apples were significantly different ($p<0.05$). With water circulation, the mean temperature of the individual RF heated apple varied from 49.2 to 53.0°C with the

standard deviation varying from 0.6 to 3.1°C (Table 2, & Fig. 6B). The mean temperature over seven apples was 51.1°C with an overall 2.2°C standard deviation. There was no significant difference ($p>0.05$) in mean temperatures of apples except between apple #3 and 5 (Table 2). Similar to observations with oranges, rotation and movement of apples in RF field reduced temperature variation significantly among the fruit and within each individual fruit (Fig.6). Table 2 shows that the temperatures at stem side (Ax1) and bottom side of fruit (Ax3) were significantly ($p<<0.05$) high compared with other locations on an apple. The path along this axis was the shortest route for RF energy to pass. The consistent hot spots on these two ends suggests that the shape of a fruit highly influences the temperature uniformity within a fruit.

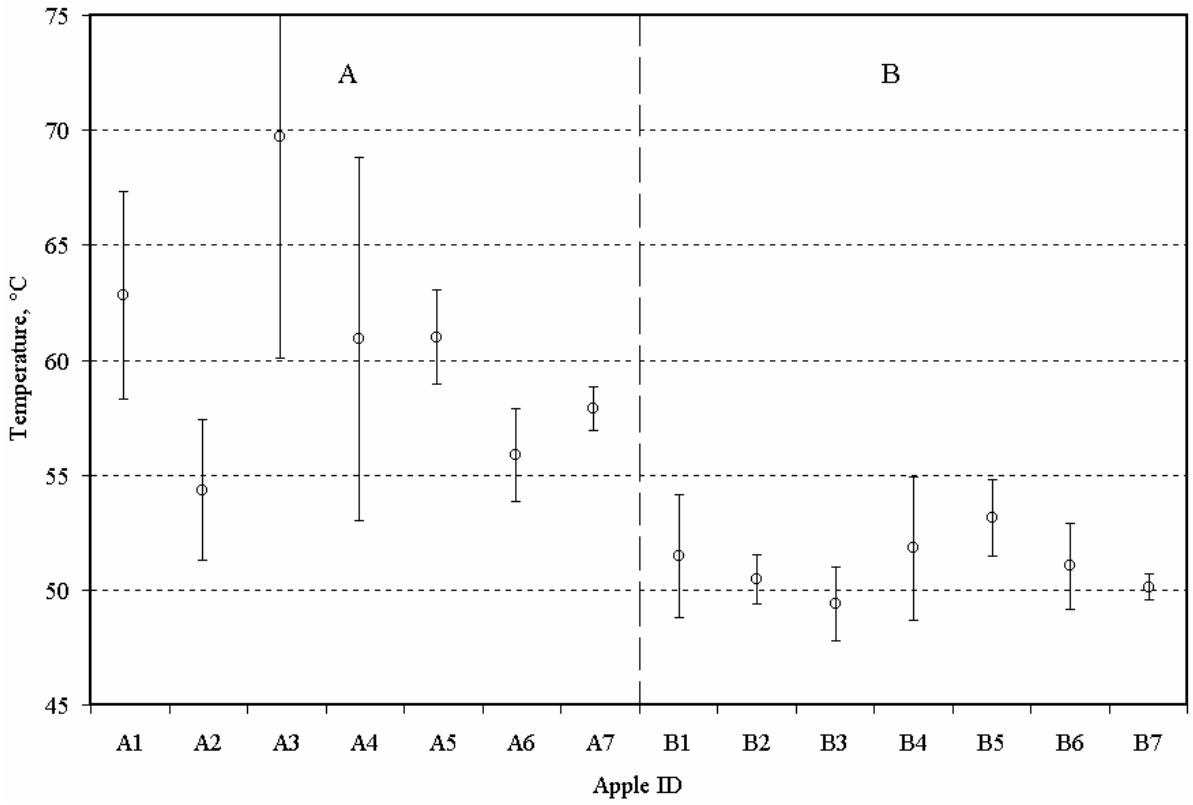

Fig. 6. Temperature variations (mean and standard deviation values over six locations) in seven apples RF heated for 6 min without (A) and with (B) water circulation from 20°C initial temperature of fruit.

Table 2. Final temperature, mean and standard deviation (STD) values for six locations in an individual apple and among seven apples heated by RF for 5.5 min. from 20°C initial fruit temperature.

Fruit	Temperature (°C)							
	Rad1	Rad2	Rad3	Ax1	Ax2	Ax3	Mean	STD
1	49.6	48.1	49.5	53.6	53.7	54.2	51.5	2.67
2	50.8	49.6	51.2	51.9	50.4	48.9	50.5	1.09
3	48.9	48.0	47.4	51.6	50.6	50.0	49.4$^{\#}$	1.60
4	49.8	48.9	48.6	55.7	53.2	54.7	51.8	3.11
5	53.1	51.1	51.3	54.1	54.2	55.2	53.2$^{\#}$	1.66
6	49.1	49.2	50.3	53.8	51.4	52.5	51.1	1.87
7	51.0	49.5	49.5	50.1	50.3	50.4	50.1	0.58
Mean	50.3ac*	49.2^{a}	49.7^{a}	53.0^{b}	52.0^{ab}	52.3^{bc}	51.1	
STD	1.46	1.05	1.40	1.87	1.68	2.53		2.15

Note : ac* *Means in row with different letters are significantly different ($p<0.05$) .*
$^{\#}$ *Means in column with # sign are significantly different ($p<0.05$).*

3.4. Comparison of RF Heating with hot air and hot water heating

Fig. 7 shows experimental time-temperature histories for oranges (fruit diameter 9 cm) when subjected to hot air, hot water and RF heating. It took about 66 and 173 min for core temperature to reach 50°C in hot water and hot air heating, respectively. In RF heating, core temperature increased linearly with the process time and heated at rate varying from 3 – 5°C/min from fruit to fruit. Please note that in the above RF heating tests, the fruit was stationary in water to allow monitoring of temperature with fiber-optic sensors, which was different from the tests for RF heating uniformity assessment where fruit was moving and rotating in water filled container. There appeared to be no marked temperature difference between core and subsurface with respect to process time during the RF heating while the temperature difference between subsurface (2 cm deep) and core was fairly large with hot water and hot air (Fig. 7). In hot air

treatment, the temperature difference persisted even after 3 hours of heating. RF heating was approximately 8.8 and 23 times faster compared with hot water and air, respectively, as it took only 7.5 min to heat from 20°C to 50°C. RF treatment has particular advantages over conventional heating in treating large fruit.

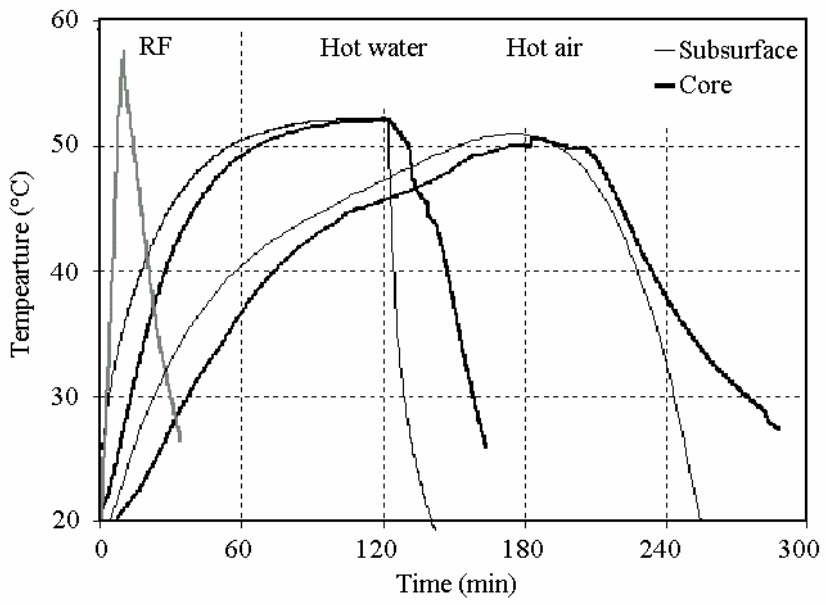

Fig. 7. Experimental heating and cooling curves for orange (9 cm diameter) center and subsurface (2 cm deep) when subjected to forced hot air (53°C air temperature, 1 m s^{-1}air speed), hot water (53°C) and radio frequency (RF: 27.12 MHz) treatments.

Fig. 8 illustrates the temperature distributions inside orange measured with infrared thermal imaging technique when subjected to RF heating for 5 and 10 min, and to hot water and hot air heating at 53°C for 10 and 20 min (initial fruit temperature, 20°C). Ten minute RF heating time was chosen to compare with other methods of heating for the same duration. RF heating resulted in fairly uniform temperatures over the entire orange and achieved the target temperature in a short time. With the hot water and hot air treatments, a large temperature gradient was observed from the surface to the core.

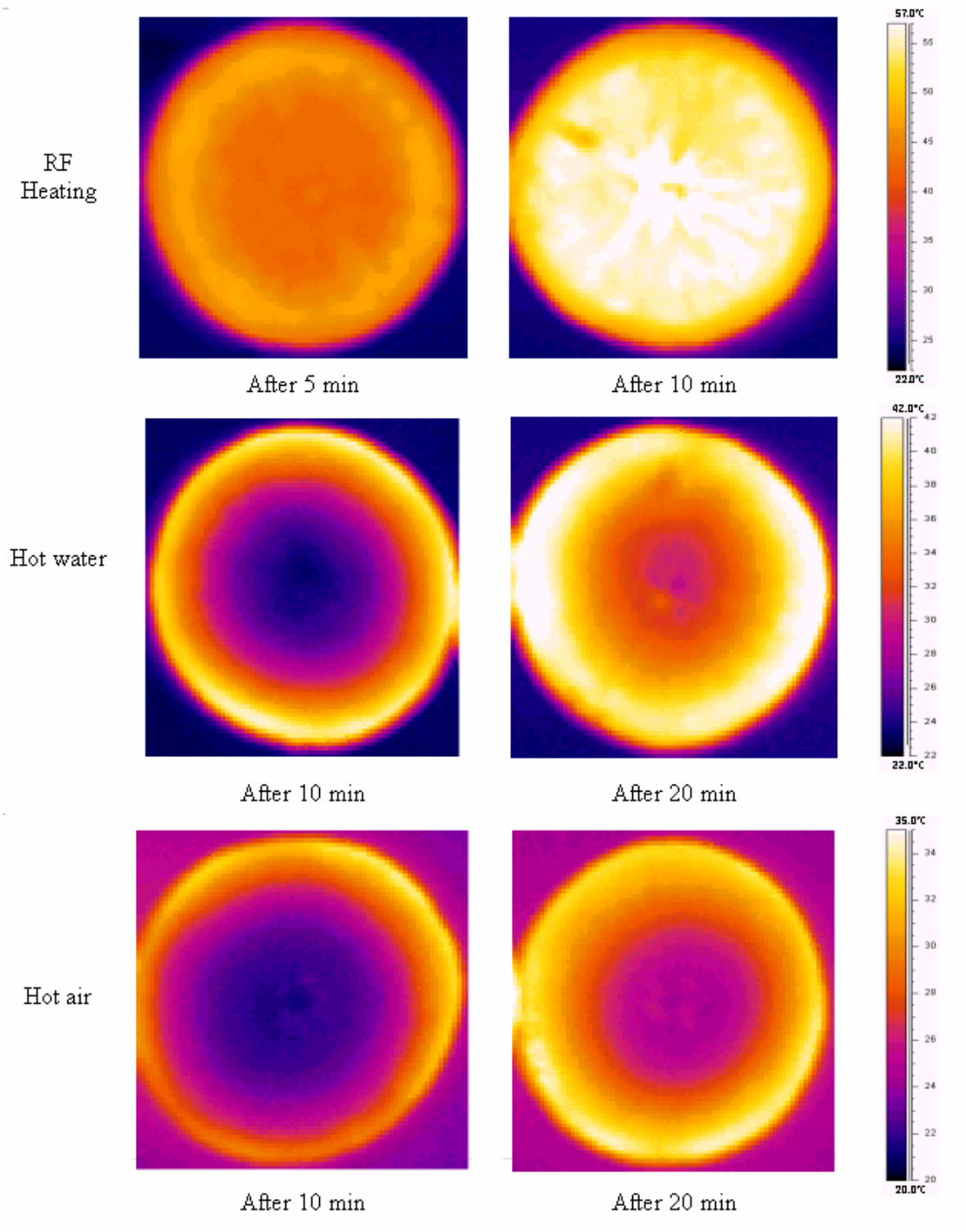

Fig. 8. Temperature distributions in oranges (9 cm dia.) when subjected to RF heating for 5 and 10 min, to hot water and hot air heating at 53°C for 10 and 20 min from 20 °C initial fruit temperature.

Table 3 shows the comparison of measured temperature by an infrared camera and by a thermocouple when oranges were subjected to RF, hot air and hot water heating. Taking into account the initial temperatures and elapsed time before the image was taken, a good agreement was obtained for both measurement methods. In general, the RF heating was more uniform and faster than hot water or hot air treatments.

Table 3. Core temperature of oranges measured by thermal imaging (T/I) and thermocouple (T/C) in hot water, hot air and RF heating.

Heating time (min)	Hot water (°C)		Hot air (°C)		RF (°C)	
	T/I	T/C	T/I	T/C	T/I	T/C
0	18	20.2	18	19.8	18	20.1
5	--	--	--	--	36	38.6
10	25	26.9	19	20.2	56	57.4
20	33	35.2	23	23.9	--	--
30	39	41.1	25	27.3	--	--
40	43	45.0	28	30.8	--	--

3.5. Design considerations for industrial scale fruit mover

The results of this study suggest that moving and rotating a fruit can overcome the obstacle of a non-uniform RF field and irregular geometry of the fruit. It is, therefore, possible to develop a RF heat treatment protocol to control insect pests in large fruit. Because the medium (water) was 85 – 90 % of the total RF heat load in our study, a major challenge in developing a continuous process using this concept relies on recovery of heat from the medium for energy savings. RF heating may be used for preheated fruit (preheating to non-damaging temperature by conventional method) to maximize energy efficiency and throughput. An industrial scale fruit mover should have a high ratio of fruit volume to total volume of heating load. For industrial scale RF heating systems, the rotation and the movement of fruit may be accomplished in a

flume that may be a part of the applicator. In a flume, a series of baffles can be placed in a staggered fashion to provide a zigzag path for fruit. The top covering plate may have corrugations to facilitate axial rotations of fruit. The water nozzles may be mounted on the side walls to propel the fruit. The flume may have a false perforated bottom through which water can be pumped out so that the buoyancy force on the fruit can be reduced and facilitate movement of fruit.

4. Conclusions

RF treatments had an advantage of fast heating over conventional hot air and hot water heating for large fruit. The fruit mover was capable of rotating the fruit on their axes and moving them in the RF field. The rotational ability of the fruit was greatly influenced by the batch size and the water circulation rate, which were determined experimentally to obtain desired rotational characteristics. For naval oranges, 12.5 % fruit volume (based on total volume of water and fruit) with a 50 l/min flow rate corresponding to 9 m s^{-1} water jet velocity at a point of exit from the nozzles were found to be best to obtain desired movement of the fruit. Similarly for 'Fuji' apples 11.0 % fruit volume and 10 m s^{-1} water jet velocity were found to be best. The rotation and movement of fruit minimized the adverse effect of the non-uniform RF field and the irregular geometry of the fruit and improved RF heating uniformity. Fruit geometry was found to influence the heating pattern. Apples with typical geometry (oval and dimples on ends) showed more variation in temperature within a fruit than oranges, which are almost spherical. Oranges were heated with less than ±2°C variation within an orange and ±3°C temperature variation among oranges. Apples were heated with less than ±2.5°C variation within an apple and ±3.5°C temperature variation among apples.

References

Burditt, A.K.J., 1982. Food irradiation as a quarantine treatment of fruits. Food Technol. November: 51–54–58–60, 62.

Calkins, C.O., 1993. Future directions in control of the Caribbean fruit fly (Diptera: Tephritidae). Flo. Entomol. 76, 263–270.

Frings, H., 1952. Factors determining the effects of radio-frequency electromagnetic fields and materials they infest. J. Econ. Entomol. 45, 396–408.

Hallman, G.J., Sharp, J. L., 1994. Radio frequency heat treatments. In: Sharp, J.L. and Hallman, G.J. (Eds.), Quarantine Treatments for Pests of Food Plants. Westview Press. San Francisco, CA, pp. 165–170.

Hansen, J., 1992. Heating curve models of quarantine treatments against insect pests. J. Econ. Entomol. 85, 1846–1854.

Hatton, T.T., Cubbredge, R.H., Risse, L.A., Spalding, D.H., Windeguth, D.L. and Chew, V, 1984. Phytotoxic responses of Florida grapefruit to low-dose irradiation. J. Ame. Soc. Hortic. Sci. 109, 607–610.

Headlee, T.J., Burdette, R.C., 1929. Some facts relative to the effect of high frequency radio waves on insect activity. J. New York Entomol. Soc. 37, 59–64.

Ikediala, J.N., Tang, J., Hansen, J., Drake, S.R., Wang, S., 2002. Quarantine treatment of fruits using radio frequency energy and an ionic-water-immersion technique. Postharvest Biol. Technol., 24, 25–37.

Lurie, S., 1998. Postharvest heat treatments of horticultural crops: commodity responses. Postharvest Biol. Technol., 14, 257–269.

Nelson, S.O., Payne, J.A., 1982. RF dielectric heating for pecan weevil control. Trans. ASAE, 31, 456–458.

Schiffman-Nadel, M., Chalutz, E., Wax, J. Dagan, M.,1975. Reduction of chilling injury in grapefruit by thiabendazole and benomyl during long term storage. J. Ame. Soc. Hortic. Sci. 100, 276–276.

Schiffman-Nadel, M., Chalutz, E., Wax, J., Lattar, F.S., 1972. Reduction of pitting of grapefruit by thiabendazole during long term cold storage. Hortic. Sci. 7, 394–394.

Sharp, J.L., Gaffney, J.J., Moss, J.I., Gould, W.P., 1991. Hot-air treatment device for quarantine research. J. Econ. Entomol. 84, 520–527.

Shellie, K.C., Firko, M.J., Mangan, R.L., 1992. Phytotoxic response of 'Dancy' tangerine to high-temperature moist forced-air treatment for fruit fly disinfestation. J. Amer. Soc. Hort. Sci. 118, 481–485.

Shellie, K.C. and R. L. Mangan. 1993. Disinfestation of subtropical commodities with hot forced air. Acta Hortic. 343, 367–370.

Shellie, K.C., Mangan, R.L.,.1995. Heating rate and tolerance of naturally degreened 'Dancy' tangerine to high-temperature, forced air for fruit fly disinfestation. HortTechnol. 5, 40–43.

Shellie, K.C. Mangan, R.L., 1998. Tolerance of navel orange to heat treatments for disinfestation of Mexican fruit fly. J. Amer. Soc. Hort. Sci. 123, 288–293.

Soderstrom, E.L., Brandl, D.G., Mackey, B.E., 1996. High temperature alone and combined with controlled atmospheres for control of diapausing codling moth (Lepidoptera: Tortricidae) in walnuts. J. Econ. Entomol. 89, 144–147.

Tang, J., Ikediala, J.N., Wang, S., Hansen, J., Cavalieri, R., 2000. High-temperature-short-time thermal quarantine methods. Postharvest Biol. Technol. 21, 129–145.

UNEP. United Nations Environmental Programme, 1992. Fourth Meeting of the parties to the Montreal Protocol on substances that deplete the ozone layer. Copenhagen, 23–35 November 1992. UNEP, Nairobi, Kenya.

[USDA] United States Department of Agriculture, 2001. Agricultural statistics. USDA, Washington, DC.

[USEPA] United States Environmental Protection Agency, 1998. Reregistration Eligibility Decision. Aluminum and Magnesium Phosphide. Cases 0025 & 0645. USEPA, Office of Pesticide Programs, Special Review and Reregistration Division.

Wang, S., Ikediala, J.N., Tang, J., Hansen, J.D., Mitcham, E., Mao, R., Swanson, B., 2001a. Radio frequency treatments to control codling moth in in-shell walnuts. Postharvest Biol. Technol. 22, 29–38.

Wang, S., Tang, J., Cavalieri, R.P., 2001b. Modeling fruit internal heating rates for hot air and hot water treatments. Postharvest Biol. Technol. 22, 257–270.

Wang, S., Tang, J., Johnson, J.A., Mitcham, E., Hansen, J.D., Cavalieri, R, Bower, J., Biasi, B., 2002. Process protocols based on radio frequency energy to control field and storage pests in in-shell walnuts. Postharvest Biol. Technol. 26, 265–273.

Wang, S., Tang, J., Johnson, J.A., Mitcham, E., Hansen, J.D., Hallman, G., Drake, S.R., Wang, Y., 2003. Dielectric properties of fruits and insect pests as related to radio frequency and microwave treatments. Biosystems Eng. 85, 201–212.

C H A P T E R 4

RADIO FREQUENCY HEATING PATTERNS AS INFLUENCED BY DIELECTRIC PROPERTIES OF CONSTITUENT PARTS OF FRUIT

S. L. Birla, S. Wang, J. Tang
Department of Biological Systems Engineering
Washington State University, 213 LJ Smith Hall, Pullman WA, 99164–6120 USA

Published in ASABE 06 Conference Proceeding paper #066052

Abstract

In this chapter, RF heating patterns in various fruits were investigated. Effect of dielectric properties of constitutional parts of fruit such as peel and pulp on the RF heating patterns was also studied. Orange, apple, grapefruit, peach, and avocado were selected for these studies. The selected fruits were placed in a fruit mover equipped with a mechanism to keep fruits rotating and moving during RF heating in a 12 kW parallel plate RF unit operating at 27.12 MHz. Dielectric properties of each fruit constitutional part were measured by open-ended coaxial cable probe method. The study showed that peel dielectric properties along with peel thickness greatly influenced the RF heating behavior of an orange and a grapefruit. Core heating was prominent in apple, peeled orange and grapefruit; whereas in whole oranges the subsurface was at higher temperature than the core. The study helped in better understanding of the complex RF heating characteristics of fruits for designing practical product specific treatment protocol. To further understand the complex RF heating, modeling of RF heating is highly recommended for predicting heating patterns in real fruit.

Keywords: Dielectric properties, Radio frequency, Heating uniformity, Heat treatment, Quarantine

1. Introduction

Interstate and international trade regulations require postharvest treatments of fresh fruits to ensure quarantine security from insect pests. The current quarantine method, i.e. methyl bromide fumigation, has posed a serious environmental health hazard; therefore its use is being phased out under the international agreement. Many researchers have explored different methods such as thermal treatment by hot water or air, irradiation, cold storage, controlled atmosphere storage etc in order to replace chemical methods. All these methods have one or other limitations, for example, conventional heating such as hot water or hot air is slow because it relies on conduction in fruit. Because of fast and volumetric in nature, radio frequency (RF) heating has been looked upon as a way to overcome the problems associated with conventional heating methods used for disinfestation of fruits (Hallman and Sharp, 1994). Many studies have explored the possible use of electromagnetic energy for heating the fresh fruit to control insect pests. Nelson (1996) reviewed the research work on the application of RF heating as a postharvest treatment to kill selected pests in some horticulture crops. They concluded that non-uniform heating of fruits was the major stumbling block in possible use of RF energy for fruit disinfestations. Recently, researchers have tried to overcome the problems and developed treatment protocols for some commodities - microwave (MW) energy for cherries (Ikediala et al., 2002) and RF energy for in-shell walnuts (Wang et al., 2002) and apples (Wang et al., 2006). Birla et al.(2004) showed a significant improvement in RF heating uniformity of large fruits such as orange and apple by immersion of fruits in water and movement and three-dimensional rotations of fruits in RF field. They reported differential RF heating rates of water and fruit as a result of difference in dielectric properties of water and fruit.

Dielectric properties, measured as permittivity, influence reflection of electromagnetic waves at interfaces and the attenuation of the wave energy within materials. The complex

relative permittivity $\varepsilon^* = \varepsilon' - j\varepsilon''$ of a material includes dielectric constant (ε′) which represents stored energy when the material is exposed to an electric field, and the dielectric loss factor (ε′′), which is the imaginary part and influences energy absorption and attenuation. The RF power absorption in any material is directly proportional to the loss factor, therefore dissimilar materials exposed to similar RF field would heat differently (Ryynänen, 1995). The dielectric loss factor in RF range is dominated by ionic conductance. Addition of salt in water increases the ionic conductivity and so the loss factor. The differential heating of fruit and water can be overcome by adjustment of dielectric properties of water with respect to fruit by addition of salt. The level of adjustment is dependent on dielectric properties of the fruit. Therefore the information of dielectric properties of fruits is essential for proper design of RF heating process.

In principle, the dielectric properties are needed to define electromagnetic fields in the objects but this is also influence by the geometry of the object and electrodes. The RF heating pattern is influenced by wavelength (λ_m) and penetration depth (d) of electro-magnetic (EM) wave relative to the size of the fruit (d). The wavelength in the lossy object depends primarily on dielectric constant whereas the penetration depth mostly decides by loss factor (Zhang and Datta, 2005). The penetration depth (d_p, m) defines the distance that an incident EM wave can penetrate beneath the surface of a material as the power decreases to 1/e (e = 2.718) of its power at the surface (Ryynänen, 1995).

$$d_p = \frac{c}{2\pi f(2\varepsilon')^{0.5}}[\{1+(\varepsilon''/\varepsilon')^2\}^{0.5} - 1]^{-0.5} \quad (1)$$

$$\lambda_m = \frac{c}{f}[\tfrac{1}{2}(\{1+(\varepsilon''/\varepsilon')^2\}^{0.5} + 1)]^{-0.5} \quad (2)$$

where c is the speed of light in vacuum, 3×10^8 m s^{-1}, f is the frequency of EM wave, Hz.

Information on dielectric property data of fruits has been published over the last several years (Foster and Schwan, 1989; Nelson, 1996; Ryynänen, 1995; Venkatesh and Raghavan, 2004). Nelson (2003) measured temperature and frequency dependent dielectric properties of many fresh fruits and vegetables in frequency range of 0.01 to 1.8 GHz. Sipaghioglu and Barringer (2003) measured dielectric properties of fruits and vegetables as a function of temperature, ash, and moisture content. Seaman and Seals(1991) measured the dielectric properties (0·15 to 6·4 GHz) of peel and pulp of apples and oranges at room temperature. They reported a large difference in dielectric properties of pulp and peel. However, no data have been reported on the temperature dependent dielectric properties of peel at 27.12 MHz frequency which are important in characterization of RF heating pattern in fruits. There is a need to measure dielectric properties of each fruit constituent parts such as peel, pulp for understanding how the dielectric properties influence the RF heating patterns.

The objectives of this study were 1) to measure dielectric properties of peel and pulp of selected fruits, and 2) to experimentally determine the RF heating pattern of the selected fruits. This study was to develop an understanding of RF heating behavior of fruits as influenced by dielectric properties of component parts. The knowledge of the RF heating pattern of fruits will help in designing practical RF energy based thermal treatments.

2. Materials and Methods

2.1. Dielectric properties measurement

Material : 'Red delicious' and 'golden delicious' apples (*Malus sylvestris*), 'navel' and 'valencia' oranges (*Citrus sinesis* L. Osbeck), 'marsh' grapefruit (*Citrus perdesi* Macfad.*)*, 'gwen' avocado (*Persea Americana*), and 'elegant lady' peach (*Prunus persica*) were purchased from local grocery store for measuring dielectric properties of pulp and peel of these fruits, and

for studying the RF heating pattern. These were selected in order to cover the wide varieties of spherical fruits. The structural and physical properties of the selected fruits are listed in Table 1.

Table 1. Physical properties of the selected fruits

Fruit	Fruit diameter cm	Peel thickness, cm	Moisture content % w.b.	Density, kg m^{-3}	Brix %
Grapefruit	8.2	0.8	91	830	8.5
Avocado	5.8	0.5	82	990	12.6
GD apple	7.5	0.01	84	760	12.8
RD apple	7.6	0.015	87	800	11.7
Navel orange	7.9	0.6	88	920	12.9
Valencia orange	7.7	0.4	86	950	11.2
Peach	6.5	0.01	87	980	13.5

Source: Nelson (1996)

Dielectric properties of samples were measured between 1 MHz and 1800 MHz using the open-ended coaxial probe technique with an Impedance Analyzer (Model 4291B, Agilent Technologies, Palo Alto). This frequency range covers three U.S. Federal Communications Commission (FCC) allocated RF frequencies (13, 27, and 40 MHz) and one microwave frequency (915 MHz) for industrial heating applications. The upper frequency (1800 MHz) is close to another FCC allocated microwave frequency (2,450 MHz).

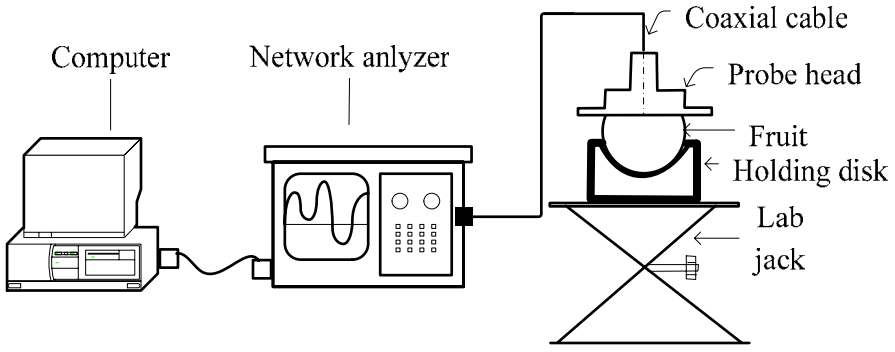

Fig. 1. Experimental set up of dielectric properties measurement

2.2. Measurement procedure

The measurement system was consisted of an open ended dielectric probe connected with an impedance analyzer, a custom built test cell equipped with a temperature control system, and a personal computer (Fig. 1). Before starting measurements, the system was calibrated following standard procedure as described by (Wang et al., 2003a; Wang et al., 2003b). The sample fruit was secured on a laboratory mini-support jack to ensure that flat surface of the sample is in close contact with the probe. For measurements on pulp, fruit was bisect equatorially and cut surface oriented horizontally. The cut face of the fruit was brought in close contact with the probe while care was taken to avoid undue pressure on the tissue which could lead to deformation of the tissues and juice expression. The dielectric properties (DPs) of apple were measured at fruit peel, sub-surface tissue exposed from 3 mm slice cut, and at core of apple. The measurements were made at different location on the apple cross-section to discern whether the spatial variation in the properties exists. DPs of grapefruit and oranges were measured for peel tissue, and for pulp tissue surface exposed by bisecting fruit equatorially. DPs of peach were measured at peel tissue surface and pulp tissues adjacent to fruit stone.

It has been speculated that disruption or damage of biological tissues could lead to alteration of dielectric properties. In order to study the effect of sample preparation technique, orange flesh and peel tissues were crushed into pulp and minced samples respectively using a domestic blender. The prepared samples were held in glass flask and dielectric probe was inserted into the sample mass.

2.3. Temperature dependent DP measurement

Accomplishing rapid heating of intact fruit tissue and maintaining the sample temperature in the test cell during DP measurement are quite difficult. Therefore orange fruit flesh was macerated into pulp and peel into minced samples using a domestic blender. It was done to

ensure proper filling of the sample in the water jacketed test cell. The prepared sample was confined in the test cell with a pressure spring to ensure a close contact between the tip of the coaxial probe and the sample during the measurements. The sample temperature was maintained by circulating a heating fluid into the cell jacket. Details of the test cell and the DP measurement procedure have been explained by Wang et al. (2003b). The dielectric properties were measured at five temperature levels (20, 30, 40, 50 and 60^{o}C) as quarantine thermal treatment requires to heat fruits to around 50°C. A type-T thermocouple (0.8 mm diameter and 0.8 response time) was used to monitor the sample temperature. All measurements were in triplicates, and the results presented as mean and standard deviation.

2.4. RF heating procedure

To study how the RF energy dissipates in different fruits, 'red delicious' and 'golden delicious' apples, 'navel' and 'valencia' oranges, 'marsh: grapefruit, 'gwen' avocado, and 'elegant lady' peach were selected to cover the wide varieties of fruits. The selected fruits were near to spherical in shape so that influence of shape factor on RF heating pattern could be controlled. The fruits were kept at room conditions for 12 h to attain equilibrium room temperature (~20°C). One fruit from each variety/class was randomly picked and a batch of eight assorted fruits was formed. Similarly another batch of eight assorted fruits was formed and fruits were peeled off to study the effect of peel on RF heating pattern. RF heating was conducted in a 12 kW, 27 MHz batch type RF heating system (Strayfield Fastran with E-200, Strayfield International Limited, Wokingham, UK). The batch of the fruits was placed in a fruit mover developed in the previous study (Birla et al., 2004), and tap water was filled up to the top of the covering plate placed over fruits. Fig. 2 shows the schematic diagram of the fruit mover system placed between two RF electrodes. The assorted fruits were kept in motion by means of water jet nozzles mounted on the periphery of the fruit mover. A thermocouple thermometer, installed on

water circulation piping, monitored the water temperature during RF heating (Fig. 2). The RF input power (10 kW) was switched off when the water temperature reached 50°C. Details of the fruit mover and operating procedure have been explained elsewhere (Birla et al., 2004). Immediately after RF heating the fruits were halved equatorially and thermal images of one-half cut section of the fruits recorded using an infrared imaging camera (ThermaCAM^{TM} Researcher 2001, accuracy ±2°C, 5 picture recordings per seconds, FLIR Systems, Portland, OR).

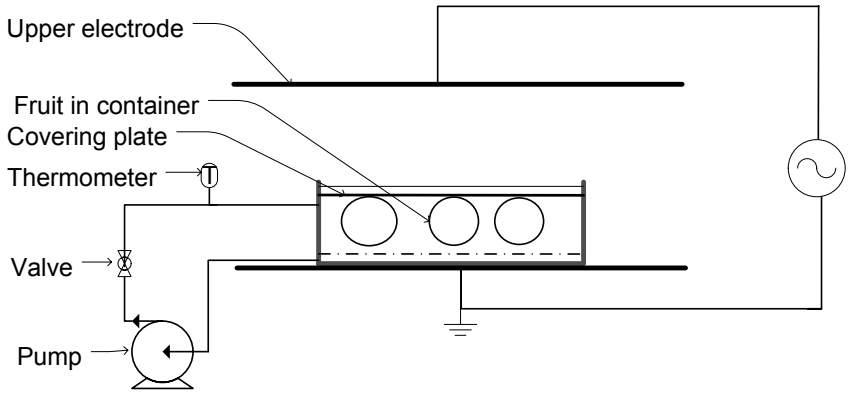

Fig. 2. Schematic diagram of the RF heating system equipped with fruit mover

3. Results and Discussion

3.1. Dielectric properties

In this study, the discussion of DP of the fruits is focused on 27.12 MHz frequency, which can be potentially used for design of RF energy based treatment protocol for postharvest insect control in fresh fruits. However we also measured DP of the fruits at other frequencies and data for 915 and 1800 MHz have been shown in Table 2 which can be used for microwave based process design. We first studied the effect of sample preparation technique on dielectric properties of 'navel' orange. Fig. 3 shows the dielectric constant and the loss factor of 'navel' orange pulp and pulp tissue, minced peel and peel tissue, and juice measured at ~20°c and 27.12

MHz. The loss factor of pulp was almost two times of that of the peel. The loss factor of the pulp was slightly smaller than that of the juice and the pulp tissue. The lower value of the pulp loss factor might be attributed by entrapped air, which whipped in during pulp sample preparation. The loss factor of the peel tissue was less than that of minced peel, and it might be due to expulsion of air from the samples. The dielectric constant of juice was around 81, which slightly higher than distilled water (78) but loss factor is ten times of that of the water. The effect of peel tissues disruption on dielectric constant was observed to be negative and the disruption of peel tissues resulted in a significantly lower value of dielectric constant. Therefore, disruption of biomaterials tissues by sample preparation technique would alter dielectric properties of the sample. The dielectric properties of orange pulp sample gave conservative estimates of the dielectric properties of fruit mass; however values were in reasonable range. In case of peel, the DP measurement with minced peel samples should not be treated as peel tissue properties.

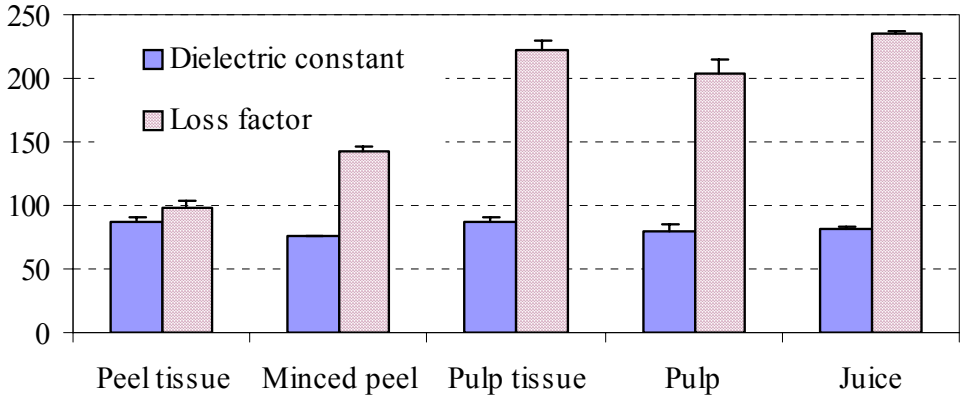

Fig. 3. Dielectric properties of navel orange pulp, minced peel, peel tissue, pulp tissue and juice at 20°C and 27.12 MHz

As DP of biomaterials are a strong function of temperature, measurements were also made at elevated temperatures and results are shown in Fig. 4. The dielectric constant of orange pulp and minced peel decreased with increasing temperature at 27.12 MHz while the loss factor

increased linearly with increasing temperature (Fig. 4a). The trend and values of the loss factor and dielectric constant were in agreement with the reported results (Wang et al., 2003b). Predominant ionic loss in RF range resulted in increased loss factor with increasing temperature. The temperature dependent loss factor can cause thermal run away in fruit especially when heating is conducted under non uniform electromagnetic field (Wang et al., 2002). Therefore it is imperative to consider this phenomenon in design of RF application. Fig. 4 also shows that the dielectric constant and loss factor of 'valencia' orange were greater than those of 'navel' orange. The difference in the dielectric properties between two cultivars was attributed by difference in peel thickness, density, and total soluble solids (Table 1). Valencia oranges were more juicer, compact than the navel oranges.

Table 2. Dielectric properties of constituent parts of the selected fruits measured at 27.12, 915 and 1800 MHz frequencies at ~20°C

Fruit	Tissue/part	27 MHz		915 MHz		1800 MHz		Penetration	Wavelength
		ε'	ε"	ε'	ε"	ε'	ε"	dp, cm	λm , cm
Grapefruit	Pulp	99.42 ±2.77	245.7 ±12.81	69.44 ±3.79	14.53 ±0.47	66.93 ±3.82	14.22 ±0.08	9.67	81.94
	Peel	65.77 ±5.40	161.67 ±44.16	51.09 ±5.06	12.93 ±2.87	48.6 ±9.21	11.89 ±2.30	11.93	100.92
Avocado	Pulp	146.73 ±16.67	574.71 ±75.66	53.1 ±3.59	24.09 ±2.06	50.95 ±3.44	17.08 ±1.27	5.89	57.51
	Stone	4.81 ±0.57	0.15 ±0.01	4.52 ±0.58	0.28 ±0.05	4.57 ±0.53	0.23 ±0.07	2573.42	504.32
	Peel	8.31 ±0.37	0.32 ±0.09	7.59 ±0.08	0.21 ±0.06	5.94 ±0.04	0.19 ±0.03	1585.65	383.66
GD apple	Sub-surface	63.58 ±4.79	67.88 ±7.63	55.08 ±4.20	7.47 ±0.72	53.89 ±3.46	9.27 ±0.69	22.94	125.02
	Core	84.86 ±7.18	132.73 ±2.51	65.02 ±1.92	12.25 ±0.64	62.67 ±1.54	12.98 ±0.67	14.60	100.48
	Middle	73.56 ±5.95	113 ±15.24	61.8 ±3.85	9.85 ±0.97	60.02 ±3.68	11.05 ±0.75	15.90	108.37
	Peel	40.2 ±1.30	22.39 ±2.94	26.94 ±3.51	3.38 ±0.59	26.34 ±3.32	3.53 ±0.78	51.61	168.48
RD apple	Sub-surface	62.38 ±5.38	67.37 ±16.70	55.68 ±3.33	7.06 ±1.04	54.35 ±3.30	8.93 ±0.90	22.94	125.98
	Core	72.31 ±2.60	115.44 ±5.14	62.14 ±0.81	9.28 ±0.59	60.64 ±0.78	10.38 ±0.37	15.57	108.33
	Peel	38.77 ±6.66	23.15 ±2.88	28.61 ±5.02	3.18 ±0.73	28.03 ±4.81	3.87 ±.64	49.24	170.77
N. orange	Pulp	84.57 ±4.51	222.48 ±11.57	72.16 ±3.95	11.61 ±0.56	70.56 ±4.25	12.21 ±0.74	10.05	87.10
	Peel	86.55 ±4.56	98.27 ±5.21	44.28 ±4.43	11.23 ±1.14	43.8 ±4.12	10.73 ±1.47	18.68	106.08
V. orange	Pulp	85.29 ±5.52	240.09 ±13.88	74.23 ±3.12	15.03 ±2.31	70.62 ±34.03	15.99 ±1.92	9.56	84.83
	Peel	95.52 ±9.44	99.41 ±16.7	43.02 ±3.95	10.73 ±1.23	40.43 ±3.61	10.24 ±1.22	19.12	102.40
Mango	Pulp	90.89 ±1.71	297.49 ±47.96	90.89 ±1.71	297.49 ±47.96	90.89 ±1.71	297.49 ±47.96	8.39	78.03
	Peel	42 ±14.14	13.4 ±5.52	42 ±14.14	13.4 ±5.52	42 ±14.14	13.4 ±5.52	86.16	168.61
Peach	Pulp	90.09 ±7.87	269.5 ±45.96	76.32 ±5.64	16.12 ±2.12	72.14 ±3.87	16.4 ±3.18	8.93	80.87
	Peel	85.06 ±3.03	213 ±5.66	74.34 ±3.83	12.5 ±2.31	68.12 ±2.87	13.1 ±2.92	10.36	88.23

69

The DP of peel and pulp tissues of various fruits measured at 27.12 MHz is shown in Figures 5 & 6. The dielectric constant and loss factor values of apple peel tissue were very small in comparison with that of pulp tissues. This is in agreement with results reported by (Seaman and Seals) (1991) in which a large difference was observed between the dielectric properties of pulp and skin of GD apples measured from 150 to 6400 GHz. The loss factor of golden delicious apple pulp was slightly higher than that of red delicious apple and this might be attributed by difference in physiochemical properties (Table 1).

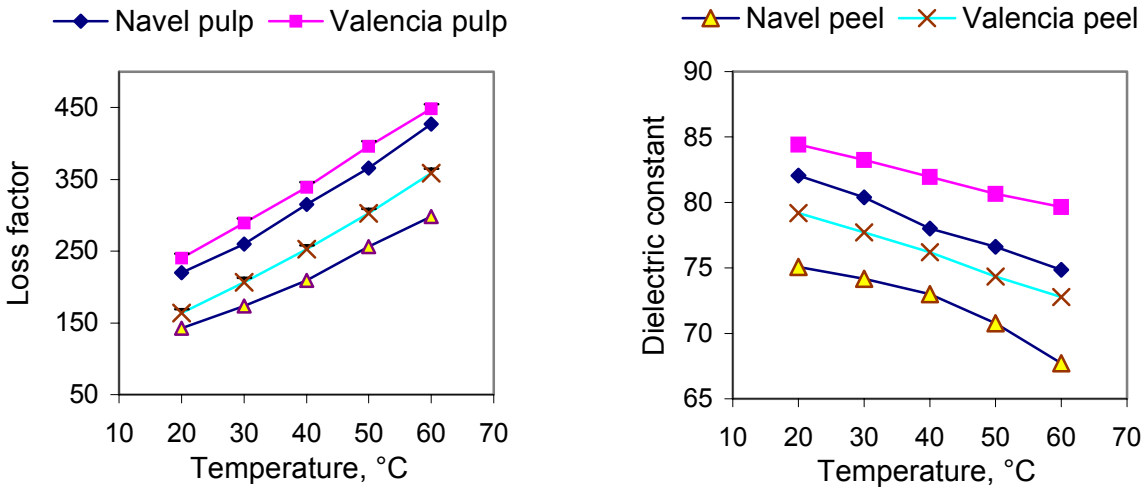

a) **b)**

Fig. 4. Dielectric loss factor and constant of pulp and minced peel of 'navel' and 'valencia' oranges measured at 27.12 MHz and temperatures ranging from 20 to 60°C.

The dielectric properties of apple tissues measured at different points on the cross section revealed that the loss factor decreases with the increasing distance of the measurement points apart from the core of the apple (Table 2). In apples physiological maturity starts from inside, therefore an observable visual color difference due to degree of maturity can be seen on the cross section. This variation affects the dielectric properties as ripening onset from core of the apple. Ikediala et al. (2000) measured the dielectric properties of red delicious apple and reported that

dielectric constant of pulp, close to the surface was higher than that of the core while the loss factor close to the core higher than that of close to the surface, especially in the RF range.

Similarly in other fruits a large difference in dielectric properties of peel and pulp were observed (Figures 5 & 6). The loss factor of avocado pulp was very high (> 600) this might be attributed by high oil and salt content in fruit pulp. Nelson (2003) and Wang et al.(2005) also reported an excessively high value of loss factor for avocado. The low values of dielectric constant and loss factor for avocado peel might be attributed by improper contact of probe to the rough skin of the fruit. Seaman and Seal (1991) experienced the similar problem with measurement of DP of apples skin. There was no much difference in dielectric constant of pulp and peel of the peach; however a difference in loss factor was noticeable (Fig. 5).

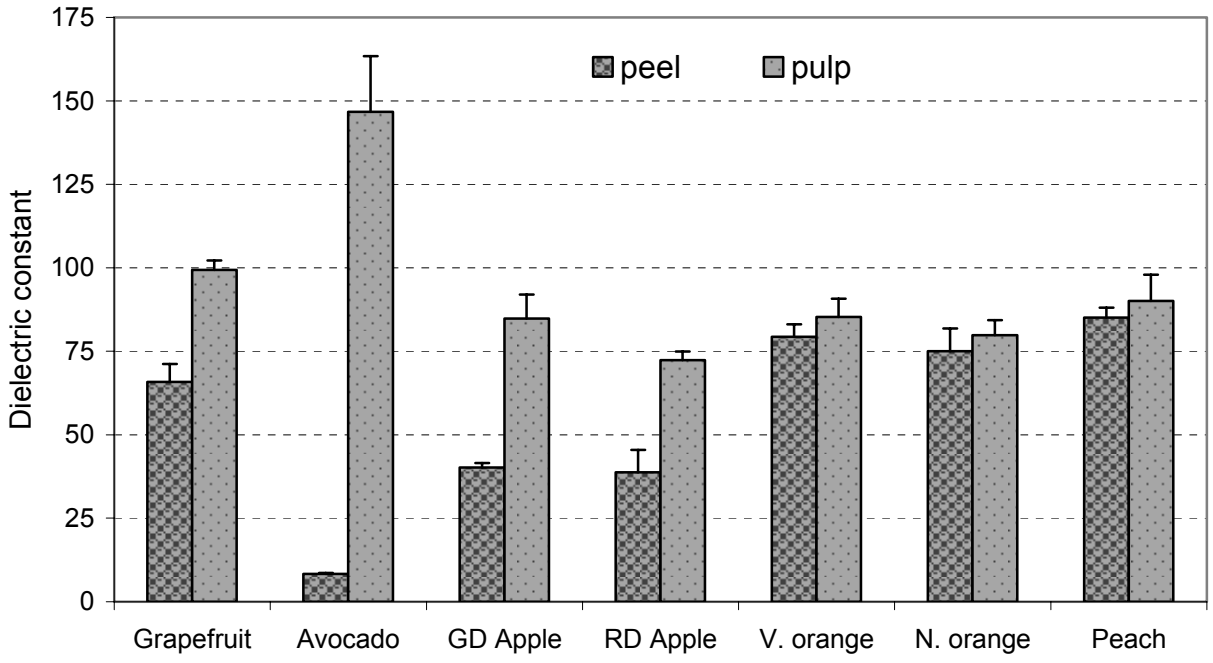

Fig. 5. Dielectric constant of peel and pulp tissues of fruits measured at 27.12 MHz and 20°C

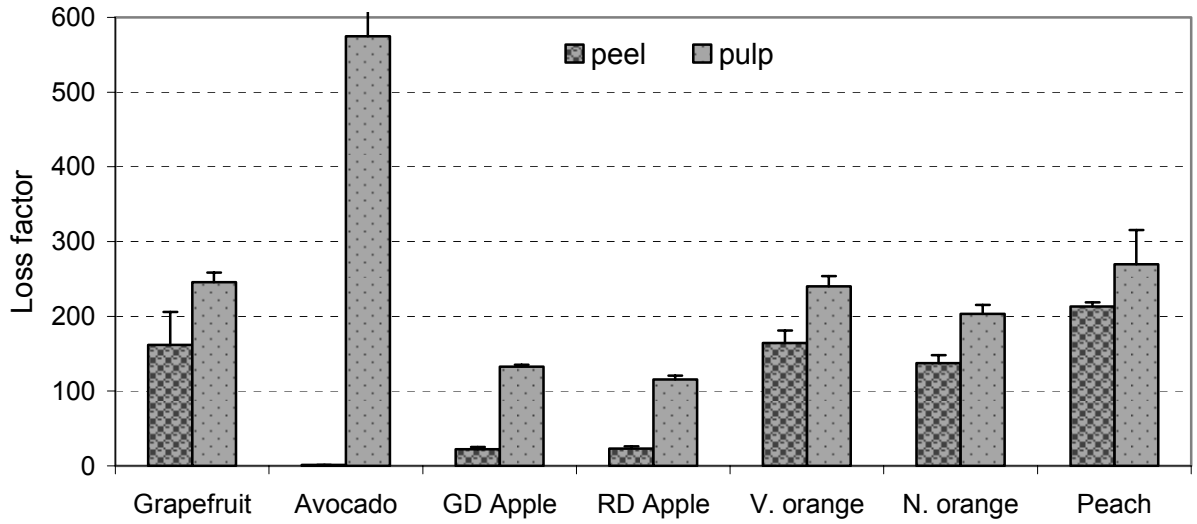

Fig. 6. Dielectric loss factor of peel and pulp tissues of fruits measured at 27.12 MHz and 20°C

3.2. Penetration depth

Penetration depth (d_p) is the function of dielectric properties of the material and frequency as related in Eq. 1. The penetration depth at 27.12 MHz frequency in the peel and pulp tissue of fruits are listed in Table 2. As it is expected a large value of loss factor of avocado pulp resulted in small value of d_p (5.9 cm). Limited penetration depths may lead to non-uniform heating in large fruits. For apple pulp, the d value was 15.6 cm which was the highest value in all the fruits. In general the penetration depth in the fruit peel was greater than that in the fruit pulp (Table 2), therefore we should expect a core heating or uniform heating provided if the fruit mass is homogenous. Penetration depth alone can not generally dictate the heating pattern, except for very large and lossy materials in microwave range (Zhang and Datta, 2005). For spherical objects Buffler and Stanford (1991) gave a criterion core focused heating in microwave range based on shell model. As per the criterion core focusing would occur if the penetration depth is less than 1.5 times of diameter of the object. For spherical object placed in the way of plane EM waves a precise criterion for surface heating was given by Kritikos and Schwan (1975) and according to it, wavelength in object should be more than 2.73 times of radius of the fruit. This

criterion is not true for lossy objects heated in parallel plate RF system. Evan (2000) has mentioned that at a given frequency, loss factor and dielectric constant are sufficient in principle to predict the heating pattern but not straightforward in deciding the heating behavior of fruit because it is also influenced by shape and size of fruit and relative distance of the fruit in between electrodes. In next section we will discuss the RF heating behavior as influenced by the DP of the fruits.

3.3. RF Heating patterns in fruits

To study the RF heating patterns, assorted whole and peeled fruits were immersed in tap water and the fruits were kept in motion during RF heating. The rotation of movement of fruits in water eliminates the fringing effect, spatial variation of electric field strength on heating pattern (Birla et al., 2004). It took six min to raise the water temperature from 20.5 to 50°C with 10 kW RF input power. Initial temperature of all the fruits was 19.5°C and final temperature profiles over fruits cross sections, recorded using the infrared imaging camera, are shown in Figs. 7a–c.

Temperature profile over the RF heated oranges shows that a maximum temperature (56°C) was recorded at subsurface whereas minimum temperature (52°C) was at core. In whole orange temperature gradient was established from sub-surface to core, whereas in peeled oranges core focus heating was observed and temperature gradient was reversed. As we have seen in previous section that dielectric properties of peel and pulp were significantly different hence heating pattern was influenced by the peel dielectric properties. In whole ‘valencia’ oranges occurrence of slightly core focused heating pattern might be attributed by thin peel layer. Core focused heating of the peeled oranges suggested that if the fruit mass is homogenous than we can expect preferentially core heating in spherical objects provided fruits are kept in motion in tap water.

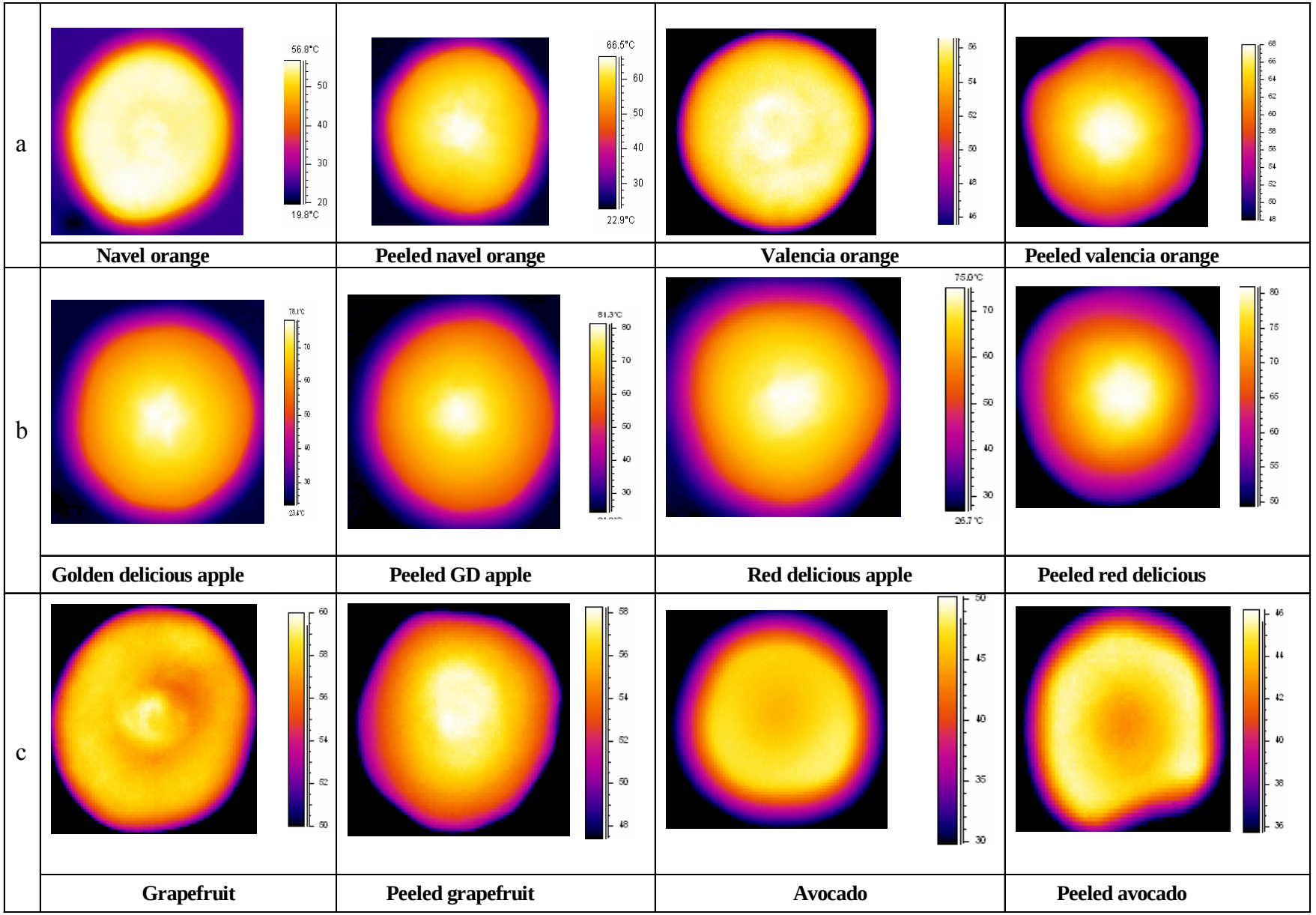

Fig. 7. Temperature profiles over the cross section of the fruits subjected to 6 min of RF heating (@10kW RF power input,19.5°C) immersed in 20.5°C tap water

Fig. 7b shows the temperature profiles on golden and red delicious apples. Under the similar RF heating conditions, apples were core heated much faster than the oranges and temperature gradient was pronounced in the apples. Temperature variation over the cross section of apple was distinct with contour of maximum temperature (80°C) at core and minimum temperature (55°C) at surface. Preferentially core heating might be further added by the fact that the loss factor of tissues increase toward core of the fruit. The values of loss factor of GD apple tissues were 67 and 132 at subsurface and core respectively (Table 2). In spite of significant difference in dielectric properties of pulp and peel of the apples (Figs. 5 & 6), the effect of the peel properties on heating pattern was not evident as it was in the oranges. This may be explained by the fact that apple peel thickness is very small (Table 1).

Similar to 'navel' oranges, RF heating of whole grapefruit resulted in a small temperature gradient from outside to inside (Fig. 7c), whereas peeled grapefruits were preferentially core heated. Only striking difference between orange and grapefruit was the thickness of the peel and that explained the concentric temperature contours. The dielectric properties of grapefruit pulp were in close range with those of the oranges (Figs. 5 & 6) therefore under the similar RF heating conditions; a rise in the temperature was more or less same as observed in the oranges. Heating pattern in avocado was surprisingly non-uniform with core of fruits i.e. hard pit was at lowest temperature (Fig. 7c). Removal of corky peel from the fruit did not show any much difference in heating pattern. The loss factor of avocado pulp was more than 600 and dielectric constant was in more than 100 even though a rise in temperature of avocado was (<50°C) least among all the fruits. The electric field strength inside the fruit is influenced by both the dielectric constant and the loss factor. Evan (2000) has given criteria for maximum heating rate of the spherical objects which are suspended in a large air gap between two electrodes. According to

this, at any constant value of ε', increasing values of ε'' increases the heating rate upto a condition $\varepsilon'' = \varepsilon' + 2$, and any further increments in the value of ε'', heating rate starts to decline. Although this criteria is valid for RF heating of fruits in a large air gap between two electrodes, but similar criteria can be developed using electromagnetic equations for water and fruit system two electrodes. This also explains the excessive high heating rate of apple in comparison of other fruits. In case of peaches preferential heating of core and stone was observed. The temperature raise was comparable with the oranges but the peel effect was not evident on the heating pattern as the peel thickness was very small (Table 1).

3.4. Practical utility of dielectric properties

Due to various factors, one can not generalize the heating patterns of the fruits. For designing RF energy based process, each class of fruit needs special considerations as heating patterns do change with constitutional parts. Phenomenon of the core focused heating of RF energy in apple can be seen as advantage in applying RF energy in conjunction with conventional heating methods. Because conventional heating establishes temperature gradient from surface to core, and combination of these two methods would solve the problems associated with these methods. A RF assisted hot water heating in which preheating of fruits (at certain temperature and for a certain time) in hot water prior to RF heating could be an answer to a quest for an energy efficient, rapid and uniform heating process (Wang et al., 2006). In case of oranges RF heating is not core focused therefore RF heating of oranges will require additional holding time in conventional heating medium to meet thermal lethality requirement at core of the fruit. As we have seen that each fruit variety exhibits different heating patterns, therefore a combination of heating methods should be explored to harness the advantage of each method. To develop a better understanding of the complex nature of RF heating pattern, it is highly desirable

to develop a computer simulation model that makes use of dielectric properties and other factors influencing heating pattern.

4. Conclusions

In this study dielectric properties of constituent parts of different fruits were measured in order to study the RF heating behavior of the fruits. Each fruit behaved differently and heating pattern was influenced not only by shape and size but also by structural parts and their dielectric properties. RF heating of a fruit would be core focused if it has uniform mass such as peeled oranges, apple etc. Due to natural variations in size, shape, and non-homogenous fruit mass, it is very difficult to achieve uniform RF heating of fruit mass. Therefore stand alone RF heating of fruits is not feasible. For fruits such as apple, peaches, which are preferentially core heated, it is an advantage to use RF energy in conjunction with conventional heating. To develop a better understanding of the complex nature of RF heating pattern, it is highly desirable to develop a computer simulation model that makes use of dielectric properties and other factors influencing heating pattern.

References

Birla, S.L., Wang, S., Tang, J., Hallman, G., 2004. Improving heating uniformity of fresh fruit in radio frequency treatments for pest control. Postharvest Biol. Technol. 33, 205–217.

Evans, S., 2000. Electromagnetic rewarming: The effect of CPA concentration and radio source frequency on uniformity and efficiency of heating. Cryobiol. 40, 126–138.

Foster, K.R., Schwan, H.P., 1989. Dielectric properties of tissues and biological materials: A critical review. Crit. Rev. Biomed. Eng 17, 25–104.

Hallman, G.J., Sharp, J.L., 1994. Radio frequency heat treatments. In: Sharp, J.L., Hallman, G.J. (Eds.), Quarantine treatments for pests of food plants. Westview Press, San Francisco, CA, pp. 165–170.

Ikediala, J.N., Tang, J., Drake, S.R., Neven, L.G., 2000. Dielectric properties of apple cultivars and codling moth larvae. Trans. ASAE 43, 1175–1184.

Ikediala, J.N., Hansen, J.D., Tang, J., Drake, S.R., Wang, S., 2002. Development of a saline water immersion technique with RF energy as a postharvest treatment against coding moth in cherries. Postharvest Biol. Technol. 24, 25–37.

Nelson, S.O., 1996. Review and assessment of radio-frequency and microwave energy for stored-grain insect control. Trans ASAE 39, 1475–1484.

Nelson, S.O., 2003. Frequency and temperature dependent permittivity of fresh fruits and vegetables from 0.01 to 1.8 GHz. Trans. ASAE 46, 567–574.

Nelson, S.O., 2004. Dielectric spectroscopy of fresh fruit and vegetable tissues, Dielectric spectroscopy of fresh fruit and vegetable tissues. ASAE, St. Joseph, Mich.

Ryynänen, S., 1995. The electromagnetic properties of food materials: a review of the basic principles. J. Food Eng. 29, 409–429.

Seaman, R., Seals, J., 1991. Fruit pulp and skin dielectric properties for 150 to 6400 MHz. J. Microwave Power EE. 26, 72–81.

Sipaghioglu, O., Barringer, S.A., 2003. Dielectric properties of vegetables and fruits as a function of temperature, ash, and moisture content. J. Food Sci. 68, 234–239.

Venkatesh, M.S., Raghavan, G.S.V., 2004. An overview of microwave processing and dielectric properties of agri-food materials. Biosyst. Eng. 88, 1–18.

Wang, S., Monzon, M., Gazit, Y., Tang, J., E. Mitcham, J., Armstrong, J. W., 2005. Temperature-dependent dielectric properties of selected subtropical and tropical fruits and associated insect pests. Trans. ASAE, 48, 1873–1881.

Wang, S., Tang, J., Cavalieri, R.P., Davis, D.C., 2003a. Differential heating of insects in dried nuts and fruits associated with radio frequency and microwave treatments. Trans. ASAE 46, 1175–1182.

Wang, S., Tang, J., Johnson, J.A., Mitcham, E., Hansen, J.D., Cavalieri, R.P., Bower, J., Biasi, B., 2002. Process protocols based on radio frequency energy to control field and storage pests in in-shell walnuts. Postharvest Biol. Technol. 26, 265–273.

Wang, S., Tang, J., Johnson, J.A., Mitcham, E., Hansen, J.D., Hallman, G., Drake, S.R., Wang, Y., 2003b. Dielectric properties of fruits and insect pests as related to radio frequency and microwave treatments. Biosyst. Eng. 85, 201–212.

C H A P T E R 5

ORANGES QUALITY AS INFLUENCED BY POTENTIAL RADIO FREQUENCY HEAT TREATMENTS AGAINST MEDITERRANEAN FRUIT FLIES

S.L. Birla[1], S. Wang[1], J. Tang[*1], J. Fellman[2], D. Mattinson[2], S. Lurie[3]

1 Department of Biological Systems Engineering, Washington State University
2 Dept. of Horticulture and Landscape Architecture, Washington State University, Pullman
3 Department of Postharvest Science, ARO, The Volcani Center, Bet-Dagan, 50250, Israel

Published in Postharvest Biology and Technology, 38(3), 66–79, 2005

Abstract

Present work explored the possibility of using radio frequency (RF) heating as a means to expedite internal fruit heating rate in water to control pests. Based on the thermal death kinetics of the Mediterranean fruit fly (Medfly), thermal treatments were designed that could provide quarantine security against fruit flies. The main objective of this research was to study the influence of those RF heat treatment on the quality of treated fruit. Treated 'Navel' and 'Valencia' oranges were evaluated for postharvest quality after 10 days of 4°C storage. The quality parameters included: weight loss, loss in firmness, color change, total soluble solids, acidity, and change in volatiles. The volatile analysis was done by the SPME-GC/MS technique. The results indicated a significant change in volatile flavor profiles upon RF heat treatments even when there was no significant difference in the other quality parameters. The treatment that raised fruit temperature from 19 to 48 °C by RF heating in saline water and held then for 15 min in 48°C hot water would meet the quarantine security without impairing the quality of the treated oranges. However sensory evaluation for market acceptability of treated oranges should be carried out for complete treatment protocol development.

Keywords: RF heating; postharvest quality; fruit flies; quarantine; hot water; orange volatiles.

1. Introduction

The Mexican fruit fly, *Anastrepha ludens* (Loew), the Mediterranean fruit fly, *Ceratitis capitata* (Wiedemann), and the Caribbean fruit fly, *Anastrepha suspensa* (Loew), are quarantine pests of citrus fruit. Due to their broad host ranges, presence of these pests in fresh produce can restrict domestic and international commerce. Citrus shipments destined for states such as California, Arizona, and Florida, as well as for export markets including Japan and other Pacific Rim countries require methyl bromide fumigation to meet import quarantine security requirements. Methyl bromide can damage some citrus, e.g. mandarin, oranges (Williams et al., 2000). Moreover it has been identified as an ozone-depleting chemical. Therefore its use is being restricted in accordance with an international agreement, the Montreal Protocol (USEPA, 1998). Currently critical use exemptions may make the fumigant available to pre-shipment and quarantine purposes, but in future use of methyl bromide is at great risk due to reduced production and increased price and future restrictions imposed on its uses under international agreements. Increasing legislative pressure on the use of chemicals for postharvest quarantine disinfestation has resulted in great interest in the development of non-chemical treatment methods.

Several alternative methods have been explored by many researchers, including ionizing radiation, cold storage, and conventional hot air and water heating. All of these methods have drawbacks. For example, a common difficulty with hot air or water heat treatments for large fruits, such as citrus and apple is the slow rate of heat transfer resulting in hours of treatment time (Wang et al., 2001b). Shellie and Mangan (1994, 1998), Sharp and McGuire (1996), Schirra et al. (2005) and Lurie et al. (2004) have extensively studied citrus heat treatments using hot

water and moist hot air. A long exposure time requirement and alterations to flavor compounds (Obenland et al., 1999) were the main difficulty in the development of quarantine treatment protocols. Radio frequency (RF) heating has been studied for selected commodities as a rapid disinfestation treatment (Headlee and Burdette, 1929; Frings, 1952; Nelson and Payne, 1982; Wang et al., 2002). RF heating has relative advantages over microwave heating because it provides larger penetration depths, possible differential heating of insects in commodities (Wang et al., 2003) and simple field patterns (Zhao et al., 2000). However a number of potential problems need to be addressed before RF heat treatments can be successfully used in commercial applications. One potential problem associated with RF heating is possible lack of uniform heating in heterogeneous media (Tang et al., 2000). A large temperature variation among and within fresh fruits reduces the effectiveness of a treatment and may cause severe thermal damage to the fruit. Recently efforts have been made to overcome non-uniform RF heating of fruit. Birla et al. (2004) have shown improvements in RF heating uniformity of orange and apple when fruit were immersed in water and kept in motion by water jets during RF heating.

Treatment protocols have been developed using RF energy that can effectively control codling moth (Wang et al., 2001a) and navel orangeworm (Wang et al., 2002) in unshelled walnuts without causing quality losses. These studies focus on dry nuts that have higher heat tolerance than fresh fruit. Exposure to high temperature can alter many fruit ripening processes, such as ethylene production, respiration, fruit softening, and cell wall metabolism, pigment, carbohydrate and volatile metabolism (Lurie, 1998). Many researchers (Shellie et al., 1993; Shellie and Mangan, 1998, Obenland et al. 1999) have reported the negative effects of heat treatment on postharvest quality of citrus fruit. Changes in flavor quality were reported in these studies even with no significant differences in soluble solids or titratable acidity after heat

treatment. The instability of fresh orange juice aroma during processing (e.g., heat treatment) and subsequent storage has been studied (Shaw, 1991). Decreased levels of characteristic fresh orange juice aroma compounds on one hand, and off-flavor formation on the other, lead to the distinct aroma differences between fresh and processed juice (Obenland et al., 1999).

Similar to development of any new process or technology, many issues have to be addressed before the RF heating method can be adopted as commercial process. As RF heating is fast very, short treatment times can be developed. The development of a treatment protocol requires establishment of process parameters and verification and validation of treatment efficacy. The knowledge of thermal death kinetics can be used in selecting time-temperature combinations for RF heat treatments to kill Mediterranean fruit fly (Medfly) in citrus fruit. The objective of this research was to evaluate different treatment conditions that can control Medfly on orange quality. The quality parameters such as weight loss, loss in firmness, color change, total soluble solids, acidity, and the change in volatile compounds from oranges were evaluated after treatments. This study will identify suitable treatment conditions to support further efficacy studies with infested fruit.

2. Materials and Methods

2.1. Thermal treatment

Freshly harvested ‘Navel’ and ‘Valencia’ oranges (Citrus sinensis L. Osbeck) were procured from Fillmore-Peru Citrus Association, California. The freshly harvested, untreated, unwashed, and unwaxed oranges were delivered overnight to Washington State University, Pullman, WA. The average fruit weight (mean±SD) was 264±21 and 255±18 g for ‘Navel’ and ‘Valencia’, respectively. The supplied oranges were stored at 4°C until used for thermal

treatments. The oranges were removed from the cold storage and left overnight at ambient temperature (~20°C) to ensure uniform initial fruit temperature. Based on the thermal death kinetics reported by Gazit et al. (2004), 100% mortality of Medfly can be achieved by exposing infested fruit to 48°C for 15 min, 50°C for 4 min or 52°C for 1 min. Therefore we chose three temperatures, 48, 50 and 52°C, and different holding times (Table 1) corresponding to one level above and one level below 100% mortality.

Table 1. Experimental design of heat treatments

Treatment name	Heat treatment description	Cultivar
RF48 +10 RF48 +15 RF48 +20	RF heating in saline water to 48°C and holding at 48°C for 10, 15 and 20 min	Valencia/Navel
RF50 +2 RF50 +4 RF50 +6	RF heating in saline water to 50°C and holding at 50°C for 2, 4 and 6 min	Valencia/ Navel
RF52 +0 RF52 +1 RF52 +2	RF heating in saline water to 52°C and holding for 0, 1 and 2 min	Navel
HW48	Hot water heating at 48°C for 2.5 h	Valencia
RFA35	Preheating in 35°C hot water for 45 min and followed by RF heating in tap water to 48°C and holding 15min	Valencia
Control	No heat treated oranges.	Valencia/Navel

Initial experiments suggested that exposure at 52°C caused irreversible and undesirable changes in the quality (flavor, and firmness) of treated Navel oranges. Therefore, for 'Valencia' oranges the 52°C RF treatment was removed and, instead, an experiment was performed to

evaluate the effect of preheating of fruit (conventional hot water heating) before RF treatment. Preheating fruit to a moderate temperature prior to RF treatment could increase throughput and reduce cost of RF equipment and RF energy on a per unit commodity basis in commercial applications. In principle, RF energy should be used sparingly as a means to overcome the problems associated with conventional heating methods so that it remains economically viable. 'Valencia' oranges were preheated in 35^{o}C hot water for 45 min. The preheated fruit were subjected to RF heating in 35^{o}C tap water to raise the fruit core temperature to 48°C, and then held at 48°C in hot water for 15 min.

The RF heating of oranges was conducted in a 12 kW batch type RF heating system (Strayfield Fastran with E-200, Strayfield International Limited, Wokingham, UK). The movement and rotation of oranges in water during RF heating for uniform heating was carried out in a fruit mover. The details of the fruit mover and operating procedure can be found elsewhere (Birla et al., 2004). In preliminary RF heating trials, it was found that 0.006 and 0.004 % NaCl salt in tap water were adequate for 'Valencia' oranges and 'Navel' oranges, respectively, in order to minimize differential heating of fruit and water. Prior to starting the RF treatment for oranges, an experiment was conducted to obtain temperature profiles of the fruit subjected to different thermal treatments. At the end of each treatment stage (preheating, RF heating, holding and cooling), two oranges were removed and thermal images were recorded by an infrared imaging camera (ThermaCAM^{TM} Researcher 2001, accuracy ±2°C, 5 picture recordings per seconds, FLIR Systems, Portland, OR). The temperature of the core and subsurface (5 mm below the surface) was measured by a pre-calibrated thermocouple (Type-T, 0.8-mm diameter and 0.8 s response time, Omega Engineering Ltd, CT) and temperature data during preheating

and cooling time were recorded every 5 s by a data logger (DL2e, Delta-T Devices Ltd., Cambridge, UK.

Eight oranges were placed in the fruit mover and water of preset salt concentration was filled to the top of the covering plate placed over oranges. Oranges were kept in motion by means of water jet nozzles mounted on the periphery of the fruit mover. The RF input power (10 kW) was switched off when the water temperature reached the treatment temperature, i.e. 48, 50 or 52°C. Oranges were then kept on hold at the treatment temperature for 0 to 20 minutes depending upon the treatment design, followed by hydro-cooling for 30 minutes in 3-4°C chilled water. The core temperature of one randomly selected fruit was measured immediately after RF heating, holding time, and cooling. For comparative study, conventional hot water heating of 'Valencia' oranges was also carried out in a water bath (Model ZD, Grant, Cambridge, UK) set at 48°C. Hydro-cooling started after the core temperature reached 47.2°C. Treated and control oranges were placed in cold storage (~5°C and ~95% RH) for 10 days. Quality analyses of 'Navel' oranges suggested that water loss from both treated and control fruit was considerable and resulted in a loss of firmness. Therefore treated and control 'Valencia' oranges were waxed (by *Carnauba* natural wax) before placing them in storage to reduce moisture loss. Each treatment combination listed in Table 1 was replicated three times.

2.2. Quality measurement

Weight, firmness and peel color of each orange were measured before and 10 days after treatment. Each fruit within a treatment group was numbered on its stem end. Color and firmness were measured at three marked spots along the equatorial fruit surface. The firmness was measured by a Texture analyzer (Model TA-XT2, Stable Micro Systems, YL, UK) which was attached with an aluminum disk (50 × 20 mm) on cross head. The fruit was kept in position on a

concave shaped Nylon disk which was secured in place on Texture analyzer base during firmness measurement. The firmness was expressed in mm deformation by a 1 kg force on the equatorial fruit surface for 10 s. The change in firmness (difference in post storage and pretreatment firmness of individual fruit) was expressed as a percentage of pretreatment firmness. A positive value suggests that there is a loss of firmness, whereas a negative value suggests that oranges became firmer after the treatments. Peel color was measured at three marked spots on an individual orange by a colorimeter (Model CM-2002, Minolta Corp., Ramsey, NJ) calibrated to a standard white reflective plate. The change in peel color was analyzed as percent change in value of L^*, C^*, h^o color system (L^* = darkness, C^* = chroma, h^o = hue angle). The post storage/treatment color was expressed as a percentage of pretreatment value of color indices, which were calculated from 'L', 'a' and 'b' values obtained before and after the treatments using the colorimeter. Total soluble solids and percent titratable acidity were measured after 10 days of storage on six oranges for each treatment. Juice was extracted from the oranges and titratable acidity (TA) was determined by end-point titration of 5 ml juice to pH 8.2 with 0.1N NaOH solution and expressed in terms of the equivalent anhydrous citric acid per 100 ml of juice. Total soluble solids (° Brix) was measured by a hand-held refractrometer (Model N-1α, ATAGO Co. Ltd., Tokyo) and expressed as percent soluble solids in juice. The treated and untreated oranges were visually inspected for external appearance, treatment damage, and decay and assessed organoleptically for any off-flavor development in the peel.

The measurements of individual quality attributes were subjected to an analysis of variance (ANOVA) and means were separated by LSD ($p<0.05$) and as multiple pair by Tukey's method (SAS Institute, 1990, Cary, NC).

2.3. Volatile compounds analysis

2.3.1. Sample preparation

After 10 days of storage, juice from six oranges (from each treatment group) was hand squeezed, filtered through cheese cloth to remove pulp and filled in a 20 ml plastic (scintillation vial with a cone cap lid). The sample vials were immediately sealed and stored in a freezer until the samples were used for SPME-GC analysis. A solid phase micro-extraction (SPME) technique was used to prepare samples for analysis by a Gas Chromotograph (Steffen and Pawliszyn, 1996). The orange juice samples were removed from the freezer just before volatile component analysis. The sample vial was immersed in tap water for thawing. In a 4 ml SPME vial one ml of juice was diluted in 1 ml of de-ionized water containing 0.65 g NaCl, according to Steffen and Pawliszyn (1996) and a 6 mm magnetic stirring bar. The vial was mounted on a SPME stand and a fiber (0.65μm thick PDMS/DVB stationary phase, Supelco Inc., Bellefonte, PA) was inserted in the headspace (Yang and Peppard, 1994; Boyd-Bland et al., 1994). The fiber was kept in the headspace for 30 min to absorb the volatile compounds and attain equilibrium (Arthur et al., 1992).

2.3.2. GC/MS analysis

The headspace sample adsorbed on the SPME fiber was injected into a Hewlett-Packard (Agilent, Avondale, PA), 5890II gas chromatograph interfaced with a 5970 mass selective detector system. The volatiles were desorbed into the injection port for 5 min set at 200^{o}C using a 0.75 mm SPME liner. The injection mode was split-less for 2 min. The MS transfer line was held at 250°C and the GC programmed according to Mattheis et al. (1991). The carrier gas (Helium) velocity was set at 30.1 cm/s through the fused silica capillary column, a DB-1 (J&W, Folsom, CA, 60 m × 0.32 mm, thickness 0.32 μm). The various flavor compounds present in the

orange juice were identified based on comparison of GC retention indices and mass spectra of those contained in the Wiley/NBS library and with those of authentic compounds under the identical experimental conditions. The data were collected and analyzed using the HP Chemstation G 1034C data processing package. The reproducibility of flavor compounds analyzed by the SPME-GC/MS was assessed by analyzing diluted identical samples in replicates and reporting the percent relative standard deviation (% RSD).

2.3.3. Determination of response factors for major flavor compounds

A standard aqueous solution was prepared to determine the response factors for major volatile flavor compounds (ethanol, ethyl acetate, ethyl butanoate, hexenal, α-pinene, β-myrcene, sabinene, limonene, γ-terpinene, 1-octanol, decanal, dodecanal, citral, trans-geraniol, L-phellandrene, and valencene). The concentration of these components in the standard solution was compared to the results of Shaw (1991) and our preliminary experiment. The response factors of these components were obtained by dividing GC peak areas by concentrations of each standard component in the standard solution.

3. Results and Discussion

3.1. Temperature profiles

Fig. 1 shows the time-temperature history at the core and sub-surface of 'Valencia' oranges (18.9°C initial temperature) subjected to RF heating in saline water (0.004%), followed by holding at 48°C for 15 min before hydro-cooling for 30 min. The core temperature of the oranges after 5.5 min of RF heating at 10 kW power input was 46.4°C whereas surface temperature was 48°C. After 15 min of holding in hot water at 48°C, the core temperature was 47.6°C and it remained above 47°C for more than 15 min. The addition of salt insured that the

core temperature was not more than that of the treatment target temperature during RF heating to avoid prolonged exposure of the core to high temperatures.

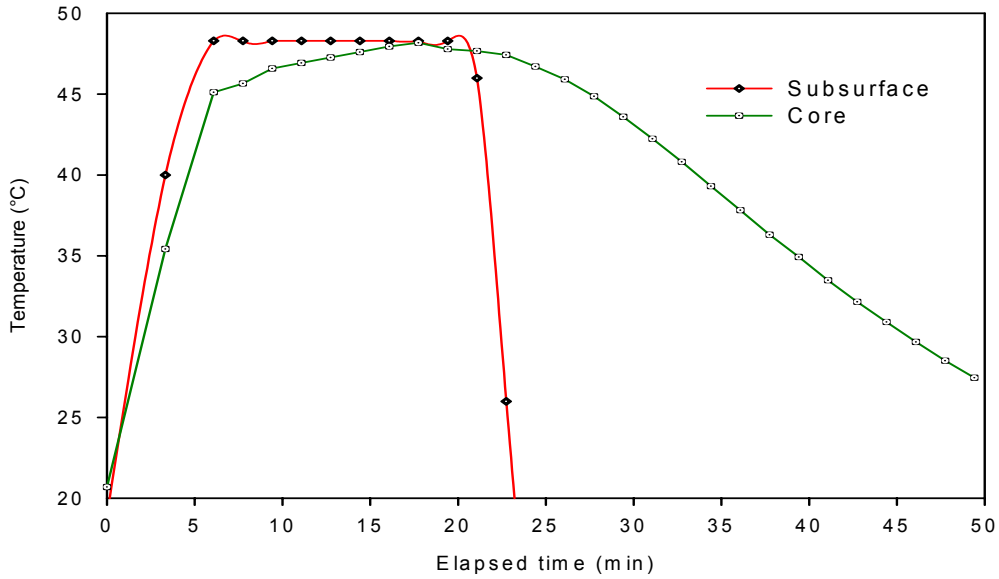

Fig. 1. Temperature-time history of subsurface (10 mm beneath surface) and core of the 'Valencia' oranges recorded during RF48°C+15 heat treatment. The oranges subjected to RF heating in 0.004% saline water for 5.5 min followed by holding at 48°C for 15 min before being cooled by 4°C water for 30 min

Fig. 2 shows time–temperature profile of the oranges subjected to preheating followed by RF heating. After 45 min of preheating at 35°C, core and subsurface (5 mm below the surface) temperatures were 29.6 and 34.6°C. Upon 2 min of RF heating in 35°C tap water with 10 kW input RF power, the core and subsurface temperatures were 46.4 and 48°C. The holding of oranges in hot water for 15 min at 48°C was carried out to insure the accumulation of thermal lethality at the core by heat transfer from hot spots to cold spots. Fig. 2 also shows the time–temperature profile of an orange subjected to 48°C hot water immersion for 2.5 h. Even after such a long exposure time core temperature of fruit was not higher than 47.2°C.

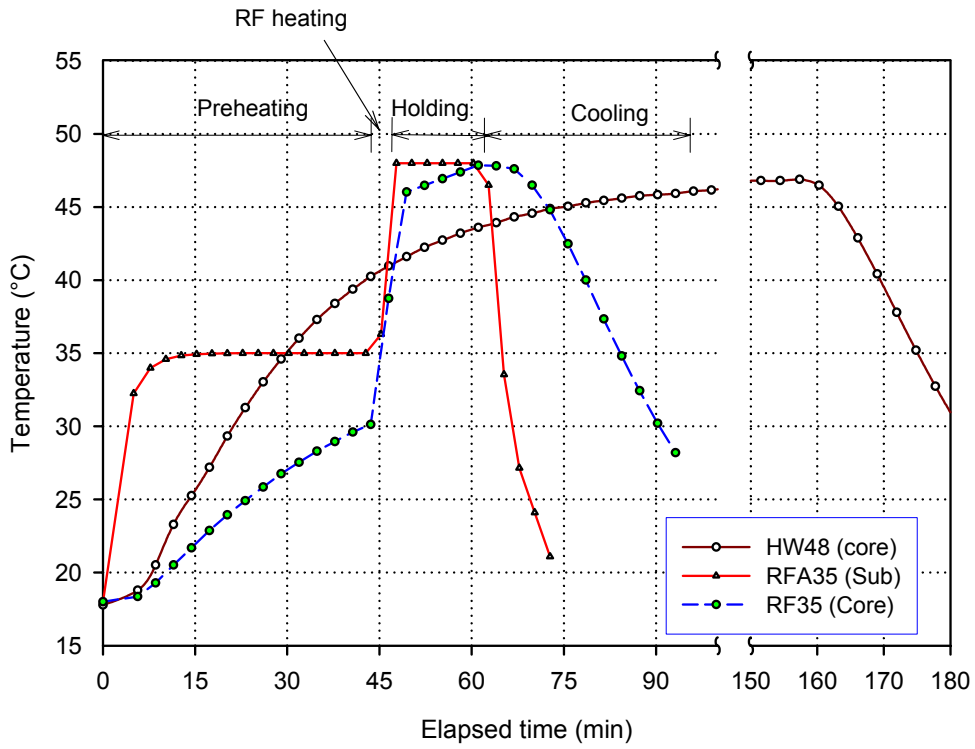

Fig. 2. Temperature-time history of 'Valencia' orange subsurface (10 mm beneath surface) and core subjected to HW48 and RFA35 (preheating in 35°C water for 45 min followed by RF heating in tap water for 2 min and holding at 48°C for 15 min) treatments

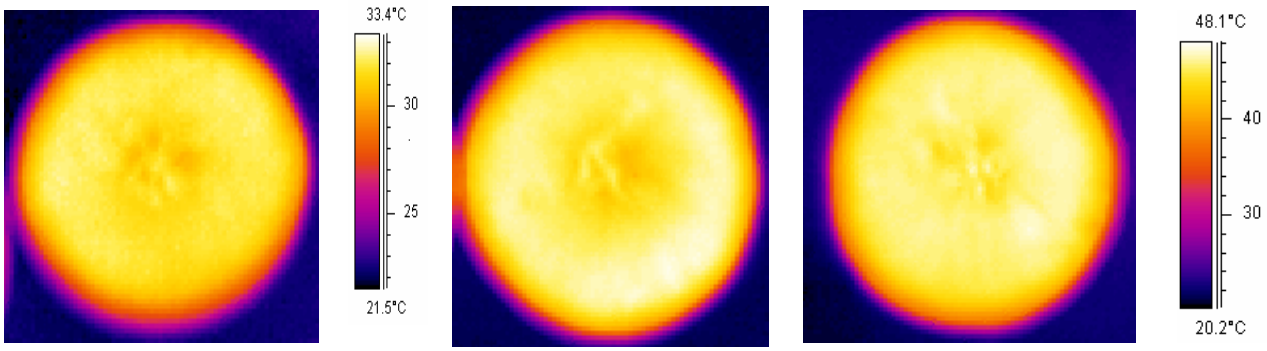

Preheating at 35°C for 45min RF heating to 48°C Holding for15 min at 48°C

Fig. 3. Thermal images of oranges taken by the infrared imaging camera during RF assisted hot water heat treatment at the end of preheating, RF heating, and holding time

Fig. 3 shows the thermal images of oranges taken during the RFA35 experiment (See Table 1); at the end of preheating, after RF heating and after holding for 15 min at 48°C. The preheating in hot water established a temperature gradient from surface to core. The preheating of the oranges insured that the core temperature remains below the treatment temperature (48°C) at the end of RF heating. A thermal image in Fig. 3 showed that 15 min holding at 48°C eliminated the temperature gradient and insured a uniform distribution of temperature in the orange. The mean temperature over the orange cross section was 47.4±1.2 and 47.8±0.3°C before and after holding, respectively.

3.2. Quality analysis

3.2.1. Weight loss

The percent weight loss after 10 days of cold humid storage (5^{o}C and 95% RH) was significantly higher in 'Navel' oranges (0.6–1.65 %) than 'Valencia' oranges (0.2–0.4 %) (Table 2). The higher weight loss in 'Navel' oranges was likely caused by no wax coating applied to oranges. Statistical analysis showed a significant effect of temperature on weight loss of the treated 'Navel'oranges. The weight loss was significantly high in all the treatments in comparison with control oranges (Table 2). Shellie and Mangan (1998) have reported that a hot water treatment (46°C for 3 h, storage for 4 weeks at 7°C and one week at 23°C) of oranges caused 10.45 % loss of moisture in comparison to 8.46% weight loss from untreated oranges. The weight loss in the 'Navel' oranges subjected to RF treatments corresponding to 48°C was (0.77–0.97 %) significantly less than (1.06–1.65%) that of treatments to which the oranges were subjected to 50 or 52°C (Table 2).

Table 2. Change in the postharvest physical quality traits of 'Navel' and 'Valencia' oranges upon 10 days of storage of oranges subjected to different thermal treatments.

Cultivar	Treatment	Weight loss (%)	Firmness change (%)	Peel color change (%)		
				L^*	h^o	C^*
Navel	Control	0.60±0.22 [a]	–8.98±9.86 [a]	99.07±1.61 [a]	99.34±2.00 [b]	100.41±2.36 [b]
	48°C+10 min	0.77±0.12 [b]	0.55±27.93 [ab]	98.85±2.04 [a]	101.09±3.02 [ab]	100.14±3.11 [bc]
	48°C+15 min	0.93±0.15 [c]	19.44±35.44 [bcd]	98.38±1.88 [ab]	102.02±2.94 [a]	100.68±2.94 [b]
	50°C+2 min	1.63±0.53 [e]	35.46±41.90 [cd]	98.47±1.88 [ab]	101.98±3.11 [a]	97.73±4.22 [cd]
	50°C+4 min	1.65±0.34 [e]	42.24±49.87 [d]	97.41±2.34 [bc]	102.09±2.98 [a]	97.15±3.74 [d]
	52°C+1 min	1.27±0.44 [de]	23.97±42.85 [bc]	97.40±2.36 [bc]	101.11±2.01 [a]	98.44±4.10 [bcd]
	52°C+2 min	1.32±0.34 [e]	16.16±23.32 [b]	97.41±2.56 [bc]	101.37±3.30 [a]	99.05±3.78 [bcd]
Valencia	Control	0.38±0.15[a]	–10.25±8.60 [a]	97.28±2.97 [a]	98.72±2.89 [a]	97.99±5.95 [bc]
	48°C +10min	0.36±0.13[a]	–12.49±14.09 [a]	98.08±2.35 [a]	99.30±2.62[a]	92.76±4.64 [d]
	48°C +15min	0.39±0.11[a]	–11.16±14.18 [a]	97.78±3.36 [a]	98.04±7.04 [a]	93.71±4.93 [cd]
	50°C+2 min	0.32±0.12[ac]	–13.26±9.99 [a]	97.25±3.81 [a]	101.37±6.36 [ac]	95.90±3.79 [c]
	50°C +4 min	0.36±0.10[ac]	–14.56±16.22 [a]	97.71±2.41 [a]	100.27±1.80 [a]	93.77±1.43 [d]
	HW48°C +155min	0.16±0.10[b]	–6.10±10.82 [a]	98.63±1.30 [a]	99.08±1.84 [a]	94.08±3.94 [cd]
	RFA35 +48°C+15min	0.24±0.06[bc]	–14.45±8.82 [a]	97.06±2.71 [a]	99.68±3.56 [a]	100.62±5.82 [ab]

[abc] Entries with different letters in same column of each cultivar are significantly different ($p<0.05$)

The application of wax coating on ‘Valencia’ oranges before storage improved moisture retention (Table 2). There was no significant weight loss in the ‘Valencia’ oranges subjected to RF heating in comparison with the control group. A significantly lower weight loss (0.16–0.24%) from ‘Valencia’ oranges subjected to HW48 or RFA35 treatments in contrast to control group (0.38%) was likely due to hydration of the orange cells during treatment, and later on retention of absorbed moisture by the wax coating. Therefore, for oranges with a wax coating, weight loss could not be used as a criterion for quality assessment as the negative effect of heat is masked by the wax coating.

3.2.2. Firmness

The loss/gain in firmness was expressed by the percentage change in firmness over the period of 10 days storage. Positive values suggest a loss in firmness and negative values show a gain in firmness upon treatment and storage. In ‘Navel’ oranges, the effect of heat was pronounced because of excessive weight loss during storage (Table 2). Except treatment RF48+10, all the other treatments caused significant loss in firmness in comparison to the control oranges. In case of ‘Valencia’ oranges, control and as well as treated oranges became firmer after 10 days of storage. There was no significant difference in firmness between control and treated oranges. This gain in firmness might be attributed to the wax coating that prevented moisture loss during storage. Even the oranges subjected to hot water treatment (HW48) did not lose firmness. Therefore, we conclude that prevention of moisture loss by the wax coating can maintain firmness.

3.2.3. Skin color

Change in skin color was calculated from the color measurement before and after 10 days of treatment. In ‘Navel oranges, L^* value of the peel was significantly lower in the oranges

subjected to a temperature of 50°C for more than 4 min or 52°C for more than 1 min in comparison to controls (Table 2). The lower value of L^* indicates a darker shade of peel color. Physical observation also suggested that 'Navel' oranges subjected to RF heat treatment at 50°C and 4 min or more holding time or exposure to 52°C lost the luster of peel surface. The loss of luster might be due to diffusion of peel essential oil from peel to hot water. The change in hue angle that signifies the shift toward yellow or red within the yellow to red quadrant was significantly high in all treatments except for the heat treatment RF48+10 (Table 2). The trend of chroma value or color intensity change was not clear but in most of the treatments the color intensity did not change significantly in comparison with the control oranges.

In 'Valencia' oranges peel color in terms of L^* did not change significantly for all treatments. The values of hue for all treatments were not statistically different from control oranges except for the treatment RF50+6 min. The color intensity of oranges was again found to be varying from treatment to treatment but in comparison with control oranges most of the treatments were not significantly different. The lowest color intensity was recorded for the treatment RF48+10 (Table 2).

3.2.4. Total soluble solids/Titratable acidity

There was no significant difference in the value of total soluble solids (TSS) for all treatments (data not shown). The mean value of TSS was 10.78±0.5 and 10.24±0.5 % for 'Navel' and 'Valencia' oranges, respectively. A sharp decrease in TA in heat-treated fruit may be an indication of heat damage (Schirra et al., 2005). But in the present study we did not find a significant difference in values of TA for all heat treatments in comparison with the control (data not shown). The mean value of acidity in treated oranges were 0.98±0.04 and 1.04±0.05 g/100 ml for 'Navel' and 'Valencia' oranges, respectively.

3.2.5. Visual observations

In the present study we observed incidences of decay and off-flavor development in the peel of oranges subjected to HW48 treatment. Shellie and Mangan (1998) reported that hot water heating (46°C for 4 h) of oranges inflicted deleterious effects on fruit flavor, and decay incidence. McGuire (1991) also reported a higher incidence of decay and off-flavor development in grapefruits that were subjected to hot water (48°C for 3 h) than in grapefruits treated by forced hot air at 48°C. The RF heat treatments did not cause any visible peel damage except for treatments at 52°C. Control oranges showed the onset of stem rot after 10 days of cold-humid storage. Upon 10 days of storage 12 % of control oranges, 22 % of HW48 and 8 % of RF52 treated oranges were found with some decay. The onset of stem rot in untreated control oranges was likely due to a large load of active pathogens, whereas an increased incidence of decay in heat-treated oranges, HW48 and RF52 was likely due to pathogens invading areas on the fruit injured by heat treatment. Mulas et al. (2001) studied the response of 'Tarocco', 'Moro', 'Sanguinello' and 'Doppio sanguigno' blood oranges to hot water heat treatment. They observed that a fruit core temperature of 44°C for 100 min or 46°C for 50 min did not induce visible damage to the fruit, but inflicted deleterious effects on quality attributes such as the development of off-flavors and off-taste, decreased fruit firmness and reduced fruit resistance to decay.

A distinct oily odor from the peel of 'Valencia' oranges was detectable by the nose in all heat treatments, however, such odor was not detected from 'Navel' oranges. The impairment of water-gas exchange by the wax coating has been studied by Cohen et al. (1990) and Baldwin et al. (1995), who reported the notable increase in the synthesis of volatiles associated with anaerobic conditions, such as ethanol, methanol, and acetaldehyde which might be the reason behind off flavors development. Secondly, the movements and rotations of oranges during RF

heating in the fruit mover might have caused peel bruising that could lead to phenomenon called O*leocellosis* –oil spotting on orange peel. This is a common peel injury of citrus fruit that is usually caused by mechanical damage that forces the toxic oil out of the oil glands. This oil kills nearby parenchyma, epidermal and subepidermal cells of the flavedo. Cells killed by oil are readily invaded by fungi resulting in increased decay (Wardowski et al., 2004). In the present study the distinct flavor development in 'Valencia' orange peel might be attributed to the combined effect of the wax coating and bruised peel oil glands. This speculation was based on the observation that no distinct off flavors from the peel of untreated, waxed 'Valencia' oranges were detected. A consideration of mechanical damage is very important in designing a system for the handling and movement of citrus fruit.

3.3. Flavor analysis

Tables 3 and 4 show the concentrations of the major volatile compounds identified in the 'Navel' and 'Valencia' orange juice samples using SPME and GC/MS techniques after treatment and 10 d of cold storage. The last row in the tables shows the percent relative standard deviation (% RSD) in each treatment for all the volatile components. In calculation of the % RSD, acetaldehyde and ethanol were excluded because of the fact that we could not accurately quantify these components in every sample since the peaks representing these components were often too small and too poorly resolved for accurate determinations. Therefore, the concentrations of acetaldehyde and ethanol may not be accurate. However, the areas were averaged for the replicates whose peaks had large enough values so we might view the effect of different heat treatments on these compounds. The values of RSD (<10 %) indicated excellent reproducibility of SPME-GC/MS analysis under the analytical conditions used. This level of reproducibility was adequate enough to separate the effect of different heat treatment regimes on the flavor

compounds. The quantitative values determined for the terpenes, esters, alcohols, and aldehydes listed in Table 4 are in agreement with reported literature values for most of the compounds found in hand squeezed unheated orange juice (Shaw, 1986; Nisperos-Carriedo and Shaw, 1990). The data in Table 4 also lists the odor threshold (OT, ppm, in water) of the major compounds as compiled by Rychlik et al. (1998).

The GC-MS analysis of untreated orange juice showed that typical citrus-like flavor was contributed by more than 31 volatile components present in varying quantities. Among those 31 flavor compounds, 16 major volatiles were selected and quantified based on their abundance in the juice and contribution in overall citrus flavor. Sizer et al. (1988) broadly categorized volatile orange flavor compounds and reported that 75–98% of flavor compounds are hydrocarbons, 0.6–1.7% aldehydes, 1% esters, 1% ketones, and 1–5% alcohols. In the present study the volatile compounds identified in the juice of both 'Navel' and 'Valencia' orange varieties were similar but abundance of many volatiles were higher in 'Navel' oranges (Tables 3 and 4).

The volatile compounds responsible for the delicate, fruity flavor of orange, including ethyl butanoate, ethyl hexanoanate, octanal (Amhed et al., 1978) were present in relatively low quantities in untreated oranges. These compounds have very low odor thresholds (ppb range) thus making them indispensable for the fresh orange flavor (Table 4). Upon heat treatments all of these components were diminished to a level at which detection and quantitation by the present method was not reproducible. Ethyl butanoate is the major volatile ester in orange juice and it is an important contributor to desirable top-notes in orange flavor (Ahmed et. al., 1978).

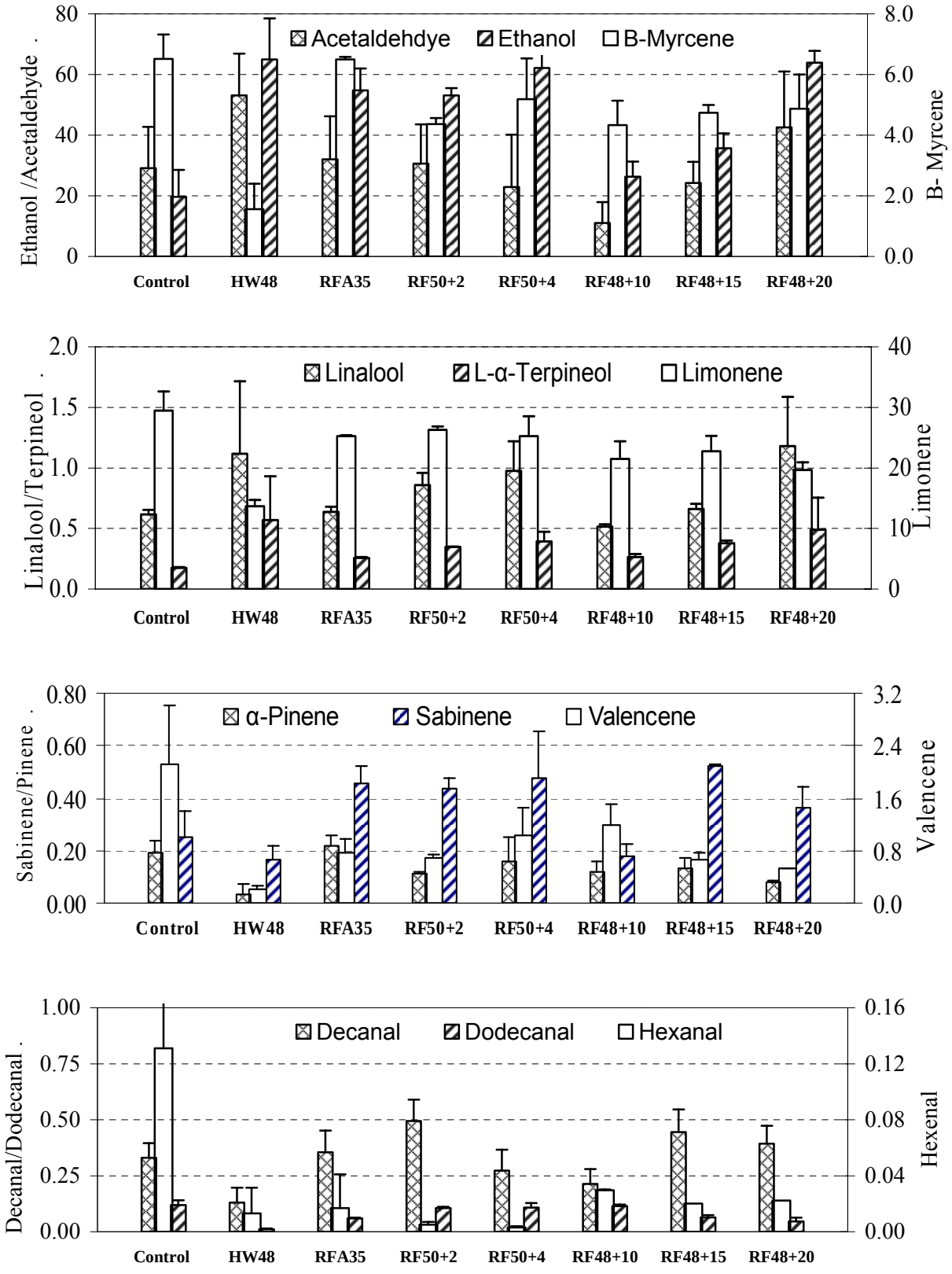

Fig. 4. Volatile compounds concentration (µg/ml, ppm) in 'Valencia' oranges subjected to different heat treatments (temperature + holding, min) and 10 days of cold storage

Table 3. Concentration (μg/ml) of the major volatiles compounds quantified using the SPME-GC/MS technique in 'Navel' oranges subjected to different RF heat treatment regimes and 10 days of cold storage

Volatile Compound	LV μg/ml	Control	52°C		50°C		48°C	
			1 min	2 min	2 min	4 min	10 min	15 min
Acetaldehyde	3–8.5[a]	38.6±3.8	39.8±36.7	41.7±12.6	40.5±41.6	37.5±20.3	35.3±5.4	45.8±8.3
Ethanol	64–900[a]	57.0±19.2	67.9±13.6	79.9±43.8	81.9±48.5	102.8±15.6	107.3±12.0	79.0±24.1
Ethyl Acetate	0.01–0.58[b]	0.11±0.03	0.05±0.01	0.02±0.02	ND	0.05±0.00	0.01±0.01	0.04±0.00
Hexanal	0.02–0.65[a]	0.06±0.01	0.01±0.00	0.00±0.00	0.02±0.00	0.02±0.01	0.02±0.02	0.02±0.00
Ethyl Butanoate	0.26–1.02[b]	0.66±0.14	0.02±0.01	0.01±0.02	0.13±0.18	0.10±0.06	0.12±0.04	0.09±0.05
α-Pinene	0–0.22[b]	0.75±0.10	0.26±0.06	0.24±0.15	0.27±0.05	0.21±0.06	0.61±0.01	0.70±0.02
Sabinene	0–0.15[b]	0.64±0.04	0.93±0.15	0.84±0.21	1.17±0.31	0.88±0.41	0.69±0.20	0.62±0.21
β-Myrcene	1.54[c]	17.5±1.1	10.5±1.7	11.4±0.5	15.5±2.6	12.2±1.7	12.8±0.8	12.8±1.8
Limonene	1–278[a]	61.2±4.1	39.6±3.9	38.0±3.0	54.4±2.9	42.8±2.1	58.0±9.4	53.2±3.2
γ-Terpinene	0.04–0.46[b]	0.01±0.02	0.02±0.03	0.05±0.01	0.12±0.04	0.08±0.10	0.05±0.02	0.04±0.03
Linalool	0.15–4.6[a]	0.58±0.18	0.95±0.19	1.23±0.42	1.11±0.15	1.14±0.25	0.95±0.05	1.23±0.09
L-α-Terpineol	0.09–1.1[a]	0.30±0.05	0.69±0.07	0.70±0.19	0.73±0.12	0.66±0.14	0.64±0.08	0.67±0.05
Decanal	0.01–0.15[a]	0.83±0.26	1.50±0.95	1.83±0.88	1.25±0.27	1.78±0.71	1.11±0.39	2.09±0.62
Dodecanal	NA	0.11±0.05	0.29±0.07	0.27±0.20	0.68±0.75	0.20±0.14	0.22±0.01	0.35±0.02
Valencene	0.8–15[b]	1.57±0.39	1.16±0.45	1.32±0.76	1.73±0.10	1.30±0.52	1.26±0.29	1.16±0.18
RSD (%)		11.5	13.5	11.5	9.7	9.9	14.8	8.5

LV – Literature values cited from [a]– *Shaw (1986),* [b] – *Nisperos-Carriedo & Shaw (1990),* [c] – Stephen & Pawliszyn (1996) ND – Not detected

Table 4. Concentration (μg/ml) of the major volatile compounds quantified using the SPME-C/MS technique in 'Valencia' oranges subjected to different heat treatment regimes and 10 days of cold storage.

Volatile Compounds	Retention time, min	LV μg/ml	OT ppm	Control μg/ml	HW48°C (2.5 hr)	RFA35 48°C+15 min	RF 50°C 2 min	RF 50°C 4 min	RF 48°C 10 min	RF 48°C 15 min
Acetaldehyde	3.83	3–8.5[a]	0.01[a]	29.1±13.6	53.1±13.7	32.1±14.2	30.7±12.8	22.9±17.3	11.0±6.9	24.2±7.0
Ethanol	4.30	64–900[a]	NA	19.7±8.8	64.9±13.5	54.8±7.2	53.1±2.5	82.2±77.0	26.3±5.0	35.7±4.9
Ethyl Acetate	6.03	0.01–0.58[b]	0.5	0.05±0.01	ND	ND	ND	ND	0.04±0.00	0.02±0.00
Hexanal	13.4	0.02–0.65[a]	0.015	0.13±0.08	0.01±0.02	0.02±0.02	0.01±0.00	0.00±0.00	0.03±0.00	0.02±0.00
Ethyl Butanoate	14.0	0.26–1.02[b]	0.001	0.52±0.06	0.12±0.08	0.21±0.02	0.03±0.00	0.02±0.02	0.27±0.12	0.18±0.00
α-Pinene	22.1	0–0.22[b]	0.030	0.19±0.05	0.04±0.03	0.22±0.04	0.12±0.00	0.16±0.09	0.12±0.04	0.14±0.03
Sabinene	23.8	0–0.15[b]	NA	0.25±0.10	0.16±0.06	0.45±0.07	0.43±0.04	0.48±0.18	0.18±0.05	0.52±0.01
β-Myrcene	24.7	1.54[c]	0.016	6.51±0.80	1.56±0.84	6.50±0.08	3.36±0.20	5.18±1.35	4.33±0.80	4.74±0.25
Limonene	26.7	1–278[a]	0.034	29.5±3.1	13.7±1.1	25.3±0.1	26.3±0.6	25.2±3.3	21.5±2.9	22.8±2.5
1-Octanol	27.5	NA	NA	0.06±0.00	0.08±0.09	0.05±0.01	0.11±0.02	0.06±0.04	0.06±0.00	0.09±0.00
γ-Terpinene	27.7	0.04–0.46[b]	NA	0.03±0.02	0.02±0.00	0.04±0.00	0.03±0.04	0.02±0.02	0.01±0.02	0.05±0.01
Linalool	28.9	0.15–4.6[a]	0.001	0.61±0.04	1.12±0.60	0.64±0.04	0.86±0.10	0.98±0.24	0.51±0.02	0.66±0.04
L-α-Terpineol	32.0	0.09–1.1[a]	NA	0.17±0.01	0.57±0.36	0.26±0.01	0.35±0.00	0.39±0.08	0.26±0.03	0.38±0.02
Decanal	32.33	0.01–0.15[a]	0.007	0.33±0.07	0.13±0.07	0.35±0.10	0.49±0.10	0.27±0.09	0.21±0.07	0.44±0.10
Dodecanal	38.57	NA	NA	0.12±0.02	0.01±0.00	0.06±0.00	0.11±0.01	0.11±0.02	0.11±0.01	0.06±0.01
Valencene	41.51	0.8–15[b]	NA	2.11±0.89	0.20±0.06	0.76±0.22	0.70±0.03	1.03±0.41	1.19±0.31	0.67±0.11
RSD (%)	--	--		13.9	21.6	2.8	20.8	4.0	15.7	9.8

OT – Odor threshold, data complied by Rychlik et al. (1998), ND – Not detected., NA – Not available

LV – Literature values cited from: a –Shaw (1986), b – Nisperos-Carriedo & Shaw (1990), c – Stephen & Pawliszyn (1996)

A general decrease in the amount of this ester is associated decreased fresh orange flavor quality (Nisperos-Carriedo and Shaw, 1990). In both varieties ethyl butanoate levels were somewhat reduced by the heat treatments (Tables 3 and 4). Heat is known to inactivate enzyme systems responsible for the synthesis of esters, but a study by Fallik et al. (1997) on apple suggested that heat treatment only temporarily inhibits aroma volatile emission, mainly esters. Therefore we would expect to see renewed biosynthesis of ethyl butanoate upon long term storage of treated oranges.

Heat treatments led to significant changes in acetaldehyde and ethanol concentrations. In the most severe heat treatment i. e., HW48 ethanol and acetaldehyde increased 2 to 3 fold (Table 4). An increase in the concentrations of the ethanol and acetaldehyde were least in the oranges subjected to heat treatment RF48+10 and RF48+15 in comparison with other heat treatments. Ethanol build-up after heat treatment is a well-documented trend shown in the literature

A study by Schirra and D'hallewin (1997) showed a two-fold increase of ethanol level in oranges after a heat treatment at 58° C for 3 minutes. In the present study we also observed the same trend of increased ethanol with increasing holding time and temperature particularly in 'Navel' oranges (Table 4). Ethanol buildup might be attributed to long exposure at high temperature, which increases the respiration rate leading to onset of the anaerobic pathway. Ethanol concentration was also considerably higher in the oranges subjected to RFA35 and HW48 heat treatments (Table 4). Obenland et al. (1999) reported that oranges exposed to 48.5°C forced air heating for more than 200 min (47.2°C core temp) caused a large increase in ethanol build up in the range of 1200 μg/ml. Though ethanol enhances other flavors, its build-up, along with acetaldehyde will lead to an off-flavor in oranges (Cohen et al., 1990).

Limonene was the most abundant volatile component in orange juice. 'Navel' oranges contained two times more limonene than 'Valencia oranges (Tables 3 and 4). The loss of limonene in thermal treatments was observed, but losses were very high (30–50%) for heat treatments HW48, RF52 and RF48+20 min (Tables 3 & 4, and fig. 4). The compound α-terpineol is a thermal degradation product of limonene and it is a known contributor to the off-flavor in orange juice at levels of 2 ppm or higher (Tatum et al., 1975). It is evident from a trend shown in Fig. 4 that decrease in limonene is associated with spiking in volatiles such as linalool and L-α-terpineol. The quantity of these components dramatically increased by more than two times in the oranges subjected to either HW48 or RF heating at 52°C (Fig. 4 & Table 3). A reduction in important flavor components and increases of linalool and L-α-terpineol concentrations upon heat treatment could be a possible explanation for poor orange juice flavor quality (Nisperos-Carriedeo and Shaw, 1990). The oranges subjected to RFA35 and RF48+10&15 heat treatments showed the minimum increase in these two components (Fig. 4).

Other significant volatile hydrocarbons influenced by heat treatment include α-pinene, sabinene, β-myrcene and valencene. The flavor compound α–pinene has a positive contribution to flavor, whereas valencene has a citrus-like aroma and sabinene contributes a warm, spicy aroma and flavor (Arctader, 1969). The flavor of β-myrcene has a musty geranium odor (Högnadòttir and Rouselff, 2003). In the present study the heat treatments RF50, RF52 and HW48 reduced α-pinene amount by half and β-myrcene by more than 25% (Tables 3 and 4). The effect of heat treatment on sabinene was not consistent; therefore a definite conclusion could not be drawn. The amount of valencene was found to slightly decrease with severity of heat treatments and maximum loss was observed in oranges treated by HW48 (Table 4). Obenland et

al. (1999) reported a substantial loss of α -pinene, β-myrcene and limonene in oranges subjected to 48.5°C high-temperature forced-air over 200 minutes.

The aldehyde hexenal, believed to contribute green, grassy orange notes, was found to decrease substantially upon heat treatments (Tables 3 and 4, and Fig. 4). Another aldehyde, decanal, contributes to the green soapy flavors in oranges (Buettner and Schieberle, 2001) was found more in 'Navel' orange (0.8 ppm) than that of 'Valencia' orange (0.33 ppm). However, Ahmed et al. (1978) found that 0.72 ppm of decanal made a negative contribution to orange juice flavor. In the present study we observed a large increase in decanal after heat treatments of 'Navel' oranges whereas heat treatments of 'Valencia' oranges did not show a consistent trend (Table 3 and 4). Obenland et al. (1999) reported an abrupt increase in the amount of decanal in oranges exposed to humid hot air of 48.5°C up to 3 hrs, but this started decreasing with further increase in exposure time.

The effect of heat treatments on some volatiles that are abundant in peel oil such as decanal, myrcene, sabinene, linalool, and limonene, should be interpreted with caution because during sample preparation some portion of the peel oil might have mixed with juice. This is due to the fact that heat-treated oranges required more hand pressure to squeeze juice from the vesicles and so peel oil might be squeezed out too. The heat might change cell wall structure and results in less extractability of juice from the sacs.

The flavor analysis enabled us to choose RF48+15 and RFA35 as potential RF heat treatments that merit further investigations for complete treatment protocol development. In the present study, the advanced SPME GC-MS technique was used for detection and quantification of the volatile components in orange juice. However, due to the extremely low concentrations of potent orange juice odorants such as methyl and ethyl esters, hexenal, octanal, etc., direct

identification and quantitation in the headspace by means of instrumental methods such as GC-MS is sometimes difficult (Buettner and Schieberle, 2001). Therefore the high sensitivity of the human nose and taste buds should be employed in a confirmatory test using sensory evaluation techniques to judge consumer acceptability of RF heat-treated oranges.

With the thermal death kinetic information for Medfly (Gazit et al., 2004) and the treatment conditions determined in this study to minimize quality changes in oranges, our next logical step will be validation by conducting in-vitro efficacy studies at Hilo (HI), USA. on infested orange fruit with the treatment conditions determined in this study.

4. Summary

RF heating was explored as a means to expedite the internal heating rate of oranges in the hot water treatment in order to decrease exposure time. The selection of time and temperature combinations for different RF heat treatments was based on the thermal death kinetics study of the Medfly. We hypothesed that a reduction in exposure time at elevated temperature would retain the postharvest quality of the treated oranges. But slow cooling after RF heating resulted in more quality damage at 52°C even for very short time exposures than at 48°C for 20 min. Considering the overall analysis of quality attributes such as color, firmness, weight loss and change in flavor components, RF treatment corresponding to a target temperature of 48°C and holding for 15 min seems to be the best case scenario. If we consider the overall prospect for developing an RF heating process, hot water preheating followed by RF heating treatment seems to be the best option for practical implementation. To validate optimal RF heat treatments, further confirmative studies are required on sensory evaluation, simulated marketing period storage, and consumer acceptability. Based on results of our previous and present studies, a next

logical step will be an efficacy test. This test is an essential step for validation of the RF heat treatment protocol.

References

Ahmed, E. M., Dennison, R. A., Dougherty, H., Shaw, P. E., 1978. Effect of selected oil and essence volatile components on flavor quality of pump-out orange juice. J. Agric. Food Chem. 26(2), 368–372.

Arctander, S., 1969. Perfume and flavor chemicals. Vol. I & II, Montclair. NJ.

Arthur, C. L., Killam, L. M., Buchholz, K. D., Pawliszyn, J., 1992. Automation and optimization of solid-phase microextraction. Anal. Chem. 64, 1960–1966.

Baldwin , E. A., Nisperos-carriedo, M., Shaw, P. E., Burns, J. K., 1995. Effect of coatings and prolonged storage conditions on fresh orange flavor volatiles, degree brix, and ascorbic acids levels. J. Agric. Food Chem. 43, 1321–1331.

Birla, S. L., Wang, S., Tang, J., 2004. Improving heating uniformity of fresh fruit in radio frequency treatments for pest control. Postharvest Biol. Technol. 33, 205–217.

Boyd-Bland, A. A., Chai, M., Luo, Y. Z., Zhang, Z., Yang, M. J., Pawliszyn, J. B., Gorecki, T., 1994. New solvent–free preparation techniques based on fiber and polymer technologies. Environ. Sci. Technol. 28, 596A.

Buettner, A., Schieberle, P., 2001. Evaluation of aroma differences between hand-squeezed juices from Valencia late and navel oranges by quantitation of key odorants and flavor reconstitution experiments. J. Agric. Food Chem. 49, 2387–2394.

Cohen, E., Shalom, Y., Rosemberg, I.,1990. Postharvest ethanol buildup and off-flavor in 'Murcott' tangerine fruits. J. Am. Soc. Hortic. Sci. 115, 775–778.

Fallik, E., Archbold, D. D., Hamilton-Kemp, T. R., Loughrin, J. H., Collins, R. W., 1997. Heat treatment temporarily inhibits aroma volatile compound emission from Golden Delicious apples. J. Agric. Food Chem. 45, 4038–4041.

Frings, H., 1952. Factors determining the effects of radio-frequency electromagnetic fields and materials they infest. J. Econ. Entomol. 45, 396–408.

Gazit, Y., Rossler, Y., Wang, S., Tang, J., Lurie, S. 2004. Thermal death kinetics of egg and third-instar mediterranean fruit fly. J. Econ. Entomol. 97(5), 1540–1546.

Headlee, T.J., Burdette, R.C., 1929. Some facts relative to the effect of high frequency radio waves on insect activity. J. New York Entomol. Soc. 37, 59–64.

Högnadòttir, Ă., Rouselff, R. L., 2003. Identification of aroma active compounds in orange essence oil using gas chromatography – olfactometry and GC/MS. J. Chrom. A 998, 201–211.

Lurie, S., 1998. Review : Postharvest heat treatments. Postharvest Biol. Technol., 14, 257–269.

Lurie, S., Jemric, T., Weksler, A., Akiva, R., Gazit, Y., 2004. Heat treatment of 'Oroblanco' citrus fruit to control insect infestation. Postharvest Biol. Technol. 34, 321–329

Mattheis, J.P. Fellman, J.K., Chen, P.M., Patterson, M.E., 1991. Changes in headspace volatiles during physiological development of Bisbee Delicious apple fruit. J. Agric. Food Chem. 39(11), 1902–1906.

McGuire, R. G., 1991. Market quality of grapefruit after heat quarantine treatments. Hortsci. 26, 1193–1395.

Mulas, M., Perinu, B., Francescani, A. H. D., D'hallewin, G., Schirra, M., 2001. Quality of blood oranges following heat treatments for disinfestingfruit fly. In: Arte´ s, F., Gil, M. I., Conesa, M. A. (Ed.), Improving Postharvest Technologies of Fruits, Vegetables and Ornamentals, 740–745.

Nelson, S.O., Payne, J.A., 1982. RF dielectric heating for pecan weevil control. Trans. ASAE 31, 456–458.

Nisperos-Carriedo, M. O., Shaw, P. E., 1990. Comparison of volatile components in fresh and processed orange juices. J. Agric. Food Chem. 38, 1048–1052.

Obenland, D. M., Arpaia, A. L., Austin, R. K., MacKey, B. E., 1999. High-temperature forced air treatment alters the quantity of flavor-related, volatile constituents present in navel and Valencia oranges. J. Agric. Food Chem. 47, 5184–5188.

Rychlik, M., Schieberle, P. Grosch, W., 1998. Compilation of odor threshold, odor qualities and retention indices of key food odorants, Deutsche Forschungsanstalt Fuer Lebensmittelchemie: Garching, Germany.

Schirra, M., D'hallewin, G., 1997. Storage performance of Fortune mandarins following hot water dips. Postharvest Biol. Technol. 10, 229–238.

Schirra, M., Mulas, M., Fadda, A., Mignani, I., Lurie, S., 2005. Chemical and quality traits of 'Olinda' and 'Campbell' oranges after heat treatment at 44 or 46 °C for fruit fly disinfestations. Lebensm.-Wiss. u.-Technol.38(5), 517–527.

Sharp, J. L., MacGuire, R. G., 1996. Control of Caribbean fruit fly (Diptera: Tephritidae) in Navel orange by forced hot air. J. Econ. Entomol. 89(5), 1181–1185.

Shaw, P. E., 1986. The flavor of non-alcoholic fruit beverages. In Food Flavors. Part B. The Flavors of Beverages; Morton, E. D., Macleod, A. J., Eds.; Elsevier: Amsterdam, pp. 337–368.

Shaw, P. E., 1991. Fruit II. In Maarse, H. (Ed), Volatile Compounds in Foods and Beverages, New York, Dekker, pp. 305–328.

Shellie, K. C., Firko, M. J., Mangan, R. L., 1993. Phytotoxic response of 'Dancy' tangerine to high-temperature, moist, forced-air, treatment for fruit fly disinfection. J. Am. Soc. Hortic. Sci., 118, 481–485.

Shellie, K. C., Mangan, R. L., 1994. Postharvest quality of Valencia orange after exposure to hot, moist, forced air for fruit fly disinfestation. HortSc. 29, 1524–1527.

Shellie, K. C., Mangan, R. L. 1998. Navel orange tolerance to heat treatments for disinfesting Mexican fruit fly. J. Am. Soc. Hortic. Sci. 123, 288–293.

Sizer, C.E., Waugh, P. L., Edstam, S., Ackerman, P.,1988. Maintaining flavor and nutrient quality of aseptic orange juice. Food Technol. 42, 152–159.

Steffen, A., Pawliszyn, J., 1996. Analysis of flavor volatiles using headspace solid-phase micro-extraction. J. Agric. Food Chem. 44, 2187–2193.

Tang, J., Ikediala, J.N., Wang, S., Hansen, J., Cavalieri, R. P., 2000. High-temperature-short-time thermal quarantine methods. Postharvest Biol. Technol. 21, 129–145.

Tatum, J. H., Nagy, S., Berry, R. E., 1975. Degradation products formed in canned single-strength juice during storage. J. Food Sci. 40, 707–709.

[USEPA] United States Environmental Protection Agency, 1998. Reregistration Eligibility Decision. Aluminum and Magnesium Phosphide. Cases 0025 and 0645. Office of Pesticide Programs, Special Review and Reregistration Division. Agricultural Statistics. Washington, DC.

Wang, S., Ikediala, J.N., Tang, J., Hansen, J.D., Mitcham, E., Mao, R., Swanson, B., 2001a. Radio frequency treatments to control codling moth in in-shell walnuts. Postharvest Biol. Technol. 22, 29–38.

Wang, S., Tang, J. Cavalieri, R.P., 2001b. Modeling fruit internal heating rates for hot air and hot water treatments. Postharvest Biol. Technol. 22, 257–270.

Wang, S., Tang, J., Johnson, J.A., Mitcham, E., Hansen, J.D., Cavalieri, R. P., Bower, J., Biasi, B., 2002. Process protocols based on radio frequency energy to control field and storage pests in in-shell walnuts. Postharvest Biol. Technol. 26, 265–273.

Wang, S., Tang, J., Cavalieri, R.P., Davis, D., 2003. Differential Heating of insects in dried nuts and fruits associated with radio frequency and microwave treatments. Trans. ASAE 46, 1175–1182.

Wardowski, W. F., Petracek, P. D., Grierson, W., 2004. Oil spotting (Oleocellosis) of citrus fruit, http://edis.ifas.ufl.edu/BODY_CH119.

Williams, P., Hepworth, G., Goubran, F., Muhunthan, M., Dunn, K., 2000. Phosphine as a replacement for methyl bromide for postharvest disinfestation of citrus. Postharvest Biol. Technol. 19, 193–199.

Yang, X., Peppard, T,. 1994. Solid-phase microextraction for flavor analysis. J. Agric. Chem. 42, 1925–1930.

Zhao, Y., Flugstad, B., Kolbe, E., Park, J. W., and Wells, J. H., 2000. Using capacitive dielectric heating in food processing and preservation – a review. J. Food Process Eng. 23, 25–55.

C H A P T E R 6

POSTHARVEST TREATMENT TO CONTROL CODLING MOTH IN FRESH APPLES USING WATER ASSISTED RADIO FREQUENCY HEATING

Wang S., Birla S.L., Tang J., Hansen, J.
Published in Postharvest Biology and Technology, 40(1), 89–96, 2006

Abstract

The present study explored the application of radio frequency (RF) energy in conjunction with conventional hot water treatment to develop feasible heat treatments. Treatment parameters were selected based minimum time-temperature conditions required for 100% mortality of fifth-instar codling moth and influence on apple quality. The treatments included preheating infested or wholesome apples in warm water at 45°C for 30 min. The preheated apples were then heated to 48°C in a hydraulic fruit mover placed between two parallel plate electrodes in a 12 kW 27.12 MHz pilot scale RF system. RF treated apples were transferred to a 48°C hot water bath and held for 5, 10, 15 and 20 min before being hydro-cooled in ice water for 30 min. The mortality of codling moths in the infested apples was assessed, and the quality of wholesome apples was evaluated by measuring weight loss, firmness, color, soluble solids content, and titratable acidity after 0, 7, and 30 days of storage at 4°C. The results showed that the treatment at 48°C for 15 min was the most practical and effective both for insect control and apple quality. However flavor analysis using SPME-GC technique has shown that there was a huge change in volatile flavor profiles in treated apples. We kept treated apple for beyond 30 days and found that in the heat treated apples incidence of decay was very high. Hence, either lower treatment temperature combined with controlled atmospheric storage should be explored for practical RF energy based treatment.

Keywords: Apple, Codling moth; Heat; Quality; Quarantine; Radio frequency

1. Introduction

The exportation of fresh apples in the United States is mainly destined for Japan and South Korea (USDA-NASS, 2004). These countries require quarantine treatments against codling moth, Cydia pomonella L. (Lepidoptera: Tortricidae). Methyl bromide (MeBr) is used in commercial treatments against codling moth in fresh products (Guance et al., 1981; Yokoyama et al., 1990; Moffitt et al., 1992; Hansen et al., 2000). Although MeBr fumigation for postharvest quarantine treatments is currently exempted from legal restrictions, the future for MeBr usage is questionable because of price increases, complicated approval process of the exempted use, and further restrictions under international regulations (USEPA, 1998). Therefore, there is a need to develop non-chemical quarantine treatment alternatives for international trade of apples.

Heat treatments are studied in laboratories to disinfest fresh horticultural products from quarantine pests, such as codling moth and fruit flies, before entering export-marketing channels (Armstrong, 1994; Feng et al., 2004; Hansen et al., 2004). Some heat treatments have been approved by the USDA Animal Plant Health Inspection Service as quarantine treatments against the eggs and larvae of targeted fruit fly pests in a number of tropical fruit, including mango, citrus and papaya (USDA-APHIS-PPQ, 2002). Heat treatments are relatively easy to apply, leave no chemical residues, and can be fungicidal. However, accomplishing disinfestation without causing deleterious effects to fruit quality is a challenging task (Armstrong, 1994). In conventional heating with water or air, the rate of thermal energy delivered to the interior of the commodities is significantly influenced by fruit size (Wang et al., 2001b). Fresh fruit are sensitive to heat and often a slight deviation from the required time and temperature would result in either unacceptable fruit quality or insect survival.

To shorten treatment time and, thereby, minimize thermal impact on fruit quality, radio frequency (RF) heating has been suggested for control of postharvest insects (Andreuccetti et al., 1994; Hallman and Sharp, 1994; Nelson, 1996; Tang et al., 2000). Recently, pilot-scale RF treatment protocols have been developed for control of codling moth (Wang et al., 2001a) and navel orangeworm (Wang et al., 2002b; Mitcham et al., 2004) in in-shell walnuts with acceptable product quality. A joint university and industry project in summer 2005 that involved scientists and engineers from Washington State University, University of California, Davis, US Department of Agriculture, Strayfield Fastran, Inc. (UK), and Diamond Walnut Co. (Stockton, CA) has successfully demonstrated that large commercial continuous RF treatments can be designed based on pilot-scale protocols to effectively control navel orangeworm, the most heat resistant field and storage pests among codling moth, Indian meal both and red flour beetle (Johnson et al., 2004), in in-shell walnuts without causing quality losses.

It is also desirable to explore the possibility of developing a short time pilot-scale heat treatment for disinfesting apples using RF energy. To avoid overheating at the contact points between fresh fruit, water immersion is used in RF heating (Ikediala et al., 2002; Birla et al., 2004). That is, fresh fruit are immersed in tap water while heated in RF systems. Since dielectric loss factors of fresh fruit are higher than those of tap water at the RF range (Wang et al., 2003), the fruit may absorb much more RF energy than the tap water, thus resulting in different heating rates. A core-focus heating in fresh fruit is observed in RF heated fruit in tap water (Ikediala et al., 2002; Birla et al., 2004). Matching electrical conductivity of the water with that of fruit pulp may help to improve the non-uniformity between the surface and the core (Birla et al., 2004). But the observed heating uniformity is not adequate to allow the development of a practical treatment for insect control in apples and oranges without causing significant quality damage.

Core heating by RF energy can be compensated with surface heating using hot water to provide more uniform final temperature distribution in fruit.

The objectives of this study were to determine the process parameters for hot water assisted RF treatment, to investigate the effectiveness of RF thermal treatments against codling moth in apples, and to evaluate the postharvest quality of treated apples.

2. Materials and Methods

2.1. Sample preparation

For efficacy tests, a 'Red Delicious' apple (size 80, diameter 8.0±0.1 cm, weight: 266±20 g) was procured from a packing house located in Yakima, WA. Codling moth larvae were reared at the USDA-ARS Yakima Agricultural Research Laboratory (YARL) in Wapato, WA. The larvae colony was fed on a soy-wheat germ-starch artificial diet at 27°C, 40–58% RH, and 16:8 h light:dark photoperiod (Toba and Howell, 1991). The insects were shipped from YARL to Washington State University (WSU) (Pullman, WA) by overnight delivery for RF and hot water treatments. Since the fifth-instars were the most heat tolerant stage of the codling moth (Yokoyama et al., 1991; Wang et al. 2002a; Wang et al., 2004), late fourth to early fifth-instars were removed from the artificial diet and used for artificial infestation of apples. Seven apples and 35 larvae per replicate were enclosed in a single ventilated plastic container. The containers were held at 22°C, 60–70% RH, and 16:8 h light:dark photoperiod for additional 2 days to allow the larvae to infest the apples and develop into fifth-instars before heat treatments.

Freshly harvested 'Red Delicious' apples (size 80, diameter 8.0±0.1 cm, weight: 266±2 g) were procured from a local orchard (Pullman, WA) for quality evaluation.

2.2. RF heating system description and treatment procedure

Apples were stored at room temperature for more than 24 h at WSU prior to the scheduled heat treatments. A preliminary experiment was conducted with 9 apples in each test to determine the temperature-time history of apple sub-surface and core temperatures, as well as the heating uniformity at various stages of the heat treatment process. Two apples were taken out after water preheating in a water bath (Model ZD, Grant, Cambridge, UK) and 7 went through RF heating in a hydraulic fruit mover. During the preheating, two thin thermocouples (Type-T, THQSS-020U-6, Omega Engineering Inc., Stamford, CT) were inserted into a randomly selected apple at about 2 (sub-surface) and 40 mm (core) below the skin, respectively. The apple sub-surface and core temperatures were recorded by a data logger (DL2e, Delta-T Devices Ltd., Cambridge, UK) with a time interval of 10 s during the water preheating, holding and hydro-cooling processes (Fig. 1).

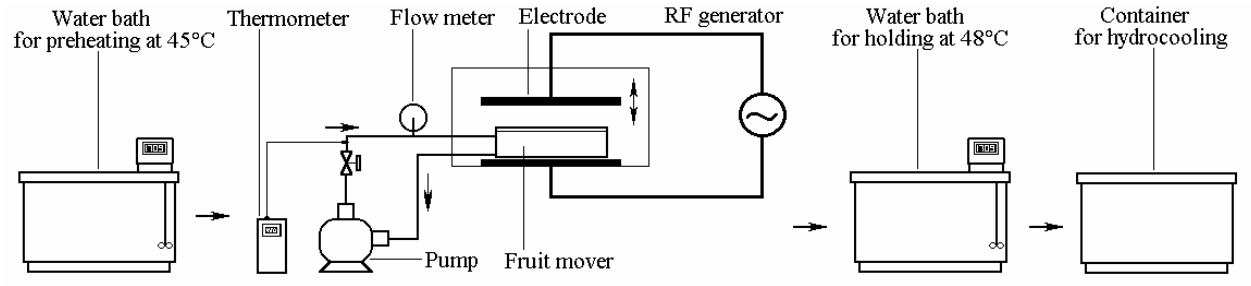

Fig. 1. Schematic view of the water assisted RF treatment process

Continuous temperature recording during RF heating was not possible due to the movement and rotation of fruit in the water medium. RF heating temperature profiles were estimated by the temperatures between the end of water preheating and the beginning of holding using a linear interpolation. At the end of each treatment stage, two apples were randomly

selected and removed for recording of the thermal imaging of two cut cross-sections, one perpendicular to the apple stem and another one along the stem. The thermal images were taken with an infra-red imaging camera (ThermaCAM^{TM} Researcher 2001, accuracy ±2°C, FLIR Systems, Portland, OR). Five seconds were required for each complete imaging process. To reduce the heat loss from the apple surface when the thermal image was taken, the half apple facing camera was surrounded with water at the treatment temperature. In each of the thermal images, 168×168 individual temperature data were collected over the whole image and about 19600 points for the targeted area of apples were used for contour plots and statistical analyses.

For each RF heating experiment, 7 randomly selected fresh apples were preheated in a circulating hot water bath at 45°C water for 30 min (Fig. 1). The preheated apples were transferred into a hydraulic fruit mover developed in our laboratory specifically for RF treatment. The fruit mover provides for a 3-dimensional rotation of the fruit by means of twelve Teflon water spray nozzles mounted on the periphery of the container, which help to rotate fruit on their axes and in a circular path. Details of the fruit mover and its operating procedure can be found elsewhere (Birla et al., 2004). The fruit mover container was filled with 45°C tap water and placed between two electrodes of a 27.12 MHz and 12 kW batch type RF heating system (Strayfield Fastran with E-200, Strayfield International Limited, Wokingham, UK). RF power was set at 6 kW and water temperature was monitored by the thermocouples in the circulation pipe outside of the RF unit during the RF heating process. The RF power was switched off once the water temperature reached 48°C.

RF heated apples were removed from the fruit mover and transferred to a hot water bath maintained at 48°C (Fig. 1). The selection of the 48°C treatment temperature was based on the reported quality of papaya after vapor heating at 47.8°C for 4 h (Hayes et al., 1984; Shellie and

Mangan, 2000) and oranges at 48°C for 15 min (Birla et al., 2005). The holding time was chosen based on the time (15 min) required to achieve 100% mortality of 600 fifth-instars of codling moth determined by the heating block system (Wang et al., 2002a). For efficacy tests, two unheated samples were used as control where one sample kept in and other in water bath , both at room temperature for 80 min. The treatments included water preheating at 45°C for 30 min, and RF heating to 48°C and holding at 48°C water for 5, 10, 15, and 20 min after the water preheating at 45°C for 30 min and prior to hydro-cooling in ice water for 30 min. The hydro-cooled apples were packed again in ventilated containers and stored at room temperature. For apple quality tests, the three relatively long holding times (10, 15 and 20 min) were used for the three heat treatments followed by the same procedure for the water preheating, the RF heating and the hydro-cooling as the efficacy tests. The hydro-cooled apples were divided into two groups for each treatment combination. A surface coating of *Carnuaba* natural wax was applied to one group (7 apples) before storage at 4°C. A group of untreated apples, control both waxed and unwaxed were also stored with the treated apples. All tests were repeated three times.

2.3. Insect mortality and quality evaluation

Efficacy of heat treatments was evaluated the following day. For each treatment, infested apples were carefully dissected and observed for any live larvae and for number of dead larvae. Average and standard deviation values of insect morality were calculated from three replicates of 7 apples for each treatment.

Postharvest quality, including weight loss, firmness, peel and pulp color, soluble solids, and titratable acidity (TA), was measured before heat treatment and after 7 and 30 days storage at 4°C after the treatment. Weight loss was expressed as percentage of weight lost from the initial weight. The firmness at three marked locations along the equatorial fruit surface was

measured by a Texture Analyzer (Model TA-XT2, Stable Micro Systems, YL, UK). The fruit was held in position on a concave shaped Nylon disc during firmness measurements. Firmness was expressed as a maximum force in Newton (N) required penetrating the 11 mm probe into 8 mm deep in the apple with 400mm/min cross head speed. Prior to measuring firmness, the marked spots were peeled off. Peel and pulp colors were measured at three marked spots on an individual apple by a colorimeter (Model CM-2002, Minolta Corp., Ramsey, NJ) calibrated to a standard white reflective plate. The color was expressed in terms of L^*, C^*, h^o color system (L^* = darkness, C^* = chroma, h^o = hue angle). Total soluble solids and percent TA were measured for control apples upon receiving and for heat treated apples at 7 and 30 days storage at 4°C. Six apples from each treatment were used for preparation of composite juice samples. TA of the samples was determined by end-point titration of 5 ml juice sample to pH 8.2 with 0.1N NaOH solution. TA is expressed in terms of the equivalent anhydrous malic acid in grams per 100 ml of juice. Total soluble solids (TSS, °Brix) was measured using a hand-held refractometer (Model N-1α, ATAGO Co. Ltd., Tokyo) with a sucrose scale calibrated at 20°C and expressed as percent soluble solids.

The measured values for individual quality attributes were subjected to a factorial analysis of variance (ANOVA) (GLM procedure, SAS Institute, 1990, Cary, NC) with storage time, wax coating, and treatment as main effects. Means were separated using Tukey's method of multiple pair-wise comparisons.

2.4. Flavor analysis

Postharvest heat treatment may induce many bio-chemical and physical changes in fresh fruits. These changes may not be reflected by physical properties such as firmness, color, TSS or acidity, however alteration in flavor profiles could be significant (Obenland et al., 1999). The

alternation in flavor volatile components after heat treatment can be a major quality determinate among consumer acceptance or rejection. There is little information available on the effect of heat treatment upon apple flavor profiles. Fallik et al. (1997) did the pioneering work and reported that heat treatment temporally inhibits aroma volatile compound emission but does not completely deteriorate flavor in Golden Delicious apples. Upon a extended storage period, heat treated apple fruit recovered the ability to produce most volatile compounds due to metabolic recovery among the enzyme systems catalyzing volatile compound synthesis. The objective of the flavor analysis is to evaluate heat-induced alteration in volatile flavor profiles after the RF treated apples were cold stored for 7 and 30 days of treatment.

2.4.1. Sample preparation

After the designated days of storage, juice from six apples (among each treatment group) was obtained using a domestic grinder, filtered through cheese cloth and filled in a 20 ml plastic scintillation vial with a cone cap lid. The sample vials were immediately sealed and stored in a freezer (<0°C) until the samples were analyzed for flavor analysis. A solid phase micro-extraction (SPME) technique was used to analyze samples by a Gas Chromotograph (GC) as described by Steffen and Pawliszyn (1996) and Song et al. (1997). The juice samples were removed from the freezer just before volatile component analysis. The sample vial was immersed in tap water for thawing. A typical sample consisted of 2.0 ml of juice in a 4.0 ml SPME vial with 0.65 g NaCl and a 6 mm magnetic stirring bar. The vial was mounted on a SPME stand and a fiber (0.65μm thick PDMS/DVB stationary phase, Supelco Inc., Bellefonte, PA) was inserted in the headspace (Yang and Peppard, 1994). The fiber was kept in the headspace for 30 min to allow volatiles molecule absorption. Volatile compounds attain equilibrium within the headspace of a SPME vial and a SPME fiber between 30–120 mins, depending on the flavor compounds

and matrix (Steffen and Pawliszyn, 1996). The volatiles from apple juice sampling attained equilibrium at 60 min, as was optimized in the Washington State University Postharvest laboratory for several types of postharvest matrices including, apple juice (Muller et al., 2005), barley slurries (Cramer et al, 2005), beet slurries (Lu et al., 2003), strawberry purees (Abonyi et al., 2003) and orange juice (Birla et al,. 2005).

2.3.2. GC/MS analysis

The headspace sample adsorbed onto the SPME fiber was injected into a Hewlett-Packard (Agilent, Avondale, PA), 5890II gas chromatograph interfaced with a 5970 mass selective detector system. The volatiles were desorbed into the injection port for 5 minutes at 200^{o}C using a 0.75 mm SPME liner. The injection mode was splitless for 2 min. The MS transfer line was held at 250°C and the GC programmed according to Mattheis et al. (1991). The carrier gas (Helium) velocity was set at 30.1 cm/s through the fused silica capillary column, a DB-1 (J&W, Folsom, CA), (60 m × 0.32 mm, thickness 0.32 μm). The various flavor compounds present in the apple juice were identified based on comparisons between GC retention indices and mass spectra of those contained in the Wiley/NBS library, along with those of authentic compounds under the identical experimental conditions. The data were collected and analyzed using the HP Chemstation G1034C data processing package. A standard aqueous solution was prepared to determine the response factors for major and minor volatile flavor compounds, such as reported by Fellman et al. (2003). The response factors of these components were obtained by dividing concentrations by GC peak areas of each standard component in the standard solution.

3. Results and Discussion

3.1. Temperature distributions of apples

Fig. 2 shows a typical temperature-time history at the core and sub-surface of 'Red-Delicious' apples (22°C initial temperature) subjected to water preheating, RF heating, holding at 48°C and hydro-cooling. After 30 min water preheating at 45°C, apple core and sub-surface (2 mm below the surface) temperatures reached 39 and 45°C, respectively. After 1.25 min of RF heating in 45°C tap water with 6 kW input RF power, the core and sub-surface temperatures reached 48 and 47°C, respectively. Holding of the apples in hot water at 48°C for a certain time period (e.g. 10 min) ensured a relatively uniform temperature profile over the entire apple cross section and provided an accumulation of thermal lethality of codling moth larvae. Hydro-cooling with 1°C water of heat treated apples expedited the cooling rate as the core temperature dropped from 48 to 19°C in 30 min (Fig. 2).

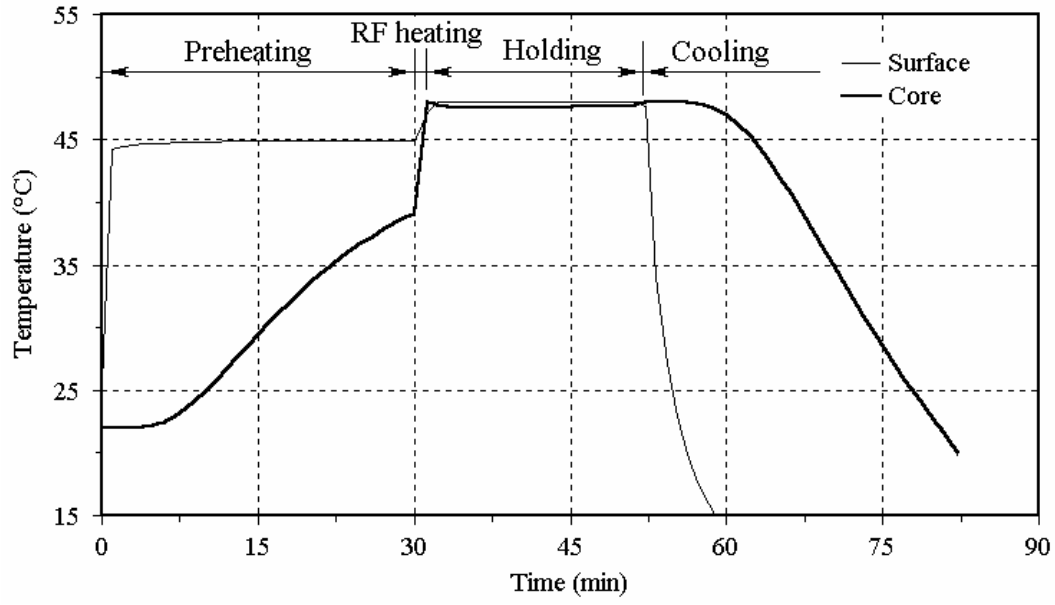

Fig. 2. Typical time-temperature history for surface and core of "Red Delicious" apples (dia: 8 cm) when subjected to water preheating (45°C, 1 m s^{-1}), RF heating (27.12 MHz, 6 kW) for 1.25 min, holding in hot water bath (48°C; 1 m s^{-1}) for 20 min, and 30 min hydro-cooling

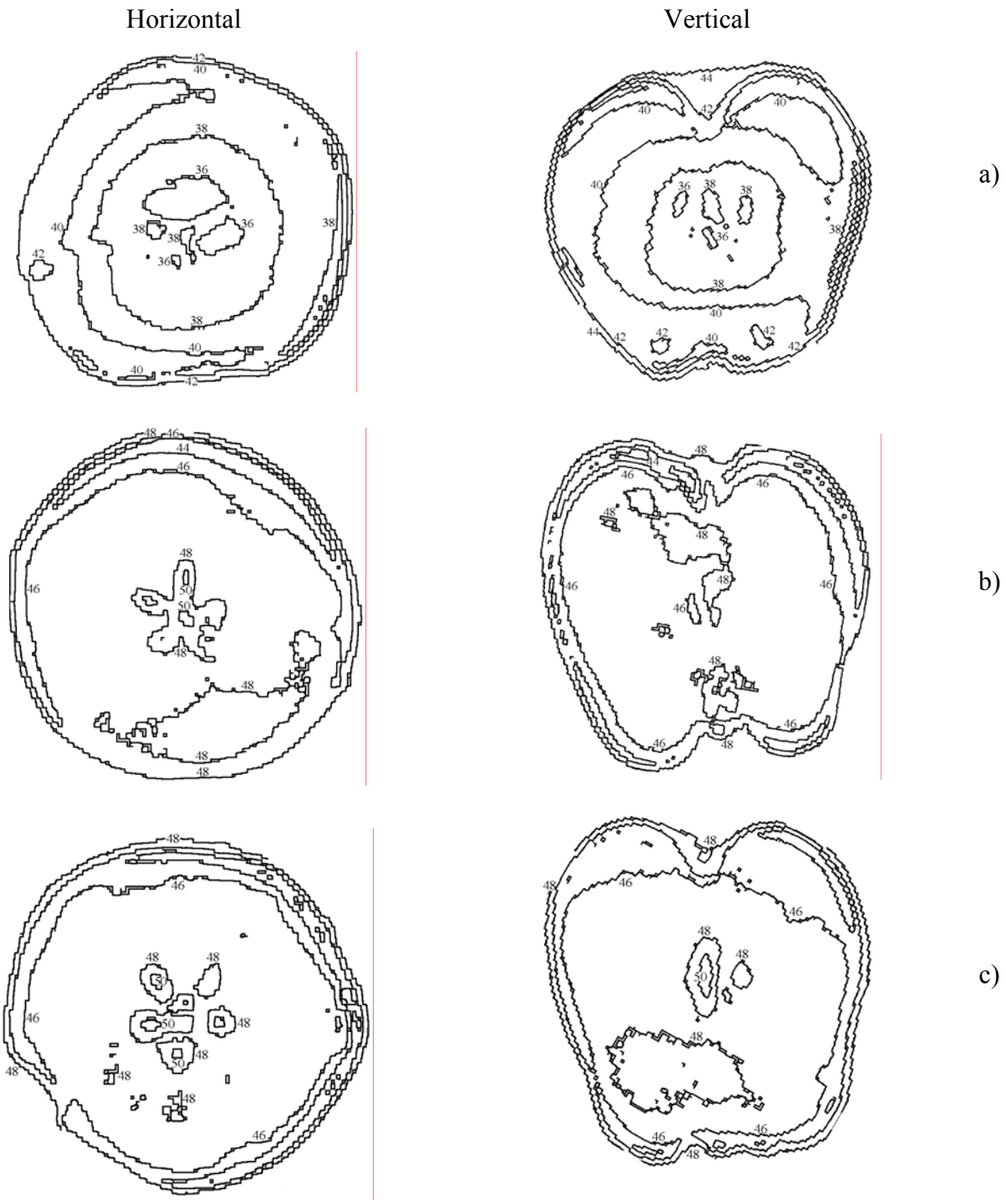

Fig. 3. Contour plot of temperature distribution obtained by thermal imaging over horizontal and vertical apple cross sections after a) water preheating at 45°C for 30 min, b) RF heating from 45 to 48°C, c) holding 10 min at 48°C water

The contour plots from thermal images of apples recorded at the end of water preheating, RF heating, holding and hydro-cooling are shown in Fig. 3. Preheating in hot water established a temperature gradient from the surface (44°C) to the core (36°C). Those two temperatures were close to those measured by thermocouples. As demonstrated in the preliminary RF heating experiment, RF heating has a core-focused heating of apples. Therefore, using preheated apples in RF assisted heating treatments resulted in a fairly uniform temperature (47.3±0.7°C) in fruit (Fig. 3b). The water preheating of apples also reduced the RF process time required to raise the fruit temperature to 48°C. The RF heating took only 1.25 min to bring overall temperature of preheated apples from 45 to 48°C. There were no drops of temperature at the apple surface when using the water to immerse apples. The apple surface temperature achieved 48°C after RF heating. Some small hot spots (50°C) along the stem and close to the air cavity and clod spots (44°C) near the subsurface were found (Fig. 3b).

Holding RF heated apples in hot water at 48°C for 10 min further reduced the temperature gradient and improved temperature uniformity (Fig. 3c). The mean temperature over the apple horizontal cross section was 47.1±1.0°C and 47.3±0.7°C before and after holding, respectively. The temperature uniformity in apples was better for those treated with RF assisted hot water heating than that of apples RF heated in matched saline solution in a fruit mover (53.6±4.8°C) (Birla et al., 2004). After the hydro-cooling for 30 min, the core and surface temperatures dropped to 18°C and 4°C, respectively (Fig. 3d). Therefore, water preheating of apples was useful in reducing RF heating time and in overcoming the limitations imposed by RF heating of fresh fruit.

3.2. Treatment confirmation studies with infested apples

Percent insect mortality (mean±SD) in unheated control apples was 5.7±2.9% and 8.6±2.9% for room temperature holding in air and water, respectively (Table 1). In general, mortality of fifth-instars in the control group was still low, suggesting that the effect of handling and shipment on mortality was negligible. Table 1 also shows the total numbers of live and dead codling moth larvae found in the heat-treated apples. After the water preheating at 45°C for 30 min, the insect mortality was 19.1%, suggesting some minor heat effect at 45°C. With the RF treatment, the insect mortality increased to 97.1 and 98.1% after 5 and 10 min holding, respectively. These mortality values were higher or comparable to 70.2±11.8% and 97.4±0.5% at 48°C for 5 and 10 min determined for fifth-instar codling moth using a heat block system (Wang et al., 2004). It took at least 15 min holding at 48°C in the water bath to ensure the death of all larvae. These results agreed with the thermal death kinetic studies on the fifth-instar codling moth using a heat block system (Wang et al., 2002a) and the infested studies in cherries (Hansen et al., 2004).

3.3. Apple quality

Table 2 shows the results of factorial ANOVA analysis performed on individual quality attributes, namely weight loss, firmness, and peel and pulp color. In presence of significant interactions among all factors, multiple pair-wise comparisons were performed to separate the main effects of individual factors on the each quality attribute. The mean listed in Table 2 for a specific factor (e.g. Storage) were calculated from the measured data over the tested range of the other two factors (e. g. coating and treatment). These values summarize overall effects of each factor.

Table 1. Total number of live and dead fifth-instar codling moth recovered from 'Red-Delicious' apples with the mortality (mean±std, %) over three replicates after being subjected into the controls at room air and water and three treatments with the same water preheating (45°C for 30 min), RF heating (27 MHz and 6 kW for 1.25 min), and hydro-cooling for 30 min (three replicates with 5 larvae per apple).

Temperature + Holding time	Total No. of alive	Total No of dead	Mortality (%)
Control at room air	99	6	5.7±2.9
Control at room water for 80 min	96	9	8.6±2.9
45°C+30 min	85	20	19.1±8.7
48°C+5 min	3	102	97.1±2.9
48°C+10 min	2	103	98.1±1.7
48°C+15 min	0	105	100±0
48°C+ 20min	0	105	100±0

3.3.1. Weight loss

Table 2 shows that 2-way and 3-way interactions among treatment factors were significant. Therefore, the main effects of wax coating, storage time and different treatments on the weigh loss were deducted from the pair-wise comparisons. Weight loss in un-waxed apples was significantly higher (1.2 %) than that of waxed apples (0.82 %). The RF heat treatments caused a significant lower weight loss from the apples in comparison with control apples. However increase in holding time after RF heating from 10 to 20 min resulted in increased weight loss. The reduced weight loss in the treated apples might be caused by the inhibition of ethylene producing enzymes or heat induced redistribution of natural wax on the apple skin. Ethylene is commonly known to be responsible for the acceleration of fruit ripening. If this is true, the heat treatment may also be good for long-term storage of apples. To corroborate this, more heat treatments should be performed to determine the overall effects of heat on the quality during extended storage time.

Table 2. Mean squares and mean values for quality attributes of 'Red delicious apples after RF heat treatments

Source	df	Weight loss (%)	Firmness (N)	Peel color			Pulp color		
				L*	h°	C*	L*	h°	C*
				Mean squares					
Waxed (W)	1	1521.67*	5.97	48.64	390.71*	599.69*	109.47	0.015	82.21*
Storage time (ST)	1	12522.56*	1370.65*	44.24	312.63*	233.75*	27.81	23.479	5.88
Treatment (T)	3	4174.86*	1204.24*	49.78	151.51*	601.05*	460.89*	36.09*	85.87*
W × ST	1	882.36*	1.99	0.53	2.9	5.22	79.77	27.96*	8.29
W × T	3	114.99*	98.16	5.83	6.41	8.98	47.78	20.04*	160.66*
ST × T	3	2145.05*	312.34*	14.48	34.76	17.32	265.07*	2.25	142.24*
W × ST × T	3	30.03*	68.82	30.02	199.13	35.88	400.76*	27.31*	82.57*
Error (df)		0.0011(32)	92.27(173)	14.42(352)	36.15(353)	26.06(352)	59.75(266)	6.7(266)	16.07(266)
Means[#]									
Waxed									
Yes		0.82[a※]	74.28	31.63	23.45[b]	24.63[b]	69.61	87.45	22.03[b]
No		1.20[b]	73.91	32.68	21.34[a]	22.02[a]	68.32	87.44	20.91[a]
Storage (Days)									
7		0.46[a+]	76.94[b]	31.65	21.45[a]	22.51[a]	69.29	87.75	21.62
30		1.56[b]	71.25[a]	32.36	23.34[b]	24.14[b]	68.64	87.15	21.32
Treatment									
Control		1.93[d]	65.71[a]	32.7	23.05[ab]	27.02[c]	72.25[b]	88.52[b]	22.46[b]
48°C +10 min		0.52[a]	76.00[b]	32.61	23.66[b]	23.71[b]	66.59[a]	87.07[a]	20.71[ab]
48°C +15 min		0.75[b]	77.81[b]	31.16	22.32[ab]	20.82[a]	67.07[a]	87.28[a]	20.29[a]
48°C +20 min		0.84[c]	76.85[b]	31.55	20.56[a]	21.74[a]	69.94[ab]	86.92[a]	22.4[b]

* Main effects and interactions are significant at $P<0.05$; df –degree of freedom.

※ Means with different letters are significantly different at $P<0.05$.

[#] Means for a factor were calculated from the measured data over the tested range of the other two factors.

3.3.2. Firmness

The effect of wax coating on firmness was not significant; however storage time and RF treatments significantly influenced the firmness. The mean firmness upon 30 days of storage of all apples at 4^{o}C was reduced from a value of 79.5 measured before treatments to 71.25 N (Table 2)**.** The firmness of RF treated apples was significantly higher than those of the control apples. This may be due to the inhibition of ethylene producing enzyme and reducing the rate of respiration. Decreased respiration translates to a reduced consumption of fruit sugars and decreased water loss during storage. This was supported by the weight loss results, which showed that heat-treated apples lost a significantly lower amount of weight as compared to the untreated apples. The effect of the wax coating on firmness was not significant.

3.3.3. Fruit color

Table 2 shows the analysis of apple peel color change in terms of value (L*), hue (h°) and chroma (C*). A decreased value of L* indicated a shift of color toward darker or gray side on the scale of light to dark (0 for dark and 100 for light). The effect of all the factors on L* value of apples was not significant but a slight decrease in L* value was observed in the RF treated apples. A change in hue angle (h°) signified the shift toward yellow or red within the yellow to red quadrant. There was a significant effect of wax coating and storage time on the hue angle. The mean value of hue angle significantly increased from 21.45 measured at 7th days of storage to 23.45 measured at 30th day after treatments. In comparison to control apples there was no significant difference in hue angle for all the heat-treated apples except for the treatment held apples at 48°C for 20 min (Table 2). Chroma is the quality that distinguishes a pure hue from gray shade. The values of chroma of heat-treated apples were significantly lower than that of the

control apples. The effects of wax coating and storage time on the hue angle were also significant.

The effect of RF treatments on L^* values of pulp was significant (Table 2). A shift of the L^* value toward darker side, means lower L^* values, suggested a conversion of starch into fruit sugars over the storage time. The RF heat treatments caused a significant decrease in L^* values of the pulp of treated fruit in comparison with control fruit. The values of hue angles were significantly lower in the apples subjected to the heat treatment in comparison with values of control apples (Table 2). The effect of the wax coating and storage time was not significant however an interaction between these factors was significant. The value of chroma for heat-treated apples was significantly altered by wax coating and thermal treatments. However, there was a significant interaction among wax coating, storage time and treatment and the main effects of the individual factor could not be separated. Therefore a trend of the pulp color change induced by heat treatments could not be determined.

3.3.4. Titrable acidity and Brix

The average values for TSS (%) and TA (g/100 ml) before treatment were 12.80±0.57% and 0.52±0.04 g/100 ml, respectively. No significant differences were observed with TSS and TA values for all of the treatments as compared to the controls stored for 7 and 30 days at 4^{o}C (data not shown).

3.4. Flavor analysis

Historically the apple aroma includes over 300 volatile compounds identified in the headspace or juice of apple cultivars (Dimick and Hoskin, 1983), but only 20 of them impart a potent characteristic flavor to the human pallet. These compounds include alcohols (6–16%), aldehydes, carboxylic esters (78-92%), ketones, and ethers (Paillard, 1990). Some are present in

very low concentrations and contribute potent aroma characteristics typical of apple aroma/flavor e.g., ethyl-2-methyl butanoate (Flath et al., 1967). The concentration of the volatile compounds increases until the apple fruits reach respiratory climacteric and afterward, particular classes of the volatiles, remain steady or their concentration then starts to decline (Mattheis et al., 1991). In this study, more than 50 volatile compounds were detected using the headspace SPME GC-MS technique in red delicious apple juice. The major 15 potent apple flavor compounds detected in the control and the RF treated apples are shown in Fig 4.

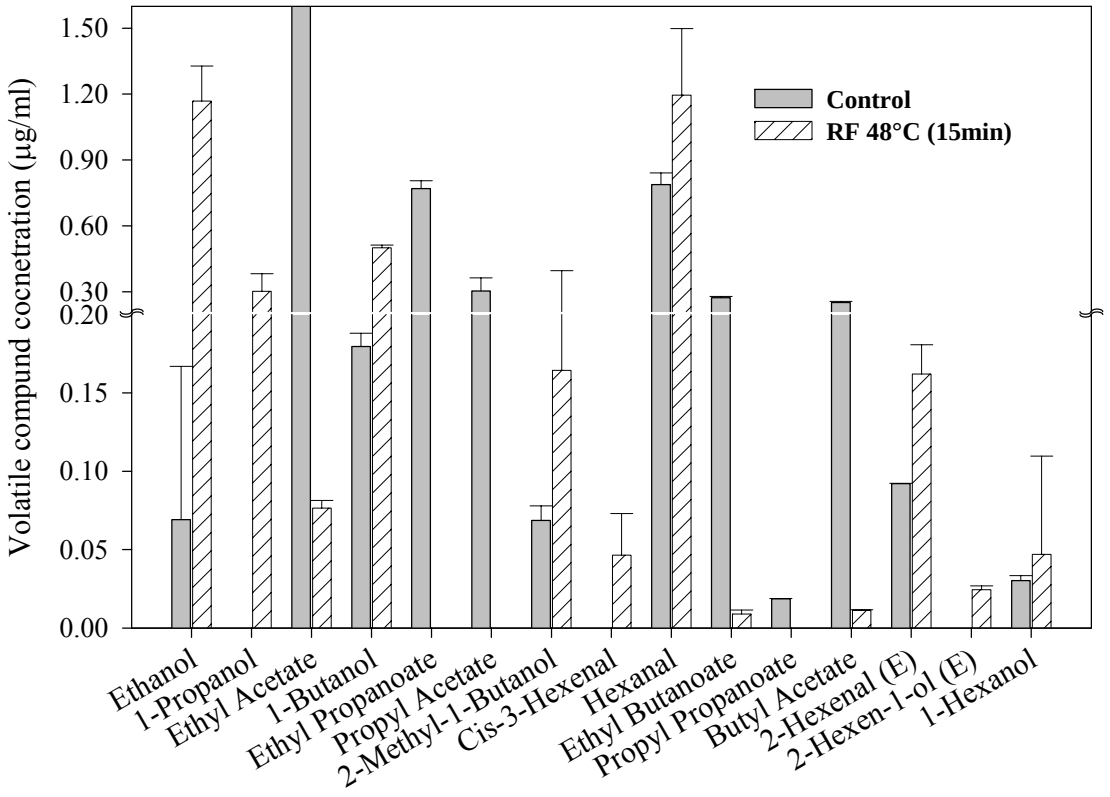

Fig. 4 Change in apple volatile profiles upon RF heating and 7 days of storage at 4°C

Fig. 4 shows that esters, aldehydes and aliphatic alcohols are the major contributors to characteristic apple-like aroma and flavor. Aldehydes impart a characteristics immature green apple flavor, whereas esters and aliphatic alcohols impart a fruity flavor (Flath et al., 1967). Generally, after the heat treatment and 4°C storage for 7 days, there were decreases in esters and increases in the alcohols and aldehydes quantities compared with the control apples (Fig. 4). A decline in ester volatiles in apples after the heat treatment was mainly attributed by a decrease in enzyme activity essential for the formation of esters (Patterson et al., 1974). In previous sections it has been shown that heat treatment did not impart undesirable changes in physical quality attributes upon apples. However, the flavor analysis suggests that heat treatment induces changes in volatile flavor profiles (Fig. 4).

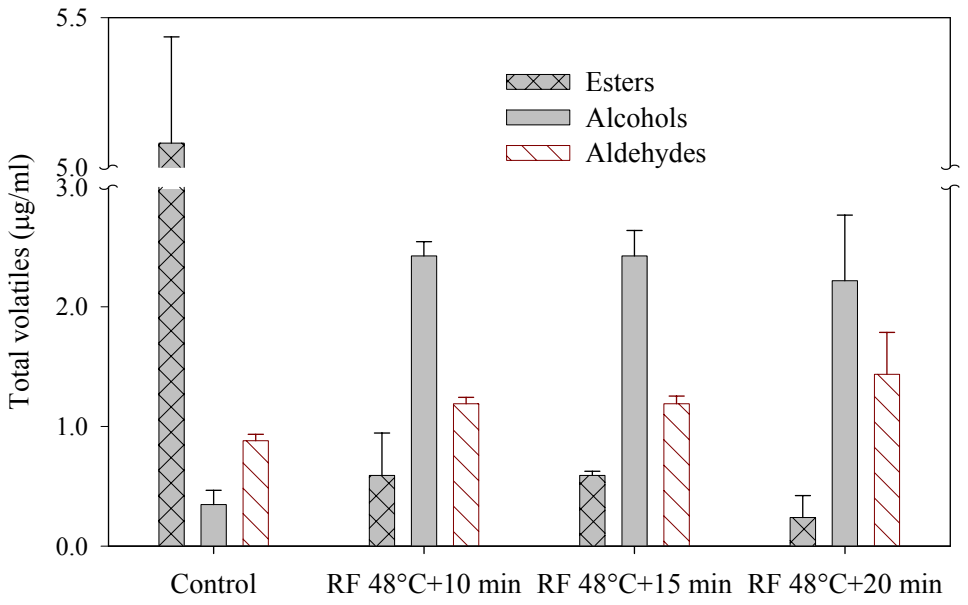

Fig. 5. Changes in the total volatile compounds namely esters, alcohols, and aldehydes after 7 days of storage of control and treated apples at 4°C temperature

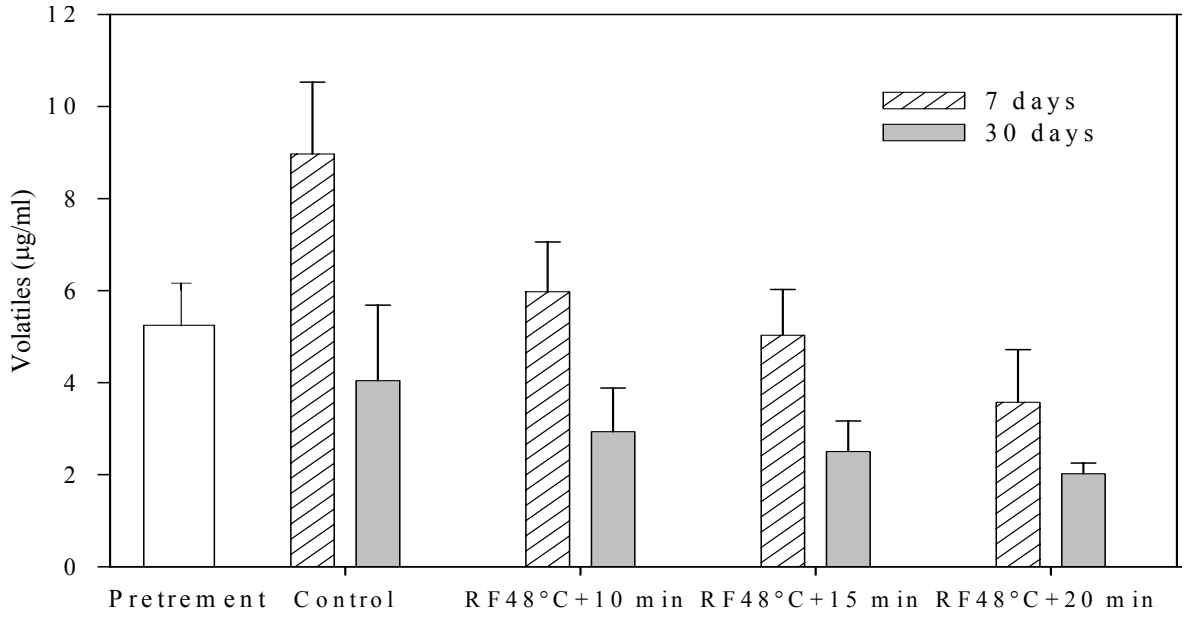

Fig. 6. Quantitatively change in volatiles compounds of 'Red Delicious' apples upon storage for 7 and 30 days after RF heat treatments (waxed and stored at 4°C)

The RF heat treatment seemed to cause a buildup in volatile compounds such as the alcohols and aldehydes as in the control apples the quantities of these volatiles were much less than that of RF treated apples (Fig. 5). The heat induced changes in the volatile flavor profiles could lead to rejection of the treated apples by consumers in spite of their favorable physio-chemical properties.

Fig. 6 shows the effect of the storage periods on apple total volatile quantities. It is quite evident that the RF heat treatments reduced the total volatiles by around 30–50% in comparison with the control apples. After 30 days of the treatment, there was a significant reduction in the volatile compounds in all the treatments. The trend can be explained by the similar observations made by Fallik et al. (1997). Over a 6 week period, they observed a steady decrease in total volatiles for the control apples. However, the heat treatment of apples (38°C for 4 days) suppressed the volatile compounds and with storage time there was a steady increase in total

volatiles and the total volatile values eventually surpassed the control apples. Their results suggested that a heat treatment (38°C for 4 days) would control postharvest pathogens and maintain fruit quality but not adversely affect apple aroma. In our study the treatment time was very short but the temperature was 10°C higher, therefore we suspect that the ester synthesizing enzyme, alcohol acetyl transferase (AAT) or the lipoxgenase (LOX) and alcohol dehyrogenase (ADH) enzymes may have been partially inactivated. These enzymes activities are important for synthesis for the major part of volatile acetate esters. It can be concluded that the treatment temperature is a major factor which alters the volatile flavors production. Hence, it is recommended that treatment temperature should be lowered to 46°C in order to retain the desirable volatile flavors. Without doubt, thermal treatment would change the flavor profile, but to assess whether the changes are acceptable by the consumer, the flavor analysis should be accompanied by sensory evaluation studies. Furthermore, studies are required to find a treatment combination that would minimize the loss of important flavor volatiles, or at least temporarily suppress them and maintain an effective mortality rate on the codling moth fruit flies at the same time. We also recommend that long term CA storage of treated apples should also be carried out in order to assess the decay susceptibility of the RF treated apple.

4. Conclusions

The hot water assisted RF treatments provided a very uniform heating over the entire cross section of apples. Heat treatments at 48°C for at least a 15 min holding period resulted in 100% mortality of fifth-instar codling moth in ‘Red Delicious’ apples. There was no significant effect of RF heat treatments on titratable acidity, soluble and solid content of apples even after 30 day storage at 4^{o}C. Although the RF heat treatments had a significant effect on firmness, weight loss, and peel and pulp color, the changes were not undesirable. The low weight loss and

retaining of firmness in heat treated apples might be considered as beneficial in view of long term storage of apples. However, further long term storage studies are required to substantiate this conclusion. Flavor analysis hinted that heat induced change in volatile flavor profile could lead to less desirability of the treated apple. To minimize the change in profile, the treatment temperature should be lowered. The conceptual design in this study can be potentially used in developing commercial water assisted RF heating process for insect control in apples. This research will be helpful for developing an effective quarantine treatment for industrial applications. More studies, namely long-term storage, sensory evaluation, and large scale efficacy demonstration, are also needed to make recommendation for application of the RF energy in conjunction with conventional hot water treatments.

References

Abonyi, B.I., Feng, H., Tang, J., Edwards, C.G., Chew, B.P., Mattinson, D.S., Fellman, J.K., 2002. Quality retention in strawberries and carrot purees dried with refractance window™ system. J. Food Sc. 67(3), 1051–1056.

Andreuccetti, D., Bini, M., Ignesti, A., Gambetta, A., Olmi, R., 1994. Microwave destruction of woodworms. J. Microwave Power EE. 29, 153–160.

Armstrong, J.W., 1994. Heat and cold treatments. In Paull, R.E., Armstrong, J.W. (eds), Insect pests and fresh horticultural products: treatments and responses, CAB International, Wallingford, UK, pp. 103–119.

Birla, S.L., Wang, S., Tang, J., Fellman, J., Mattinson, D., Lurie, S., 2005. Quality of oranges as affected by potential radio frequency heat treatments against Mediterranean fruit flies. Postharvest Biol. Technol. 38, 66–79.

Birla, S.L., Wang, S., Tang, J., Hallman, G., 2004. Improving heating uniformity of fresh fruit in radio frequency treatments for pest control. Postharvest Biol. Technol. 33, 205–217.

Cramer, A.C. J., Mattinson, D. S., Fellman, J. K., Baik, B.K., 2005. Analysis of volatile compounds from various types of barley cultivars. J. Agric. Food Chem. 53, 7526–7531.

Dixon, J., Hewett, E. W., 2000. Factors affecting apple aroma/flavor volatile concentration: a review. New Zealand J.Crop Horticul. Sc. 28, 155–173.

Feng, X., Hansen, J.D., Biasi, B., Mitcham, E.J., 2004. Use of hot water treatment to control codling moths in harvested California 'Bing' sweet cherries. Postharvest Biol. Technol. 31, 41–49.

Fallik, E., Archbold, D.D., Hamilton-Kemp, T.R., Loughrin, J.H., Collins, R.W., 1997. Heat treatment temporarily inhibits aroma volatile compound emission from golden delicious apples. J. Agric. Food Chem. 45, 4038–4041.

Flath, R., Black, D.R., Guadagni, D.G., McFadeen, W.H., Schultz, T.H., 1967. Identification and organoleptic evaluation of compounds in Delicious apple essence. J. Agric. Food Chem. 15, 29–35.

Guance, A.P., Madsen, H.F., McMullen, R.D., 1981. Fumigation with methyl bromide to kill larvae and eggs of codling moth in 'Lambert' cherries. J. Econ. Entomol. 74, 154–157.

Hallman, G.J., Sharp, J.L., 1994. Radio frequency heat treatments. In: Sharp, J.L. and Hallman, G.J. (Eds.), Quarantine treatments for pests of food plants. Westview Press, San Francisco, CA, pp. 165–170.

Hansen, J.D., Drake, S.R., Moffitt, H.R., Robertson, J.L., Albano, D.J., Heidt, M.L., 2000. A two-component quarantine treatment for postharvest control of codling moth on apple cultivars intended for export to Japan and Korea. HortTechnol. 10, 186–194.

Hansen, J., Wang, S., Tang, J., 2004. A cumulated lethal time model to evaluate efficacy of heat treatments for codling moth Cydia pomonella (L.) (Lepidoptera: Tortricidae) in cherries. Postharvest Biol. Technol. 33, 309–317.

Hayes, C.F., Chingon, H.T.G., Nitta, F.A., Wang, W.J., 1984. Temperature control as an alternative to ethylene dibromide fumigation for the control of fruit flies (Diptera: Tephritidae) in papaya. J. Econ. Entomol. 77, 683–686.

Ikediala, J.N., Tang, J., Hansen, J., Drake, S.R., Wang, S., 2002. Quarantine treatment of fruits using radio frequency energy and an ionic-water-immersion technique. Postharvest Biol. Technol. 24, 25–37.

Johnson, J.A., Valero, K.A., Wang, S., Tang, J., 2004. Thermal death kinetics of red flour beetle, Tribolium castaneum (Coleoptera: Tenebrionidae), J. Econ. Entomol. 97, 1868–1873.

Klein, J. D., Lurie, S., 1990. Prestorage heat treatment as a means of improving post storage quality of apples. J. Amer. Soc. Hort. Sci. 1115(2):265–269.

Lu, G., Fellman, J. K., Edwards, C. G., Mattinson, D. S., Navazio, J., 2003. Quantitative determination of geosmin in red beets (Beta vulgaris L.) using headspace solid-phase microextraction. J. Agric. Food Chem. 51, 1021–1025.

Lurie, S., 1998. Review : Postharvest heat treatments. Postharvest Biol. Technol., 14, 257–269.

Luire, S., Klein, J. D., 1990. Heat treatment of ripening apples: Differential effects on physiology and biochemistry. Physiol. Plant. 78, 181–186.

Mattheis, J.P. Fellman, J.K., Chen, P.M., Patterson, M.E., 1991. Changes in headspace volatiles during physiological development of Bisbee Delicious apple fruit. J. Agric. Food Chem. 39, 1902–1906.

Mitcham, E.J., Veltman, R.H., Feng, X., de Castro, E., Johnson, J.A., Simpson, T.L., Biasi, W.V., Wang, S., Tang, J., 2004. Application of radio frequency treatments to control insects in in-shell walnuts. Postharvest Biol. Technol. 33, 93–100.

Moffitt, H.R., Drake, S.R., Toba, H.H., Hartsell, P.L., 1992. Comparative efficacy of methyl bromide against codling moth (Lepidoptera: Tortricidae) larvae in Bing and Rainier cherries and confirmation of efficacy of a quarantine treatment for Rainier cherries. J. Econ. Entomol. 85, 1855–1858.

Muller, I., Mattinson, D.S., Fellman, J.K., 2005. Relationships between preharvest horticultural oil application and postharvest behavior of ‘Golden Delicious’ apples: effect on volatile aroma production. Proceedings of the 5th International Postharvest Symposium. Acta Hortculturae #682, pp. 999–1005.

Nelson, S.O., 1996. Review and assessment of radio-frequency and microwave energy for stored-grain insect control. Trans. ASAE 39, 1475–1484.

Obenland, D. M., Arpaia, A. L., Austin, R. K., MacKey, B. E., 1999. High-temperature forced air treatment alters the quantity of flavor-related, volatile constituents present in navel and Valencia oranges. J. Agric. Food Chem. 47, 5184–5188.

Paillard, N. M. M. 1990. The flavour of apples, pears and quinces. In: Morton, I.D.; Macleod, A. J. ed. Food flavours, Part C. The flavour of fruits. Amsterdam. The Netherlands, Elsevier Science Publishing Com. Inc. 1–41.

Shellie, K.C., Mangan, R.L., 2000. Postharvest disinfestation heat treatments: response of fruit and fruit fly larvae to different heating media. Postharvest Biol. Technol. 21, 51–60.

Steffen, A., Pawliszyn, J., 1996. Analysis of flavor volatiles using headspace solid-phase micro-extraction. J. Agric. Food Chem. 44, 2187–2193.

Song, J., Gardner, B.D., Holland, J.F., Beaudry, R.M., 1997. Rapid analysis of volatile flavor compounds in apple fruit using SPME and GC/time-of-flight mass spectrometry. J. Agr.Food Chem. 45, 1801–1807.

Tang, J., Ikediala, J.N., Wang, S., Hansen, J.D., Cavalieri, R.P., 2000. High-temperature-short-time thermal quarantine methods. Postharvest Biol. Technol. 21, 129–145.

Toba, H.H., Howell, J.F., 1991. An improved system for mass-rearing codling moths. J. Entomol. Soc. B. C. 88, 22–27.

USDA-APHIS-PPQ. 2002. Treatment manual: interim edition. U. S. Dep. Agric., Animal Plant Health Inspection Service, Plant protection Quarantine, Riverdale, MD.

USDA-NASS. 2004. Agricultural statistics 2004. Chapter V: Statistics of fruits, tree nuts and horticultural specialties. U. S. Dep. Agric., Nat. Agric. Stat. Serv. Washington, D.C.

(USEPA) United States Environmental Protection Agency, 1998. Reregistration Eligibility Decision. Aluminum and Magnesium Phosphide. Cases 0025 and 0645. Office of Pesticide Programs, Special Review and Reregistration Division. Agricultural Statistics. Washington, D.C.

Wang, S., Ikediala, J.N., Tang, J., Hansen, J.D., Mitcham, E., Mao, R., Swanson, B., 2001a. Radio frequency treatments to control codling moth in in-shell walnuts. Postharvest Biol. Technol. 22, 29–38.

Wang, S., Tang, J. Cavalieri, R.P., 2001b. Modeling fruit internal heating rates for hot air and hot water treatments. Postharvest Biol. Technol. 22, 257–270.

Wang, S., Ikediala, J.N., Tang, J., Hansen, J.D., 2002a. Thermal death kinetics and heating rate effects for fifth-instar Cydia pomonella (L.) (Lepidoptera: Tortricicae). J. Stored Prod. Res. 38, 441–453.

Wang, S., Tang, J., Johnson, J.A., Mitcham, E., Hansen, J.D., Cavalieri, R.P., Bower, J., Biasi, B. 2002b. Process protocols based on radio frequency energy to control field and storage pests in in-shell walnuts. Postharvest Biol. Technol. 26, 265–273.

Wang, S., Tang, J., Johnson, J.A., Mitcham, E., Hansen, J.D., Hallman, G., Drake, S.R., Wang, Y., 2003. Dielectric properties of fruits and insect pests as related to radio frequency and microwave treatments. Biosystems Eng. 85, 201–212.

Wang, S., Yin, X., Tang, J., Hansen, J., 2004. Thermal resistance of different life stages of codling moth (Lepidoptera: Tortricidae). J. Stored Prod. Res. 40, 565–574.

Yokoyama, V.Y., Miller, G.T., Dowell, R.V., 1991. Response of codling moth (Lepidoptera: Tortricidae) to high temperature, a potential quarantine treatment for exported commodities. J. Econ. Entomol. 84, 528–531.

Yokoyama, V.Y., Miller, G.T., Hartsell, P.L., 1990. Evaluation of a methyl bromide quarantine treatment to control codling moth (Lepidoptera: Tortricidae) on nectarine cultivates proposed for export to Japan. J. Econ. Entomol. 83, 466–471.

Yang, X., Peppard, T,. 1994. Solid-phase microextraction for flavor analysis. J. Agric. Chem. 42, 1925–1930.

C H A P T E R 7

MODELING OF RADIO FREQUENCY HEATING OF FRUITS

S. L. Birla, S. Wang, J. Tang

Department of Biological Systems Engineering, Washington State University Pullman, WA

Prepared manuscript for Journal of Food Engineering.

Abstract

The present study investigated influence of different factors on radio frequency (RF) heating uniformity of fruits in a parallel plate applicator. Finite element-based software FEMLAB was used to model coupled electromagnetic and heat transfer equations in three dimensional (3-D) domain and to study RF heating as influenced by dielectric properties of the fruit and its surrounding medium, size and shape of fruit. Model fruit was prepared from 1% gellan gel for experimental validation of the simulation results. The results showed that spherical fruit surrounded with air between RF electrodes and placed in the proximity of electrodes would not heat uniformly. Immersing fruits in water helped to reduce uneven heating within a fruit, but created a new problem because fruits heat differently at different horizontal positions. Horizontal and vertical fruit positions with respect to electrodes significantly influenced the heating patterns inside the fruit. The study corroborated that movement and rotation of fruit is the only plausible solution for improving heating uniformity of spherical fruits. The developed computer model can be used for prediction of the heating pattern of individual fruit as influenced by dielectric properties, size, shape, and surrounding media to design thermal treatments of specific commodities.

Keywords: Dielectric properties; RF heating; Heating pattern; Quarantine, Heating uniformity

1. Introduction

Radio frequency (RF) heating has been studied as a rapid disinfestation treatment by many researchers (Frings, 1952; Nelson & Payne, 1982; Wang, Tang, Johnson, Mitcham, Hansen, Cavalieri et al., 2002). A number of problems remain to be addressed before RF heat treatments can be successfully used in commercial applications for heat sensitive products. The most significant problem associated with RF heating is the lack of uniform heating of heterogeneous products, such as fruits (Tang, Ikediala, Wang, Hansen & Cavalieri, 2000). Large temperature variations among and within fresh fruit reduce the effectiveness of a treatment and may cause severe thermal damage to the fruit. In order to overcome non-uniform RF heating of fruits Ikediala, Hansen, Tang, Drake & Wang (2002) suggested a saline water immersion technique, but for large fruits such as apples and oranges uneven heating inside the fruit was still unacceptable. Birla, Wang, Tang & Hallman (2004) showed improved in RF heating uniformity in oranges and apples when the fruit were immersed in water and kept in motion by water jets during RF heating. However, even after rotating and moving fruits in the RF field, non-uniform heating was evident in some fruits. Computer simulation models can be an effective tool to examine the causes of non-uniform heating and in finding solutions to overcome this problem.

After an extensive literature review, Yekolov (2001) concluded that there is still a lack of studies on modeling of RF heating of food materials though extensive research has been conducted on simulation of microwave heating. Neophytou and Metaxas (1996; 1997; 1998; 1999) started electromagnetic field modeling for industrial scale RF heating systems. Their extensive work involved comparison of solution from both electrostatic and wave equations. They recommended that for small size applicators, solution of Laplace equation is adequate, whereas for large size electrodes, wave equations should be used. Recently Chan, Tang &

Younce (2004) developed a simulation model for a RF parallel plate heating system, in which electromagnetic (EM) wave equations were solved using the finite element method. All the above efforts were focused on modeling EM fields and predicting of power density profiles. Yang, Zhao & Wells (2003) added heat transfer module in modeling of RF heating of vegetable seeds packed in a rectangular box. They used the commercial software TLM-FOOD HEATING to solve the EM field by the transmission line method and the heat diffusion by the standard explicit finite difference time domain method. They reported discrepancies between simulated and experimental results, especially at the edges of the box. Veen, Goot, Vriezinga, Meester & Boom (2004) derived a simplified expression for an EM field in very small spherical object immersed in an infinitely large surrounding medium. However, for large fruits such as oranges and apples, this expression is inappropriate. Marra, Lyng, Romano & McKenna (2007) modeled RF heating of a cylindrical luncheon meat roll in a 600 W RF oven operated at 27.12 MHz frequency. Their study successfully solved coupled EM and heat transfer equations using the commercial finite element method based software FEMLAB.

The overall goal of this study was to develop an effective simulation tool to predict the transient temperature profile of fruit in RF treatments and assist in optimization of process parameters to maintain fruit quality. Specific objectives were to develop a computer model by solving coupled quasi-static EM field, and heat and momentum transfer equations using FEMLAB software, to validate the predicted temperature distributions of a gel slab by experiments, to apply the validated model to better understand RF heating patterns in fruit as influenced by shape, size, relative position, and surrounding media, and finally to suggest means to reduce non-uniform heating of fruits in postharvest insect control using RF energy.

2. Materials and Methods

2.1. Physical model

The RF heating system consists of a generator, an applicator and a metallic enclosure. The most common type of applicator is a pair of parallel plates connected with a tank circuit. The dielectric material is sandwiched between two electrodes to form a working circuit (Wang, Ikediala, Tang, Hansen, Mitcham, Mao et al., 2001). The top electrode plate, with adjustable height, is inductively coupled to the tank oscillator circuit via feed strips. RF heating involves EM interaction of the lossy material (dielectric material having considerable power dissipation capability) placed between two electrode plates. The absorbed RF power per unit volume (Q, W m^{-3}) in the material is proportional to the square of the electric field strength ($\boldsymbol{E}$, V m^{-1}) and directly proportional to the dielectric loss factor (ε'') and the frequency (f, Hz) (Choi & Konrad, 1991):

$$Q = 2\,\pi\, f\, \varepsilon_{o}\, \varepsilon''\, \boldsymbol{E}_{rms}^{2} = \pi\, f\, \varepsilon_{o}\, \varepsilon''\, \left|\boldsymbol{E}\right|^{2} \tag{1}$$

where ε_0 is the permittivity in free space (8.85×10^{-12} F m^{-1}) and $\boldsymbol{E}_{rms}$ is the root mean square value of the electric field, which is equal to $\sqrt{2}$ times of the E-field amplitude.

Evaluation of the absorbed RF power density at any point inside the material requires the electric field strength value, which is impractical to measure because the value of '$\boldsymbol{E}$' at any point within the material depends on the geometry of the object and electrode configuration (Marshall & Metaxas, 1998). Therefore, it requires solving the EM field equations. EM waves between 1 and 200 MHz frequency fall within the radio band, and at 27 MHz the wavelength is about 11 m in free space. In the present study, the electrode size (1.05 m × 0.80 m) was very small compared with the wavelength of 27.12 MHz used in our study. Therefore the primary

mode of RF energy interaction was modeled as a quasi-static electrical field between two electrodes. Our approach was to systematically study the effect of the parameters that would significantly influence the heating patterns. Those parameters include the geometry of the object, relative location of the object in between the electrodes, and dielectric properties of the object and its surroundings.

2.1.1. Governing equations

The electric field at any point inside the electrodes is governed by Eq. (2), which is derived from a quasi-static approximation of Maxwell's EM equations (Roussy & Pearce, 1995):

$$-\nabla \cdot ((\sigma + \mathrm{j}\, 2\pi f\, \varepsilon_o \varepsilon')\nabla V) = 0 \tag{2}$$

where $\mathrm{j} = \sqrt{-1}$, ε' is the dielectric constant, and σ is the temperature-dependent conductivity (S m^{-1}) and related to the dielectric loss factor as ($\sigma = 2\pi f \varepsilon_o \varepsilon''$) in the RF range (Guan, Cheng, Wang & Tang, 2004). The scalar voltage potential (V, V) is related to the electric field by $\boldsymbol{E} = -\nabla V$, hence temperature dependent dielectric properties were sufficient to calculate the electric field strength at each point in the considered domain.

The absorbed RF power raises the temperature of the fruit, hence heat transfer takes place inside and outside the fruit. The geometry of most fruits such as cherries, apples, and oranges can be approximated as a sphere. Thermal diffusion in solid objects is governed by the Fourier transient transfer equation, but when immersed in fluid (water or air) it is governed by momentum transport and continuity equations (Zhang, Jackson & Ungan, 2000):

Continuity equation $\nabla . \boldsymbol{u} = 0$ (3)

Energy conservation equation $$\frac{\partial T}{\partial t} + \boldsymbol{u}.\nabla T = \frac{k}{\rho C_p}\nabla^2 T + \frac{Q}{\rho C_p} \quad (4)$$

Momentum equation $$\rho \frac{\partial \boldsymbol{u}}{\partial t} + \rho(\boldsymbol{u}.\nabla)\boldsymbol{u} = -\nabla P + \mu \nabla^2 \boldsymbol{u} + \boldsymbol{F}_b \quad (5)$$

where C_p is the specific heat (J kg^{-1} K^{-1}), k is the thermal conductivity (W m^{-1} K^{-1}), t is the time (s), T is the temperature (K), ρ is the density of the fruit (kg m^{-3}), and μ is the viscosity of the medium (Pa s). Similar to Eqs. (4) and (5) with the velocity component $\boldsymbol{u}$ (m s^{-1}) in x-direction, the momentum and energy transport in y and z directions can be written with corresponding velocity components $\boldsymbol{v}$ and $\boldsymbol{w}$. The numerical solution of Eq. (5) requires pressure (P, N m^{-2}) to specify at least one point of the domain.

Buoyancy force ($\boldsymbol{F_b}$, N m^{-3}) in z-direction can be calculated from the Boussinesq approximation, whereby variations in density due to temperature are ignored but change in buoyancy force due to differential temperature is considered for the set up of a flow field.

$$\boldsymbol{F_b} = \rho_m g \beta \Delta T \quad (6)$$

where g is the gravitational acceleration (m s^{-2}), β is the volumetric thermal expansion coefficient (K^{-1}), ΔT is the excess temperature from the reference one (K), and ρ_m is the fluid density the at reference temperature (kg m^{-3}). If the buoyancy force is the sole cause of motion, the convection is defined as free convection.

2.1.2. Geometric model and boundary conditions

It is impossible to take into account every details of the RF machine parts in the computation domain, as it demands excessive computer resources (Chan et al., 2004). One quarter of the RF electrode and the container was modeled to take advantage of the system symmetry. The upper electrode plate was drawn as an embedded element in 3-D to avoid a large

number of mesh elements for a thin electrode plate. Symmetric surfaces were assigned thermal and electrical insulating boundary conditions as shown in Fig. 1.

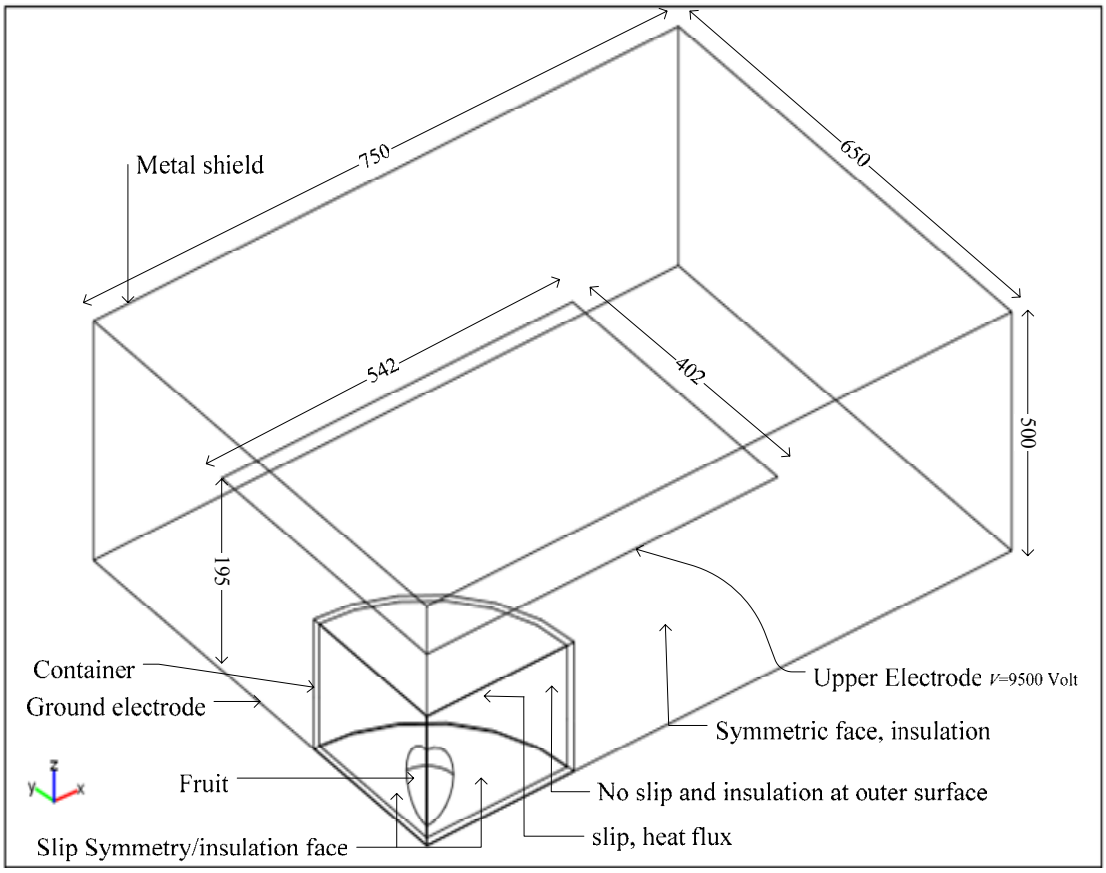

Fig. 1. Geometrical model of one quadrant of RF heating system (dimensions are in mm)

Source electric potential (V) was applied to the upper electrode of the applicator and the bottom of the enclosure served as an electrical ground return ($V = 0$). An electrically shielding boundary condition was applied to the metallic enclosure walls such that $\boldsymbol{n}\cdot(\sigma\nabla V) = 0$ where $\boldsymbol{n}$ is the unit vector normal to the surface. A thermal boundary condition of convective heat transfer was applied to the outer surfaces of the container (405 mm dia. × 127 mm height, made of 6.25 mm thick polyethylene sheet). The water-air interface in the container was assigned to a convective heat transfer boundary condition. The convective heat transfer coefficient was

assumed to be 20 W m^{-2} K^{-1} for water-air and container-air interfaces (Wang, Tang & Cavalieri, 2001). At fruit-water and container wall-water interfaces no-slip boundaries were imposed in the momentum equations. At the water-air interface, the velocity in the normal direction (***w***) and shear stress in the horizontal direction were assumed to be zero. Since solving Navier-Stokes equations needs to specify pressure at least at one point in the domain, atmospheric pressure was assigned at the top corner point of the container.

2.1.3. Solution methodology

Commercial finite element method based software FEMLAB (V3.2, COMSOL Multiphysics, Burlington, MA, USA) was used to solve the coupled electromagnetic, momentum and transport equations. Various steps involved in the modeling with FEMLAB software are outlined in Fig. 2. The computational scheme was to simultaneously solve the highly non-linear equations. An unstructured mesh consisting of Lagrange quadratic elements was created. To solve temperature and velocity values at the interfaces of spherical objects and surrounding media accurately, a relatively fine mesh was generated near the interfaces. A FEM solution was considered converging until the difference in maximum temperature between successive calculations was less than 0.1 % for a doubling of the number of elements. In the convergence studies, simulation results were found to be meshing independent when mesh sizes were reduced to $1/20^{th}$ of the maximum dimension of the domain. The optimum mesh generation yielded 3,641 nodes and 26,880 elements. The 'UMFPACK' differential equation solver in FEMLAB was used to achieve convergence. All computer simulations were performed on a Dell 670 work station with two each Dual-Core, 2.80 GHz XEON processors and 12 GB RAM running a Windows XP 64-bit operating system. Simultaneous solutions of coupled transient equations took 12 h for a 600 s RF heating process with 0.001s initial and 1 s maximum time steps.

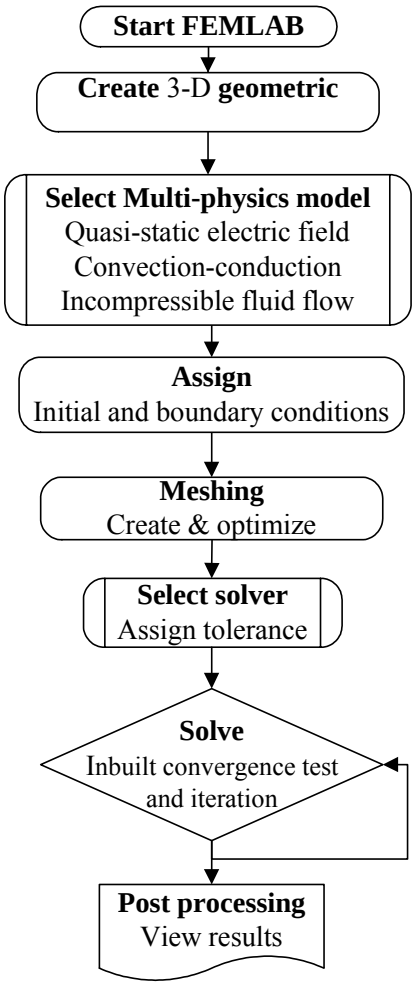

Fig. 2. FEMLAB modeling steps

2.1.4. Model input

Modeling of the RF heating process required knowledge of dielectric, thermal and physical properties of the load and surrounding medium. Density, thermal conductivity, and specific heat were assumed to be temperature-independent, whereas the dielectric properties of the materials were assumed to be temperature-dependent over the treatment temperatures range from 20 to 60°C for postharvest pest controls. Regression expressions obtained from the analysis of reported dielectric properties data were used in the model. Table 1 summarizes the properties of the various materials used in the simulations.

Table 1. Electrical and physical properties of gel ball and water used in simulation

Material proprieties	Gel ball	Water	Orange	Polypro pylene	Air
Thermal conductivity (*k,* W m^{-1} K^{-1})[#]	0.53	0.56	0.58	0.2	0.025
Density (ρ, kg m^{-3}) [#]	1010	1000	920	900	1.2
Specific heat (C_p, J kg^{-1} K^{-1})[#]	4160	4180	3600	1800	1200
Viscosity (μ, Pa s) [#]	N/A	0.001	N/A	N/A	0.000001
Exp. coefficient (β, K^{-1})	N/A	0.0003	N/A	N/A	0.002
Dielectric constant (ε')*	–0.21T+86.76	–0.48T+84.74	–0.206T+88.2	2.0[v]	1
Loss factor (ε'')*	4.36T+129.4	0.33T+11.1[@]	4. 89T+123.3	0.0023[v]	0

Source :* (Wang et al., 2003a; Wang, Tang, Johnson, Mitcham, Hansen, Hallman et al., 2003b)

[#] (Rehman, 1995) [@] (Stogryn, 1971) [v] (Von Hippel, 1954)

In the RF range, it is impractical to measure impressed voltage between two electrodes without distorting the electric field (Marshall & Metaxas, 1998). Metaxas (1996) showed that for a typical industrial-scale system the voltage varies by only 7% between standby and full load. Therefore, a constant electric potential on the upper electrode is a realistic assumption. The analytical solution of Laplace equation for the electric potential between RF electrodes and heat dissipation in a slab sandwiched between electrodes can be coupled together and an expression for electric potential on upper electrode can be obtained as (Metaxas, 1996):

$$V = \left(d_{air} \sqrt{(\varepsilon')^2 + (\varepsilon'')^2} + d_{mat} \right) \left(\sqrt{\frac{\rho C_p}{\pi f \varepsilon_o \varepsilon''} \frac{dT}{dt}} \right) \tag{7}$$

where d_{air} and d_{mat} are air gap and slab thickness (m), respectively.

The electric potential was estimated using the heating rate of a 1% gel slab (405×405×47 mm^3) in the12 kW RF unit. Procedure details are elaborated in the next section.

2.2. Model validation

2.2.1. Model fruit preparation

As a first step to validate the simulation model, it was more convenient to use a consistent homogonous sphere subject. Thus, we developed a homogeneous model fruit made of 1% gellan gels. Wang, Tang, Cavalieri & Davis (2003a) used gellan gel to prepare a model insect to study differential heating between insects and walnuts. One percent gellan gum dispersion (Kelcogel, Kelco Division of Merck and Co., San Diego, CA) in deionized water was prepared and the solution was heated to 90°C in 15 min (Tang, Tung & Zeng, 1995). To be consistent with the dielectric properties of real fruits, 0.17% $CaCl_2$ salt was added into the hot gellan gum solution. A polypropylene mould consisting of two hemispherical halves of 80 mm diameter was used to form the model fruit. The hot solution was poured into the mould though a hole in one half and allowed to cool at room temperature for 30 min to insure gel setting and easy removal of the ball (Tang, Tung & Zeng, 1997). The dielectric properties of 1% gellan gel with 0.17% $CaCl_2$ salt measured and reported by Wang et al. (2003a) over 20 to 60°C used in the computer simulation.

2.2.2. Experimental procedure for validation

A 12 kW parallel plate RF heating system (operating at 27.12 MHz, Strayfield Fastran with E-200, Strayfield International Limited, Wokingham, UK) was used for experimental validation of the simulation results. The computer model was first validated with a slab load. A slab ($405 \times 405 \times 47$ mm^3) made from 1% gellan gel was RF heated for 10 min with a 160 mm electrode gap to estimate input voltage on the upper electrode of the RF machine to be used for simulation purposes. The thermal image of the top surface of the gel slab was recorded using an

infrared camera (ThermaCAM^{TM} Researcher 2001, accuracy ±2°C, FLIR Systems, Portland, OR, USA).

A simulation model prepared for a spherical fruit was validated with an experimental heating profile of the model fruit. The prepared model fruit (gellan gel ball) were allowed to equilibrate to room temperature (approximately 20°C) prior to the experiment. To study the effect of the horizontal position of the fruit in the circular container, four model fruits were placed in the corners and one at the center of the container. The model fruits were secured at 25 mm above the container bottom. The container with fruits was placed at the center of the ground electrode. Ikediala et al. (2002) suggested immersion of fruit in saline water to minimize localized heating at contact surfaces. Therefore, in one experiment tap water (σ = 320 μS/cm at 20°C) was poured into the container that completely immersed the gel balls. To study the effect of fruit peel on the heating pattern, whole navel oranges and peeled oranges were RF heated in the water-filled container.

Experimental heating patterns were obtained by varying the vertical position of the model fruits between electrodes with respect to the bottom electrode. The core temperature of centrally placed fruit was recorded and logged during the RF heating experiment using a fiber optic sensor (UMI-8, FISO Technology, Quebec, Canada). In additional experiments, five model fruits were RF heated in a fruit mover developed by Birla et al. (2004) to study the effect of rotation and movement of fruits during RF heating. The RF heated fruit was immediately bisected vertically and a thermal image was recorded with the infrared camera for one of the cut surfaces within 10 s to avoid the surface cooling.

2.3. Modeling of fruit rotation

It has been demonstrated experimentally that rotation and movement of fruit during RF heating improves the heating uniformity (Birla et al., 2004). However, simulation of RF heating of rotating and moving fruits is very difficult because of the associated moving boundary conditions. To simplify simulation for this study, fruits were assumed to rotate on their own axes and each spot on any particular orbit was equally exposed to RF energy. The spherical fruit was further assumed to be composed of six stratified layers and RF energy absorbed on a particular layer to be uniform because of the 3-D rotation. This assumption was based on a concentric temperature contour over the fruit cross section observed with thermal images (Birla, Wang & Tang, 2006). In computer simulation, power density was integrated over the individual layer and the total power density was divided by volume of the layer to estimate an average power density over the individual layer.

3. Results and Discussion

3.1. Estimation of electric potential

Fig. 3a shows the experimental temperature profile of the gel slab subjected to 10 min RF heating in a 160 mm electrode gap. Using the average slab temperature rise (12.7°C) and dielectric properties of the gel at 25°C in Eq. (7) the input voltage was estimated to be 8,162 V. Since Eq. (7) is valid for an infinitely large slab and electrode dimensions (based on the assumption of no fringing field), the estimated voltage was not actual value. In simulation, various input voltage values were tried for predicting the realistic transient temperature. As a result, 9,500 V on the upper plate was selected for all further simulations. The simulated temperature distribution of the gel slab was in good agreement with the experimental one both in

pattern and absolute temperatures (Fig. 3b). Marshall and Metaxas (1998) used a similar approach in an attempt to model RF-assisted heating of particulates in a similar type of RF system. Upon validation of the FEMLAB model for the slab, the model was further used to characterize the RF heating pattern of spherical objects, as influenced by the dielectric properties of medium and fruit as well as locations of the fruit relative to electrodes.

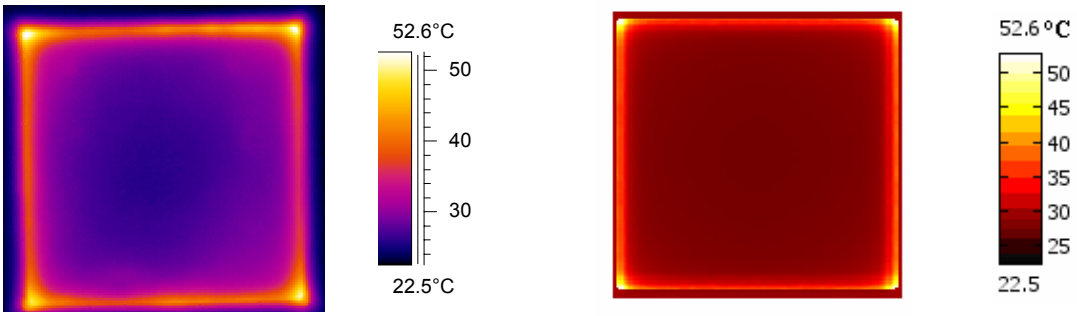

a). Experimental b). Simulation

Fig. 3. Comparison of experimental and simulated surface temperature distribution of 1% gel slab (405 × 405 × 47 mm^3 with 20°C initial slab temperature) subjected to 10 min of RF heating in a 160 mm electrode gap

3.2. RF heating of spherical balls in air

Fig. 4a shows the simulated temperature profiles of the model fruits placed at different locations between two RF electrodes. The fruit section close to the bottom electrode or near the upper electrode heated much more than other portions of the fruit, likely because of the high electric field concentration. The maximum difference between hot and cold portions ranged between 5 and 12°C. It was also corroborated by the experimental temperature profile of the RF heated gel balls hanging in the air either 25 mm above the bottom electrode or 25 mm below the upper electrode (Fig. 4b).

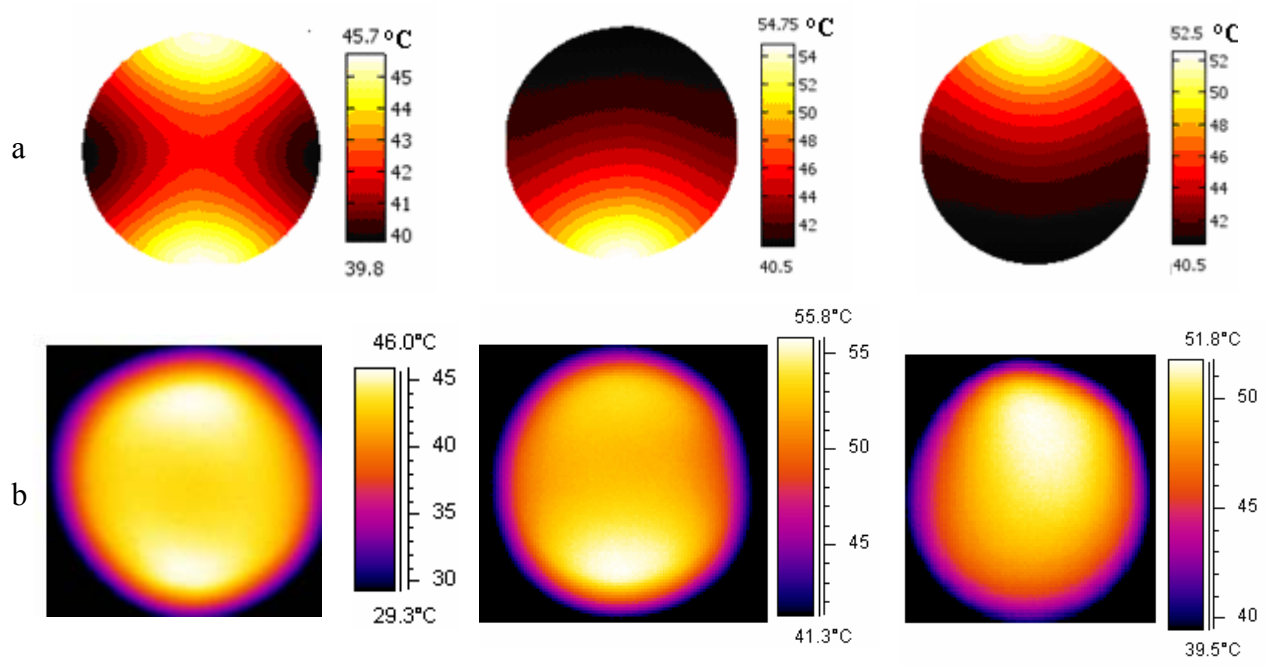

Fig. 4. Simulated (a) and experimental (b) temperature distributions after 14 min of RF heating of the model fruit (Φ80 mm) placed at the middle, toward the bottom and toward the top of a 160 mm eletrode gap

We may conclude from the above results that uniform RF heating of the fruits in air would not be possible. However, if the gap between two electrodes is very large and the fruit is positioned in the middle of the electrodes gap, somewhat uniform fruit heating can be anticipated. But, this is not practical for industrial applications because a large gap reduces the electric field strength and the heating potential, results in slow heating rates. Hallman & Sharp (1994) summarized the experience of many researchers and concluded that localized heating of fresh fruits is the major obstacle in using RF energy for fresh fruits.

3.3. RF heating pattern in fruit immersed in water

Fig. 5 shows that immersion of fruit in water radically changes the heating patterns of fruit and greatly enhances power coupling. The fruits placed near the container perimeter were heated predominantly at the segment of the fruit close to the container wall whereas the center-

placed fruit predominantly heated at the lower half of the fruit. The maximum temperature difference between corner and center-placed fruits ranged between 10 and 15°C. Since water provides the path of least resistance, electric field deflection occurred in water but not in air. The temperature profile along the radial distance as shown in Fig. 5c corroborated that simulation and experimental results agreed.

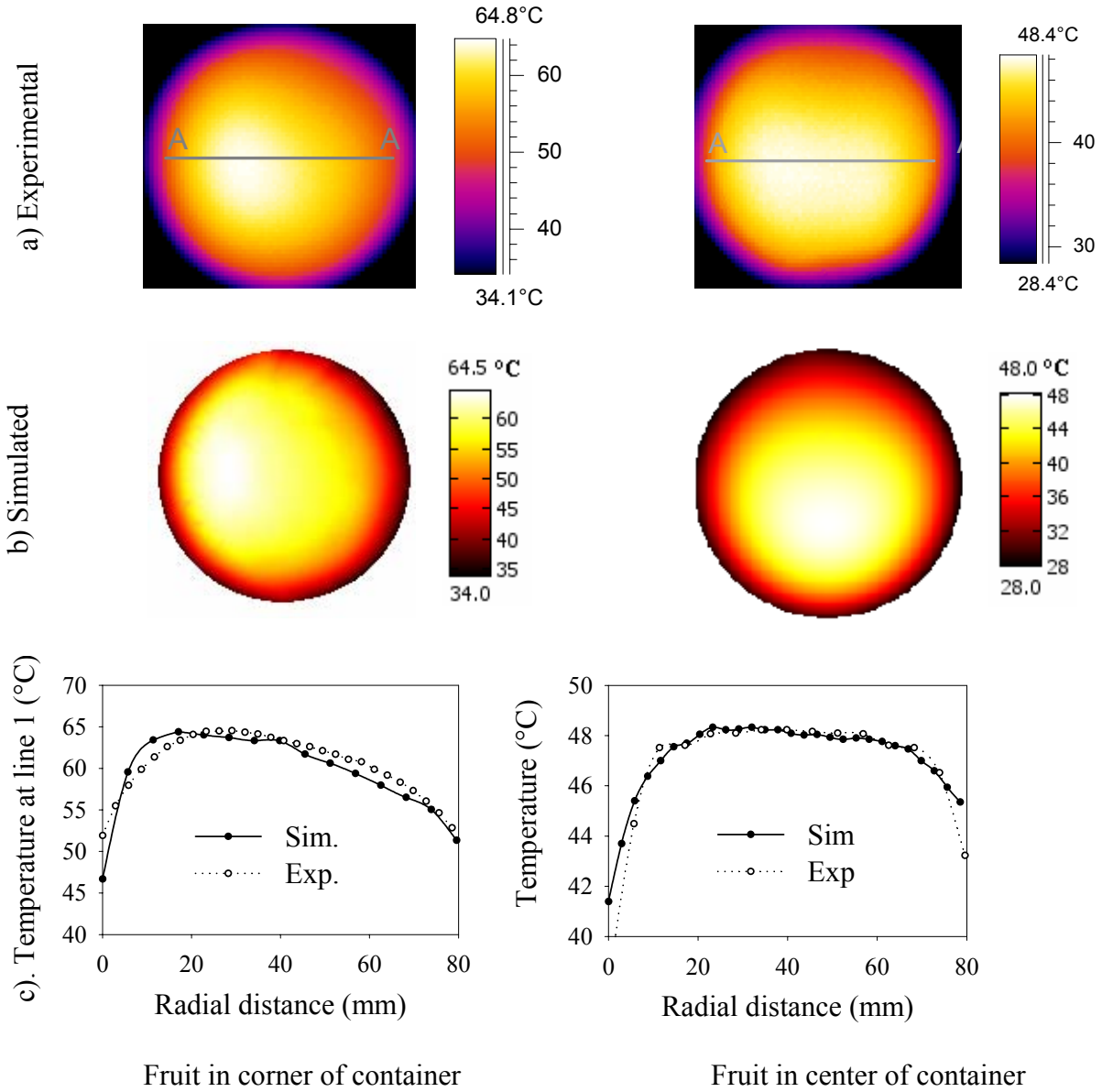

Fig. 5. Experimental (a) and simulated (b) temperature distributions inside model fruit (Φ80 mm) and at horizontal radial line A-A (c) after 7 min of RF heating in a 195 mm electrode gap

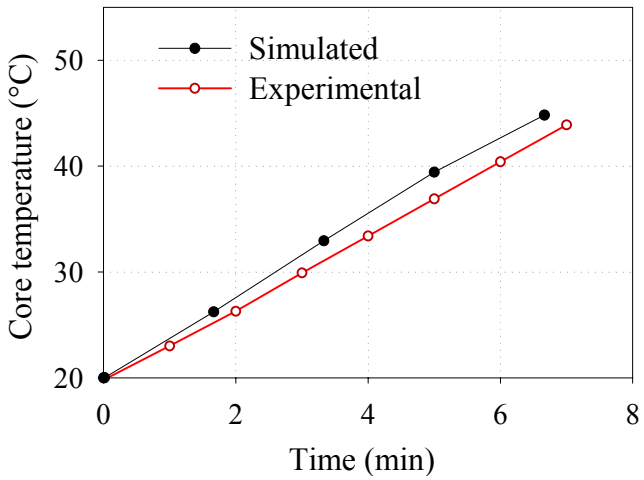

Fig. 6. Simulated and experimental time-temperature histories at the core of the centrally placed model fruit in a water filled container after RF heated for 7 min in a 195 mm electrode gap

It is also corroborated by the experimental and simulated time-temperature history at the core of the centrally placed gel ball as shown in Fig. 6. Ikediala et al. (2002) used the saline water immersion technique to minimize the uneven heating of cherries. Although immersion minimized the contact heating of cherries, non-uniformity over the cross section of cherries may still result in unacceptable quality (Ikediala et al., 2002). Non-uniform heating over cross sections of fruit becomes more pronounced in large size fruits, such as oranges and apples. To overcome this problem, Birla et al. (2004) developed a mechanism to move and rotate fruits in water during RF heating.

3.4. Effect of fruit rotation

Fig. 7 shows the effect of rotation and movement of a fruit-water mix on the heating pattern of fruits. It was quite logical that the rotation of the fruits during RF heating evened out the effect of proximity of the fruit to electrodes and container walls. The heating patterns in the experiment and the simulation were similar; however temperature raise differed because of the nature of the fruit movement and rotation. The simulated fruit was kept in the center, whereas the

experimental model fruit moved along the peripheral of the rectangular fruit mover. It should be noted that rotation and movement of fruit did not guarantee uniform heating all over the cross section of the homogenous fruit mass because of the difference in dielectric properties of the medium and fruit. A saline water immersion technique or differential startup temperature should be adopted along with fruit movement and rotation during RF heating to minimize differential heating between fruit and water.

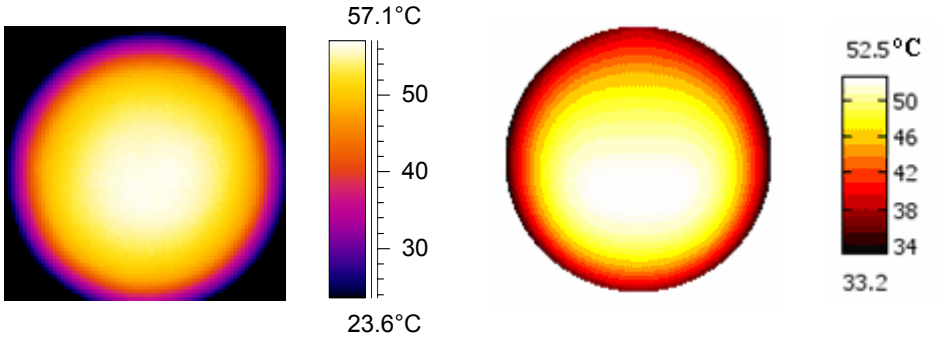

Fig. 7. Experimental and simulated temperature distributions of model fruits rotating and moving in the fruit mover (Birla et al., 2006) after 6 min of RF heating in a 195 mm electrode gap

3.5. Effect of dielectric properties of medium and fruit

3.5.1. Loss factor (LF) of water

Fig. 8 shows the simulated effect of increasing the loss factor of the surrounding media on the heating pattern of model fruit. An increase in the water loss factor (by increasing salinity) reduced the peak temperature inside the fruit, as saline water was likely to provide a conductive media for EM energy to pass through the path of least resistance.

Fig. 8b summarizes the results of a series of simulations with water loss factor value ranging from 20 to 180. Increasing water loss factor increased temperature in water but the

temperature started to decline after a certain loss factor value (~80). Altering the dielectric properties of water by addition of salt minimizes the differential heating between the fruit (oranges and cherries) and water (Birla et al., 2004; Ikediala et al., 2002). Differential heating between fruit and water can be minimized by appropriately matching dielectric properties of the water with that of fruit.

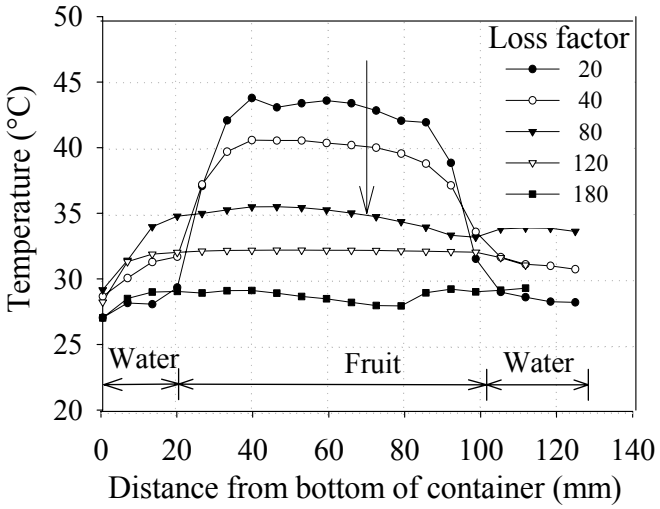

a). Temperature profile along the container height

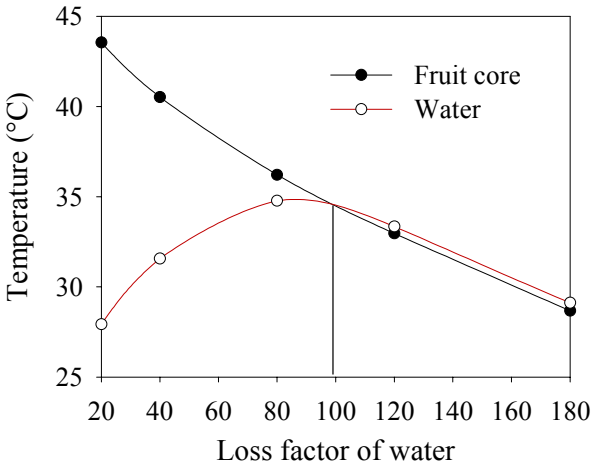

b). Temperature at fruit core and water surface

Fig. 8. Simulated and analytical effects of the water loss factor on heating patterns inside the model fruit (80 mm) subjected to 7 min RF heating in a 195 mm electrode gap

3.5.2. Loss factor of fruit

Fig. 9 shows the simulated effect of increasing the fruit loss factor on the heating pattern of model fruit placed in the center of the water-filled container (7 min of RF heating with a 195 mm electrodes gap).

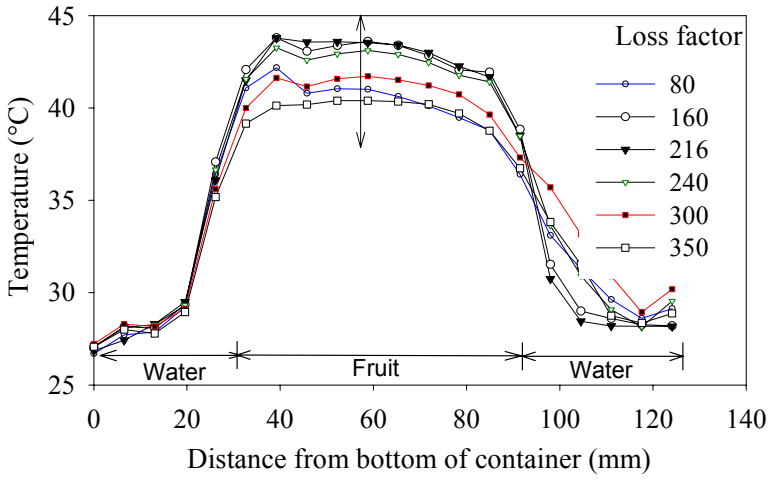

a).Temperature at vertical line dawn from the fruit core

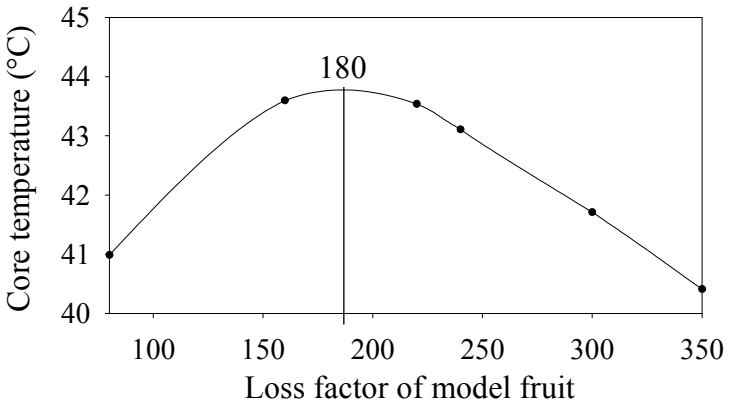

b). Temperature at fruit core

Fig. 9. Simulated effects of the dielectric loss factor of the model fruit (80 mm) on the temperature distribution inside the fruit immersed in the water after RF heating for 7 min in a 195 mm electrode gap

The simulation results showed that increasing the loss factor (LF) of fruit resulted in increasing heating rate only to a certain value (LF = 180), which was contrary to a general belief that increasing loss factor constantly increases heating rate inside the fruit. But beyond that value increasing loss factor diminished the heating rate inside the fruit. This can be explained by the fact that power density is proportional directly not only to the loss factor, but also to the square of electric field intensity. Increasing loss factor decreases the electric field intensity hence maximum heating rate occurs at particular loss factor value. An expression for limiting LF value as a function of the dielectric properties of a surrounding medium was derived by Birla (2006). Now with this simulation model and analytical expression a faster heating of apple (LF = 120) in comparison with oranges (LF = 220) can be explained.

3.6. Practical application of model

The computer model developed in this study was cable to predict the transient temperature profiles using physical and temperature-dependent dielectric properties, which are needed to design a RF heating process for disinfection of fruits. Having predicted the time-temperature profile in large fruit, one can decide the adequacy of the heating process based on information about the thermal death kinetics of microorganism/insect pests and quality degradation kinetics. In the present model we assumed constant voltage over the entire upper electrode, however, in practice this would not be true due to the effects of distributed system parameters and high frequency. To take these factors into account for the proper design of a whole RF system, an EM wave equation should be solved for domains including an RF generator, tank circuit and applicator.

4. Conclusions

A computer model based on finite element method was developed to the quasi-static electric fields in an RF heating system. The coupled Maxwell's EM equations and Navier-Stokes equations were solved for a 3-D model using FEMLAB software. The simulation results were validated with experimental temperature profiles of gellan gel model fruit. The experimental and simulation results were found to be in agreement, as the model was able to predict transient temperature profiles using physical and temperature-dependent dielectric properties. The validated computer model was further used to study the effects of dielectric properties of the medium and fruits, and effect of fruits rotation. Non-uniform heating is attributed to shape, dielectric properties, and relative position of the fruit in the container. The predicted temperature profile may be useful for designing an RF heating process in disinfestation of fruits. The developed model can be used as a tool to study the heating pattern of various fruits as influenced by dielectric properties of peel, pulp, and inner core.

Nomenclature

C_p	Specific heat (J kg^{-1} K^{-1})	*Greek symbols*	
$\boldsymbol{E}$	Electric field strength (V m^{-1})	ρ	Density (kg m^3)
f	Frequency (Hz)	σ	Ionic conductivity (S m^{-1})
$\boldsymbol{F_b}$	Buoyancy force (N m^{-3})	ε'	Dielectric constant
g	Gravitational acceleration (m s^{-2})	ε''	Dielectric loss factor
h	Heat transfer coefficient (W m^{-2} K^{-1})	ε_o	Permittivity of free space (F m^{-1})
j	Complex number operator	ω	Angular frequency, (rad s^{-1})
k	Thermal conductivity (W m^{-1} K^{-1})	∇	Delta operator
P	Pressure (N m^{-2})	β	Expansion coefficient (K^{-1})
Q	Power Density (W m^{-3})	μ	Viscosity (Pa s)
T	Temperature (K)	*Subscripts*	
t	Time (s)	air	Air
$\boldsymbol{u}$	Velocity (m s^{-1})	m	Medium
V	Electric potential (Volt)	s	slab/sphere

References

Birla, S. L. (2006). Potential of radio frequency heating of fresh fruits as an alternative quarantine method. PhD dissertation: Washington State University, Biological Systems Engineering.

Birla, S. L., Wang, S., & Tang, J. (2006). Radio frequency heating patterns as influenced by dielectric properties of constituent parts of fruits. In: *Proc. ASABE, Paper no. 066052. Portland*: ASABE.

Birla, S.L., Wang, S., Tang, J., Hallman, G., 2004. Improving heating uniformity of fresh fruit in radio frequency treatments for pest control. Postharvest Biol. Technol. 33, 205–217.

Chan, T.V.C.T., Tang, J., Younce, F., 2004. 3-Dienstional numerical modeling of an industrial Radio frequency heating systems using Finite elements. J. Microwave Power EE. 39, 87–105.

Choi, C.T.M., Konrad, A., 1991. Finite-Element Modeling of the RF Heating Process. IEEE Trans. Magn. 27, 4227–4230.

Frings, H., 1952. Factors determining the effects of radio-frequency electromagnetic fields and materials they infest. J. Econ. Entomol. 45, 396–408.

Guan, D., Cheng, M., Wang, Y., Tang, J., 2004. Dielectric properties of mashed potatoes relevant to microwave and radio-frequency pasteurization and sterilization processes. J. Food Sci. 69, FEP30–FEP37.

Hallman, G.J., Sharp, J.L., 1994. Radio frequency heat treatments. In: Sharp, J.L., Hallman, G.J. (Eds.), Quarantine treatments for pests of food plants. Westview Press, San Francisco, CA, pp. 165–170.

Hippel, A.R.v., 1954. Dielectric Materials and Applications. The Technology Press of MIT and John Wiley and Sons, New York.

Ikediala, J.N., Hansen, J.D., Tang, J., Drake, S.R., Wang, S., 2002. Development of a saline water immersion technique with RF energy as a postharvest treatment against coding moth in cherries. Postharvest Biol. Technol. 24, 25–37.

Marshall, M.G., Metaxas, A.C., 1998. Modeling of the radio frequency electric field strength developed during the RF assisted heat pump drying of particulates. J. Microwave Power EE. 33, 167–177.

Marra, F., Lyng, J., Romano, V., McKenna, B., 2007. Radio-frequency heating of foodstuff: Solution and validation of a mathematical model. J. Food Eng. 79, 998–1006.

Metaxas, A.C., 1996. Foundations of electoheat – A unified approach. John Wiley & Sons, NY.

Nelson, S.O., 1996. Review and assessment of radio-frequency and microwave energy for stored-grain insect control. Trans. ASAE 39, 1475–1484.

Nelson, S.O., Payne, J.A., 1982. RF dielectric heating for pecan weevil control. Trans. ASAE 31, 456-458.

Neophytou, R.I., Metaxas, A.C., 1996. Computer simulation of a radio frequency industrial system. J. Microwave Power EE. 31, 251–259.

Neophytou, R.I., Metaxas, A.C., 1997. Characterisation of radio frequency heating systems in industry using a network analyser. IEE Proceedings-Science Measurement and Technology 144, 215–222.

Neophytou, R.I., Metaxas, A.C., 1998. Combined 3D FE and circuit modeling of radio frequency heating systems. J. Microwave Power EE. 33, 243–262.

Neophytou, R.I., Metaxas, A.C., 1999. Combined tank and applicator design of radio frequency heating systems. IEE P-Microw. Anten. P. 146, 311–318.

Rehman, S., 1995. Food Properties Handbook. CRC Press, New York, 500 pp.

Roussy, G., Pearce, J.A., 1995. Foundations and industrial applications of microwave and radio frequency fields: physical and chemical processes. John Wiley & Sons, New York, 475 pp.

Stogryn, A., 1971. Equations for calculating the dielectric constant of saline water. IEEE Trans. Microw. Theory Tech. MTT-19, 733–736.

Tang, J., Tung, M.A., Zeng, Y., 1995. Mechanical properties of gellan gels in relation to divalent cations. J. Food Sci. 60, 748–752.

Tang, J., Tung, M.A., Zeng, Y., 1997. Gelling properties of gellan solutions containing monovalent and divalent cations. J. Food Sci. 62, 688–692, 712.

Tang, J., Ikediala, J.N., Wang, S., Hansen, J.D., Cavalieri, R.P., 2000. High-temperature-short-time thermal quarantine methods. Postharvest Biol. Technol. 21, 129–145.

Veen, M.E.v.d., Goot, A.J.v.d., Vriezinga, C.A., Meester, J.W.G.d., Boom, R.M., 2004. On the potential of uneven heating in heterogeneous food media with dielectric heating. J. Food Eng. 63, 403–412.

Wang, S., Tang, J., 2001a. Radio frequency and microwave alternative treatments for insect control in nuts: Review. Agric. Eng. J. 10, 105–120.

Wang, S., Tang, J., Cavalieri, R.P., 2001b. Modeling fruit internal heating rates for hot air and hot water treatments. Postharvest Biol. Technol. 22, 257–270.

Wang, S., Tang, J., Cavalieri, R.P., Davis, D.C., 2003a. Differential heating of insects in dried nuts and fruits associated with radio frequency and microwave treatments. Trans. ASAE 46, 1175–1182.

Wang, S., Tang, J., Johnson, J.A., Mitcham, E., Hansen, J.D., Cavalieri, R.P., Bower, J., Biasi, B., 2002. Process protocols based on radio frequency energy to control field and storage pests in in-shell walnuts. Postharvest Biol. and Technol. 26, 265–273.

C H A P T E R 8

DESIGN FEASIBILITY OF CONTINUOUS RF HEATING PROCESS FOR FRESH FRUIT DISINFESTATION

Abstract:

Many researchers have explored using Radio Frequency (RF) energy to disinfest fresh fruit. However, this research was focused on batch-type RF heating processes, whereas industrial continuous treatment systems should be compatible with washing, sorting, and other facilities currently used in packing houses. For example, the fresh fruit industry desires continuous fruit disinfestation treatment systems that can be integrated into their packing operations. To address this need, a feasibility study was undertaken to design a continuous RF heating process for fresh fruits. A 25 kW RF MagnaTube® unit was modified to perform continuous RF treatment of oranges and apples. To study the influence of pipe inclination angle, fruit properties, and flow rate on fruit heating rates, an analytical expression was derived. The experimental and analytical results showed that control of retention time of the fruit in RF electrode section was important to achieve the desired heating rate. Because fruits rolled on a particular axis, predominate heating was observed at the periphery. This problem can be overcome by mounting a spiral flight conveyor inside the tube to facilitate three-dimensional rotation of fruits and precise control over residence time during conveying though an RF heating zone. The study concluded that development of RF energy-based continuous heating process for fresh fruit should be pursued further.

Keywords: RF heating, disinfestation, heat treatment, quarantine, radio frequency.

1. Introduction

Researchers have demonstrated that RF heating is rapid, volumetric, and selective in nature (Tang et al., 2000). In spite of these advantages, its application to food processing is currently limited to baking and drying non-food materials. Contributing to this untapped potential is that most of the studies so far used a batch-type RF system, when industrial applications require a system in which products can be continuously treated. When Houben et al. (1993) studied continuous RF heating for sausage emulsion in a 10 kW RF unit by pumping the food through a 50 mm pipe surrounded by RF electrodes, they found a large difference in temperature of the emulsion at the core and near the wall of the pipe. Other studies by Zhong et al. (2003) & (2004) on heating performance of 1% carbomethylcellulose (CMC) solution and water continuously flowing through a vertical pipe enveloped with RF electrodes corroborated those results. Awuah et al. (2002) studied the continuous RF heating of starch solutions and reported that system and product parameters greatly influenced temperature change across the applicator tube (Piyasena and Dussault, 2003).

Wang et al. (2005a) developed a large-scale semi-continuous treatment protocol for disinfestation of walnuts. They showed that in the large scale continuous treatment intermittent stirring of the product promised to heat the product evenly Our Previous studies with batch-type RF treatment have shown that the problem of non-uniform RF heating of fruits can be resolved by moving and rotating the fruits during treatment. Applying this innovation to a continuous RF treatment system, a water-fruit mix flowing through an inclined tube in a RF system was hypothesized as an effective treatment. The present study was undertaken to test this hypothesis and study the feasibility of continuous RF heating of fresh fruits in a Magna tube RF machine.

2. Materials and Methods

2.1. RF machine

A 25 kW RF unit (MagnaTube, Fastran Strayfield, UK) originally developed for continuous pasteurization of liquid foods was modified to flow fresh fruit and water through a Teflon pipe (100 mm ID, 3 m length). The RF heating system consisted of a RF power generator, an RF power applicator, and circular heating tube (Fig. 1). The RF applicator consisted of two spiral ribbon electrodes, two power feed strips, two tuning inductors, and two auxiliary inductance coils (Fig. 1). The generator supplied the RF power to electrodes wrapped around a Teflon tube. The 3 m long tube was enveloped with 1.5 m long RF electrodes spirally wrapped around the middle of the pipe (Fig. 1). Maximum RF power coupling was tuned by a moving pair of variable inductors.

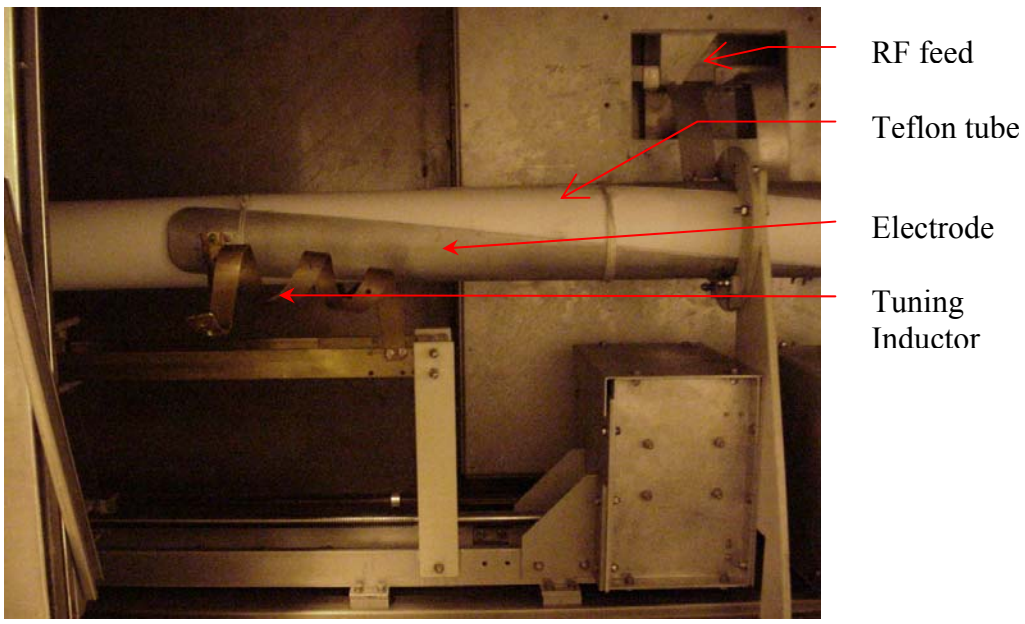

Fig. 1. Two split-ribbon electrodes wrapped around a Teflon tube

2.2. Continuous process design consideration

To build on existing knowledge about the importance of uniform heating within RF energy-based thermal treatments for fresh fruits, a detailed review of the literature was conducted. Houben et al. (1991) and Zhong et al. (2003) emphasized the need to minimize differential heating of fluid in tubes. In a laboratory-scale batch type fruit mover, Birla et al. (2004) demonstrated that rotating and moving fruit in an RF field can improve heating uniformity. To accomplish rotation and movement of fruit in a continuous flow process within a pipe, a fruit-water mix was fed from the lower end of an inclined pipe to roll spherical fruit inside the container. Translatory motion of the fruit was assumed to equally expose fruit surfaces to the RF field. Temperature rise in the fruit and water should thus be directly related to residence time in the RF heating zone, which would be a function of the fruit and tube geometry, water flow rate, density difference, and inclination angle of the tube. To determine these process parameters, a mathematical model based on flow governing mechanisms was developed.

2.3. Mathematical modeling for fruit movement in inclined pipes

Fig. 2 shows the graphical sketch of a spherical fruit with a volume (V_s, m^3) and radius of .04 m, translating upward at a velocity of v_f (m s^{-1}) and ω angular velocity in water. Since water density (ρ_w =1000 kg m^{-1}) is higher than fruit density ($\rho_{s,}$=~900 kg m^{-1}) a relative upward velocity (v_r, m s^{-1}) of fruit with respect to water velocity ($v_{w,}$ m s^{-1}) at instant 't' is $v_r = v_f - v_w$ The flow was assumed to be fully developed in the pipe inclined θ angle with horizontal. As the fruit rolls upward in the pipe, various forces control its upward velocity. It was appropriate to decompose forces into components normal and tangential to the plane of the pipe as shown in Fig. 2. The net weight normal to the plane of the pipe is balanced by a normal contact force ($\boldsymbol{F}_c$). The net weight component tangential to the plane of pipe is balanced by the hydrodynamic

resistance produced by the translation and rotation of the sphere (Prokunin and Williams, 1996). The resistance to translation causes the sphere to rotate in the usual contact rolling direction, which in turn causes an opposing torque (Chhabra and Ferreira, 1999; Chhabra et al., 2000; Zhao et al., 2002).

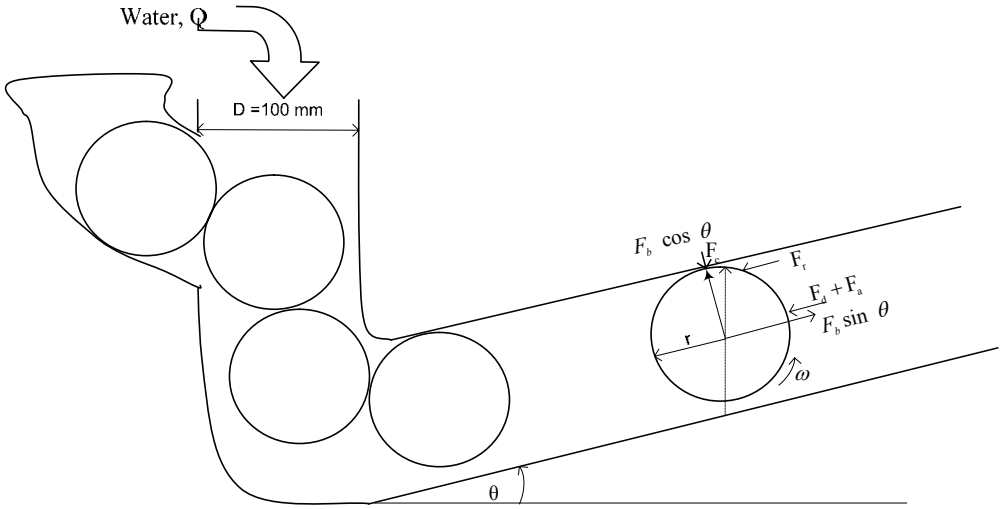

Fig. 2. Schematic diagram of forces on a spherical fruit rolling upward inside an inclined pipe

$$\underset{\text{Net force}}{\sum \boldsymbol{F}} = \underset{\text{Buoyancy}}{\boldsymbol{F}_b \sin\theta} - \underset{\text{Drag}}{\boldsymbol{F}_d} - \underset{\text{Rolling}}{\boldsymbol{F}_r} - \underset{\text{Added mass}}{\boldsymbol{F}_a} \quad (1)$$

The first term on the right-hand side of Eq. (1) is the buoyancy force exerted by water on the fruit, which is the main cause of upward movement of the fruit in the pipe. Due to sphere rotation and translation, drag force ($\boldsymbol{F_d}$), rolling friction force ($\boldsymbol{F_r}$), and added mass inertia force ($\boldsymbol{F_a}$) oppose the motion of fruit (Galvin et al., 2006; Jan and Chen, 1997). The rolling friction at the fruit-pipe wall contact surface provides the torque to the fruit to rotate as it moves up. According to Newton's 2nd law for rotational motion, rolling friction on linearly accelerating spherical fruit (moment of inertia, I =2/5 m r^2) can be determined. The last term in Eq. (1) is contributed by acceleration of spherical fruit due to added mass inertia.

$$V_s \rho_s \frac{dV}{dt} = V_s (\rho_w - \rho_s) \, g \sin\theta - \frac{\pi}{2} C_d \rho_w r^2 v_r^2 - \frac{2}{5} V_s \frac{dV}{dt} - C_A \rho_s V_s \frac{dV}{dt} \qquad (2)$$

$$V_s \rho_s (1.4 + C_A \frac{\rho_w}{\rho_s}) \frac{dv_r}{dt} = V_s (\rho_w - \rho_s) \, g \sin\theta - \frac{\pi}{2} C_d \pi r^2 \rho_w v_r^2 \qquad (3)$$

$$\frac{dv_r}{dt} = \frac{(\rho_w - \rho_s) \, g \sin\theta}{(1.4\rho_s + C_A \rho_w)} - C_d \frac{3 \rho_w}{8 r (1.4\rho_s + C_A \rho_w)} v_r^2 \qquad (4)$$

$$\frac{dv_r}{dt} = a + b C_d v_r^2 \qquad (5)$$

$$where \; a = \frac{(\rho_w - \rho_s) \, g \sin\theta}{(1.4\rho_s + C_A \rho_w)} \qquad b = \frac{-3 \rho_w}{8 r (1.4\rho_s + C_A \rho_w)}$$

The added mass coefficient (C_A) for a sphere in free fall varies from 0.5 to 1.05, depending on the ratio (ρ_s / ρ_w) of densities of sphere and water (Jan and Chen, 1997). However, there is no information about C_A for a sphere rolling up inside a pipe. Linear velocity of the fruit was estimated by numerically solving Eq. (5). The numerical results were then compared with experimental observations.

Because the drag coefficient (C_d) is a function of velocity (v_r), Eq. (5) becomes nonlinear, and a closed-form solution for linear velocity impossible. Hence the finite difference numerical technique was adopted to discretize Eq. (5) for solving the linear velocity of fruit in the inclined pipe as below:

$$v_{r\,i+1} = v_{r\,i} + (a + b C_d v_r^2)(t_{i+1} - t_i) \qquad (6)$$

A program was written in MATLAB to solve Eq. (6) for the linear relative velocity of the fruit in the inclined pipe. At every time step the drag coefficient was evaluated based on the following criteria (Jan and Chen, 1997):

In stoke range, (Reynold No. Re = $v_r\, d/\mu < 1$) $C_d = \frac{24}{Re}$ (7)

where μ is the water viscosity.

Transition region: $1 < Re < 10{,}000$ $C_d = \frac{24}{Re} + \frac{3}{Re^{1/2}} + 0.34$ (8)

Newton's Law region: $10{,}000 < Re < 200{,}000$ $C_d \sim 0.4$ is nearly constant. (9)

2.4. RF heating procedure

A feasibility study was conducted on the modified 25 kW RF heating system in which a fruit-water mix was fed from the lower end of an inclined tube as shown in Fig. 1. Navel oranges (990 kg m^{-3}) and red delicious apples (850 kg m^{-3}) from a local grocery store were kept at room temperature. The RF machine was set for maximum power coupling for flowing water by changing tuner positions and inductors. At a 38.9 *l*/min flow rate and 25 kW input power, the rise in water temperature was 19.9°C from an initial 13°C in 18 s retention within the RF heating section. Based on the water heating rate, the power coupling efficiency was 92%. Residence time in the RF heating zone was determined by recording the time required for fruit traveling from start to end of the electrode. Since preheating fruits prior to RF heating is known to help cut down energy demand and treatment time, one experiment involved preheating oranges in a 35°C water bath for 45 min before feeding with tap water in the RF machine. This experiment was important for exploring the possibility of practical continuous RF treatment. Once the fruit came out from the inclined tube at the upper end, temperatures at the core, stem, and navel ends of the fruit were measured using a thermocouple thermometer (Type-T, 0.8 mm diameter and 0.8 s response time, Omega Engineering Ltd, CT). The RF-heated fruits were halved and thermal images of the cut surfaces were recorded using an infrared imaging camera (ThermaCam®, manufacturer).

3. Results and Discussion

3.1. Linear velocity of fruit in pipe

An inclination angle of 12° was chosen based on required residence time and adequacy of fruit rolling in the heating section. Increasing inclination angle of tube resulted in a reduced residence time, whereas decreasing this angle slowed fruit movement. It was obvious from Eq. (6) that the residence time was a function of water flow rate, density of fruit and water, and viscosity of water (e.g., the drag coefficient depends on it).

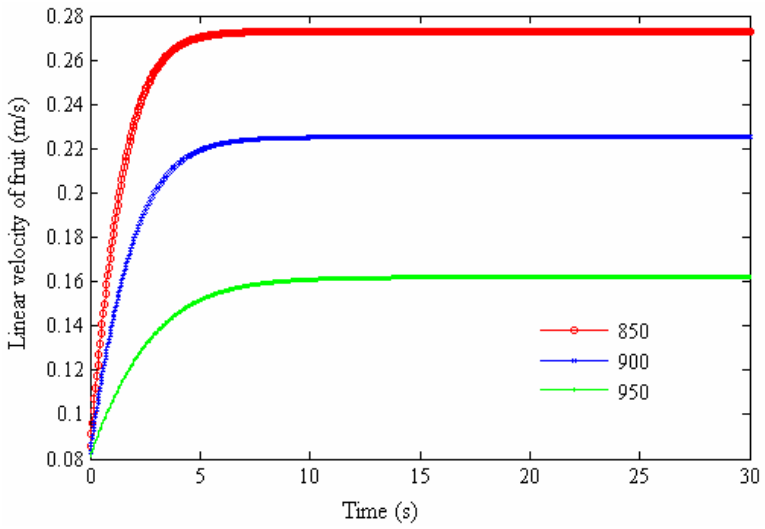

Fig. 3. Effect of fruit density (kg m^{-3}) on the linear velocity of fruit in an inclined pipe

For oranges (300 ± 25g) and apples (200 ± 20g) at a 39.8 *l*/min water flow rate, the experimentally determined residence times in a 1.5 m long RF heating section were 16 ± 2 s and 12 ± 3 s, respectively. The difference is mainly attributed to density, as the apples (850 kg m^{-3}) were much lighter than the oranges (990 kg m^{-3}). Numerical simulation of fruit linear velocity suggested that the fruits attended the terminal velocity in 3–5 s after release at the lower end of the tube (Fig. 3). The numerically calculated residence times were 12 and 8 s for oranges and apples, respectively, which were shorter than the experimental values due to non-spherical fruit

geometry and the assumption of fully developed flow. The criteria for estimating the drag coefficient still needed to be confirmed by experimental methods. After a range of C_A values (0.5–2.5) was tried, C_A 2.0 was found to give closest approximation of residence time, which was highly influenced by density (e.g., increasing fruit density resulted in slower upward movement of fruit; Fig. 3). Interestingly, numerical calculation with different sized fruits hinted that smaller fruit would move slower than larger fruit in the inclined tube (Fig. 4), which was not verified experimentally.

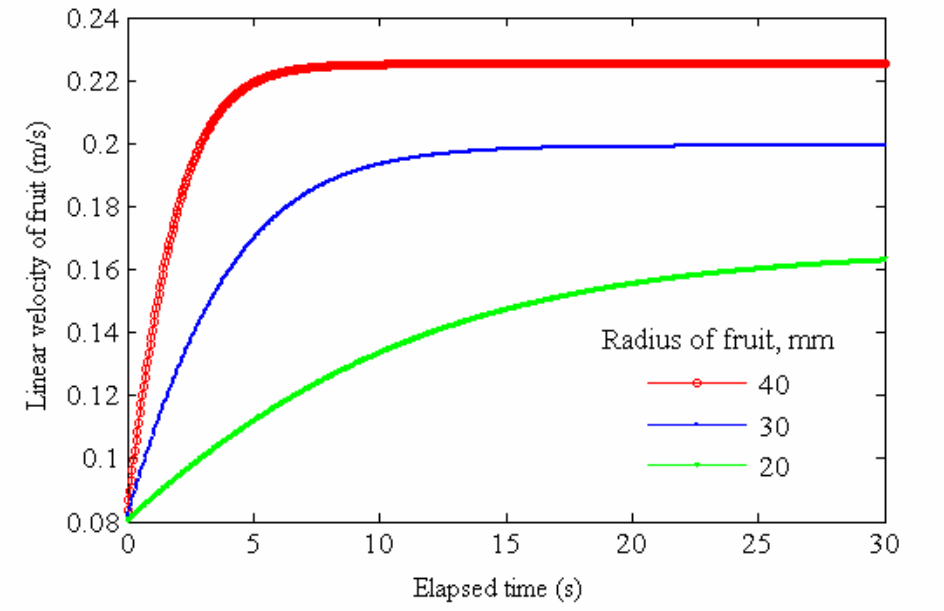

Fig. 4. Simulated effect of fruit size on a linear fruit velocity (900 kg m^{-3}) profile

3.2. Temperature profile

At full RF power (25 kW) and water flow rate of 39.8 *l*/min, the temperature rise in oranges and apples was 14 and 24°C, respectively. In oranges, excessive heating was observed at the fruit periphery (Fig. 5) due to rolling on a particular axis from variable mass distribution. Table 1 shows that temperature variations within oranges (0.6–1.4 °C SD) were lower compared to that among oranges (1.7–2.4 °C SD). This might be due to different residence times of

individual fruit, as linear velocity depended on the rolling ability of individual fruit inside the pipe. Fig. 5 shows that the temperature variation in apples was higher than that of oranges. Core heating in apples was observed even if the fruits were subjected to 3-D rotation and movement during RF heating (Birla et al., 2006).

Heating uniformity over the fruit cross-section was found to be a problem in the inclined pipe. The oranges required rotation on all axes to expose every part equally, as was provided in the fruit mover. Even a slight change in residence time produced a large variability in temperature among fruits; therefore, strict control over residence time is an important parameter. In the setup described here, the residence time of individual fruit could not be controlled. To achieve more uniform heating within a continuous RF heating process, fruit need to be rotated in 3-D and the residence time set the same for all fruit.

After preheating (35°C in hot water bath for 45 min) and RF heating of oranges, their average temperature was 51.69°C, with a 1.94°C standard deviation (Table 3). Such results confirm that RF is more effective than conventional heating for accomplishing the last lag of heating in the thermal treatment. In the case of apples, preheating prior to RF heating of fruit holds a potential to develop continuous treatment.

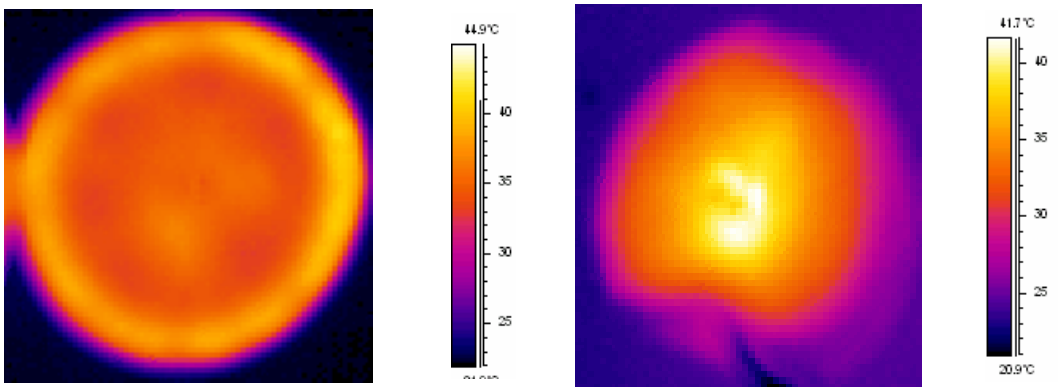

Orange **Apple**

Fig. 5. Temperature profile in oranges and apple after RF heating in a Magna tube from an initial temperature of 20°C

Table 1. Temperature distribution in RF-heated oranges (i.e., continuous feeding of oranges in an RF tube with 13.8°C water and a flow rate of 39.8 l/min)

Orange	Temperature, °C				
	Core	Stem end	Navel end	Average	Std
1	36.90	37.10	38.10	37.37	0.64
2	32.80	31.10	35.90	33.27	2.43
3	33.70	35.10	35.70	34.83	1.03
4	33.20	31.60	34.40	33.07	1.40
5	31.10	32.30	31.30	31.57	0.64
6	32.70	33.90	33.70	33.43	0.64
7	33.30	34.70	33.90	33.97	0.70
8	31.70	32.80	33.40	32.63	0.86
9	35.40	37.20	35.80	36.13	0.95
10	34.80	36.00	36.00	35.60	0.69
Avg	33.56	34.18	34.82	**34.19**	
Std	1.74	2.20	1.88		**1.95**

Note: *Water temperature increased by only 6°C*

Table 2. Temperature distribution in RF-heated apples (i.e., continuous feeding of apples in an RF tube with a water flow rate of 39.8 l/min)

Apple	Temperature, °C				
	Core	Stem end	Navel end	Average	Std
1	41.20	49.60	44.90	45.23	4.21
2	43.60	50.50	48.90	47.67	3.61
3	39.20	43.90	41.70	41.60	2.35
4	40.90	42.20	44.10	42.40	1.61
5	45.00	46.80	50.50	47.43	2.80
6	56.40	55.00	53.20	54.87	1.60
7	54.80	48.00	46.00	49.60	4.61
8	45.80	43.00	42.70	43.83	1.71
9	45.90	42.50	41.80	43.40	2.19
Avg	45.87	46.83	45.98	**46.23**	
Std	6.00	4.37	4.07		**4.71**

Table 3. Temperature distribution in RF-heated oranges (i.e., fruit were fed one at a time, with an initial temperature of 35°C and residence time of 16 s)

Orange	Temperature °C				
	Core	Stem end	Navel end	Average	Std
1	54.20	53.60	52.70	53.50	0.75
2	50.40	49.20	52.30	50.63	1.56
3	50.70	52.60	48.90	50.73	1.85
4	50.30	55.20	54.20	53.23	2.59
5	52.60	53.10	50.80	52.17	1.21
6	49.60	50.90	49.20	49.90	0.89
Avg	51.30	52.43	51.35	**51.69**	
Std	1.74	2.11	2.09		**1.94**

4. Recommendations

Figs. 2 & 3 demonstrate that oranges tend to become overheated on their rotational periphery and this might be the result of fruits rolling on particular axes inside the RF applicator tube. This problem can be overcome by mounting a spiral flight conveyor inside the tube to facilitate 3-D rotation of fruits and precisely control the residence time during conveying though the RF heating zone.

Extensive testing with a fruit mover indicates that temperature variation within and among fruits is unavoidable irrespective of how adequate the rotation during RF heating because of natural variation and heterogeneity within fruits (Birla et al., 2006). However, because apples are predominately core-heated, preheating this fruit in hot water/air prior to subjecting to RF heating holds potential for its application to a continuous process. Such a finding confirms the feasibility of developing a RF energy-based continuous heating process for fresh fruit.

References

Awuah, G.B., Ramaswamy, H.S., Piyasena, P., 2002. Radio frequency (RF) heating of starch solutions under continuous flow conditions: effect of system and product parameters on temperature change across the applicator tube. J. Food Process Eng. 25, 201–223.

Birla, S.L., Wang, S., Tang, J., 2006. Radio frequency heating patterns as influenced by dielectric properties of constituent parts of fruits, Proc. ASABE, Portland, Paper no. 066052.

Birla, S.L., Wang, S., Tang, J., Hallman, G., 2004. Improving heating uniformity of fresh fruit in radio frequency treatments for pest control. Postharvest Biol. Technol. 33, 205–217.

Chhabra, R.P., Ferreira, J.M., 1999. An analytical study of the motion of a sphere rolling down a smooth inclined plane in an incompressible Newtonian fluid. Powder Technol. 104, 130–138.

Chhabra, R.P., Kumar, M., Prasad, R., 2000. Drag on spheres in rolling motion in inclined smooth tubes filled with incompressible liquids. Powder Technol. 113, 114–118.

Galvin, K.P., Zhao, Y., Davis, R.H., 2006. Time-averaged hydrodynamic roughness of a noncolloidal sphere in low Reynolds number motion down an inclined plane. Phys. Fluids 13, 3108–3119.

Houben, J.H., Vanroon, P.S., Krol, B., 1993. Continuous Radiofrequency Pasteurization in Sausage Manufacturing Lines. Fleischwirtschaft 73, 1146–1149.

Jan, C.D., Chen, J.-C., 1997. Movements of a sphere rolling down an inclined plane. J. Hydraulic Res. 35, 689–706.

Piyasena, P., Dussault, C., 2003. Continuous radio-frequency heating of a model viscous solution: influence of active current, flow rate, and salt content of temperature rise, Canadian Biosystems Engineering ,45, 3.27-3.34

Prokunin, A.N., Williams, M.C., 1996. Spherical particle sedimentation along an inclined plane at high Reynolds numbers. Fluid Dyn. 31, 567–572.

Wang, S., Monzon, M., Tang, J., Johnson, J.A., Mitcham, E., 2005. Large-scale radio frequency treatments for insect control in walnuts, In the Proceedings of 10th Annual International Research Conference on Methyl Bromide Alternatives and Emissions Reduction, San Diego, CA.

Tang, J., Ikediala, J.N., Wang, S., Hansen, J.D., Cavalieri, R.P., 2000. High-temperature-short-time thermal quarantine methods. Postharvest Biol. Technol. 21, 129–145.

Zhao, Y., Galvin, K.P., Davis, R.H., 2002. Motion of a sphere down a rough plane in a viscous fluid. Int. J. Multiphas. Flow 28, 1787–1800.

Zhong, Q., Sandeep, K.P., Swartzel, K.R., 2003. Continuous flow radio frequency heating of water and carboxymethylcellulose solutions. J. Food Sci. 68, 217–223.

Zhong, Q.X., Sandeep, K.P., Swartzel, K.R., 2004. Continuous flow radio frequency heating of particulate foods. Innovative Food Sc. Emerging Technol. 5, 475–483.

CONCLUSIONS & RECOMMENDATIONS

This research was an effort to explore the use of electromagnetic energy to disinfest fresh fruits in response to the urgent need to develop alternative quarantine treatment methods to methyl bromide. Despite the substantial penetration depth of RF energy in fresh fruits, heating uniformity is the major stumbling block in the development of RF energy-based treatments. This research was undertaken to deal with non-uniform RF heating of fruits and develop practical treatment protocols for disinfesting fresh fruits. Major findings and recommendations are as given below:

1. To understand the heating patterns of fresh fruits in a parallel plate RF system, a simulation model was developed using FEMLAB software to solve coupled electromagnetic and Navier-Stokes equations and predict transient temperature profiles.
2. The simulation model developed for this study investigated the effects of various factors influencing fruit heating uniformity.
3. Simulation and experimental results corroborated that moving and rotating fresh fruits in water during RF heating is the best available approach to deal with uneven RF heating due to variable fruit geometry and positioning.
4. Fruit movement and rotation did not necessarily guarantee uniform heating of fruits because of different dielectric properties of the medium and fruit.
5. Differential heating or preferential heating of the core of fruit over the surface can be a blessing in disguise for development of practical RF treatment in the case of RF-assisted hot water treatment of apples.

6. Although RF-assisted hot water treatment was efficacious against codling moth in apples, significant alteration to the flavor profile raised questions about consumer acceptability and long-term storability.
7. Because the safety margin between efficacious and detrimental temperature-time combinations was found to be very narrow, high-temperature short-time RF treatments are questionable for fresh fruit.
8. A preliminary feasibility study of continuous RF treatment indicated it is possible to accomplish continuous RF treatment in a series of inclined RF tubes.

The following areas need further research to address the issues associated with developing RF energy-based treatment protocols:

1. Since high-temperature short-time (> 48°C) RF energy-based thermal treatment is not feasible for fruit, lower temperature (< 48°C) RF thermal treatments should be explored.
2. Modeling of the parallel plate RF applicator should include the RF generator and solve Maxwell's wave equation for electric fields at any point in the domain to help simulate the RF heating pattern in an industrial-scale RF system.
3. The model should also be modified to simulate a heterogeneous fruit matrix and validate the efficacy of RF-based thermal treatments for targeted insects in host commodities.
4. An experimental setup that provides movement and rotation of fruits in a continuous flowing stream is needed to demonstrate continuous RF heating.
5. A detailed economic and cost-benefit analysis in industrial-scale systems will be required before the technology is adopted by fresh fruit packing houses.